ISSN 1881-7831 Online ISSN 1881-784X

DD&T

Drug Discoveries & Therapeutics

Volume 10, Number 5
October, 2016

Topic:
Oligonucleotides

Editor:
Masahiro Murakami

IRCA
BSSA

IACMHR

www.ddtjournal.com

DD&T
Drug Discoveries & Therapeutics

ISSN: 1881-7831
Online ISSN: 1881-784X
CODEN: DDTRBX
Issues/Year: 6
Language: English
Publisher: IACMHR Co., Ltd.

Drug Discoveries & Therapeutics is one of a series of peer-reviewed journals of the International Research and Cooperation Association for Bio & Socio-Sciences Advancement (IRCA-BSSA) Group and is published bimonthly by the International Advancement Center for Medicine & Health Research Co., Ltd. (IACMHR Co., Ltd.) and supported by the IRCA-BSSA and Shandong University China-Japan Cooperation Center for Drug Discovery & Screening (SDU-DDSC).

Drug Discoveries & Therapeutics publishes contributions in all fields of pharmaceutical and therapeutic research such as medicinal chemistry, pharmacology, pharmaceutical analysis, pharmaceutics, pharmaceutical administration, and experimental and clinical studies of effects, mechanisms, or uses of various treatments. Studies in drug-related fields such as biology, biochemistry, physiology, microbiology, and immunology are also within the scope of this journal.

Drug Discoveries & Therapeutics publishes Original Articles, Brief Reports, Reviews, Policy Forum articles, Case Reports, News, and Letters on all aspects of the field of pharmaceutical research. All contributions should seek to promote international collaboration in pharmaceutical science.

Editorial Board

Editorial and Head Office:

Pearl City Koishikawa 603,
2-4-5 Kasuga, Bunkyo-ku,
Tokyo 112-0003, Japan
Tel.: +81-3-5840-9697
Fax: +81-3-5840-9698
E-mail: office@ddtjournal.com

Drug Discoveries & Therapeutics

Editorial and Head Office

Pearl City Koishikawa 603, 2-4-5 Kasuga, Bunkyo-ku,
Tokyo 112-0003, Japan

Tel: +81-3-5840-9697, Fax: +81-3-5840-9698
E-mail: office@ddtjournal.com
URL: www.ddtjournal.com

Editorial Board Members

CONTENTS

Volume 10, Number 5, 2016

Editorial

Reviews

Original Article

Commentary

Editorial

DOI: 10.5582/ddt.2016.01073

Therapeutic oligonucleotides and delivery technologies: Research topics in Japan

Masahiro Murakami*

Laboratory of Pharmaceutics, Faculty of Pharmacy, Osaka Ohtani University, Osaka, Japan.

Summary **Oligonucleotides have been gaining considerable attention as promising and effective candidate therapeutics against various diseases. This special issue is aimed at providing a better understanding of the recent progress in the development of oligonucleotide-based therapeutics to encourage further research and innovation in this field to achieve these advancements. Several Japanese scientists have been invited to contribute to this issue by describing their recent findings, overviews, insights, or commentaries on rational designing of therapeutic oligonucleotide molecules and their novel delivery technologies, especially nanocarrier systems.**

Keywords: Oligonucleotide, drug delivery, chemical modification, conjugation

In new drug discovery, the inhibition of cellular mRNA relevant to diseases has become an attractive strategy, while the molecular biology of diseases has been revealed at gene levels (*1*). Functional oligonucleotides such as antisense and small interfering RNA oligonucleotides (ASO and siRNA, respectively) are currently recognized as promising therapeutic entities that are effective for not only intractable diseases and genetic disorders but also various illnesses that do not have adequate existing therapies. Although an oligonucleotide-based therapy is supposed to be specific for the sequence of its targeted gene, initial clinical trials have taught us safety and efficacy lessons (*2,3*). Oligonucleotides are polyanionic macromolecules and naturally instable against degradation by nucleolytic enzymes in the body. Therefore, their self-mediated transportation into targeted cells is limited, which may cause off-target effects, non-specific immune stimulation, or both. This is also partly due to the lack of safe and effective *in vivo* delivery techniques. Viral and non-viral artificial carriers have been reported as effective carrier systems for specific targets (*4,5*). However, the safety of these *in vivo* carriers including their materials or sources is another inevitable problem in the development of systemic delivery systems for oligonucleotides (*6*). Thus, the major challenge for the clinical application of ASO and siRNA is solving the oligonucleotide stability issues and their delivery to specific targets.

The remarkable progress in unraveling the medicinal chemistry of nucleic acids in the last decade has improved the *in vivo* stability and target affinity of synthetic oligonucleotides using chemical modifications or rational designs (*7*). These advances have also promoted the feasible use of synthetic oligonucleotides as therapeutics. After the successful introduction of phosphorothioate modifications into ASO (*8*), various chemical modifications improved its stability against different nucleases as well as the binding affinity for target mRNA. These modifications include the use of locked nucleic acids (LNAs), 2′-*O*-methoxyethyl, and a constrained ethyl bridge nucleic acid (BNA). Recently, Yokota and co-workers (*9,10*) reported a novel DNA/RNA heteroduplex oligonucleotide (HDO) and its α-tocopherol conjugate as a targeting ligand. This α-tocopherol HDO conjugate showed significantly high specificity for the target and exerted remarkably potent gene-silencing efficacy *in vivo*. Obika and co-workers (*11,12*) have greatly contributed to the development of synthetic oligonucleotides including LNAs and BNAs. In this special issue, they have provided their recent results of the synthesis of 5′-thio-modified

**Address correspondence to:*
Dr. Masahiro Murakami, Laboratory of Pharmaceutics, Faculty of Pharmacy, Osaka Ohtani University, 3-11-1 Nishikorikita, Tondabayashi, Osaka 584-8540, Japan.
E-mail: murakam@osaka-ohtani.ac.jp

2′-deoxy-5-methylcytidine ASO and the influence of this modification on the stability of ASO, which was demonstrated in *in vitro* and *in vivo* experiments. In contrast, the cost of manufacturing oligonucleotides appears to have increased with the advancement in chemical modifications and complicated molecular designs. Chemical modification should alter the physicochemical properties of oligonucleotides to affect their distribution in the body. Therefore, a significant increase in affinity and specificity for target genes is considered essential for such synthetic oligonucleotides. Nishikawa provides his insights on the issue while introducing a unique self-gelatinizable nucleic acid technology and DNA hydrogel.

The development of an effective and safe delivery system or technology is essential for the success of synthetic oligonucleotides. The laboratory of Kataoka (*13,14*) has developed polyplex nanomicelles composed of poly(ethyleneglycol)-polycation block copolymers as gene delivery systems that are leading the field of nanocarrier system development. Miyata reviews the recent discoveries of polymer-based carriers for systemic oligonucleotide delivery. Negishi and co-workers introduced a non-invasive gene delivery technology based on the combination of lipid bubbles and ultrasound, in addition to an overview of the research conducted in this area. Asami and co-workers reviewed the recent technologies of conjugating a functional ligand for effective targeting and introduced their novel HDO and α-tocopherol conjugate.

Oral drug delivery is the most popular and patient-friendly route of administration but developing an effective delivery system for oligonucleotides remains a major challenge. The bottleneck in developing nucleic acid-based oral therapeutics has been their low bioavailability, which leads to high costs because of drug loss in the alimental canal based on their instability and impermeability. We provide a commentary that describes the potential benefits of the colorectal route as another platform for the development of oral oligonucleotide therapeutics and introduce the liver-targeted enteral siRNA delivery technology we recently developed (*15*). The importance of targeting or the availability of oligonucleotides in targeted tissue is highlighted in contrast to systemic availability, which does not directly reflect the effects of oligonucleotide.

The editor hopes that this special issue will provide a better understanding of the recent progress in the development of oligonucleotide-based therapeutics and, thereby, encourage further research and innovation in this field for achieving advancements.

Acknowledgements

I would like to express my gratitude to Dr. Tang W. and Dr. Nakata M. for their supportive management of this special issue.

References

1. Martinez T, Jimenez AI, Paneda C. Short-interference RNAs: becoming medicines. EXCLI J. 2015; 14:714-746.
2. Barros SA, Gollob JA. Safety profile of RNAi nanomedicines. Adv Drug Deliv Rev. 2012; 64:1730-1737.
3. Coelho T, Adams D, Silva A, *et al*. Safety and efficacy of RNAi therapy for transthyretin amyloidosis. N Engl J Med. 2013; 369:819-829.
4. Schott JW, Morgan M, Galla M, Schambach A. Viral and synthetic RNA vector technologies and applications. Mol Ther. 2016; 24:1513-1527.
5. Juliano RL. The delivery of therapeutic oligonucleotides. Nucleic Acids Res. 2016; 44:6518-6548.
6. Akhtar S, Benter I. Toxicogenomics of non-viral drug delivery systems for RNAi: potential impact on siRNA-mediated gene silencing activity and specificity. Adv Drug Deliv Rev. 2007; 59:164-182.
7. Grunweller A, Hartmann RK. Chemical modification of nucleic acids as a key technology for the development of RNA-based therapeutics. Pharmazie. 2016; 71:8-16.
8. Eckstein F. Phosphorothioates, essential components of therapeutic oligonucleotides. Nucleic Acid Ther. 2014; 24:374-387.
9. Nishina K, Piao W, Yoshida-Tanaka K, *et al*. DNA/RNA heteroduplex oligonucleotide for highly efficient gene silencing. Nat Commun. 2015; 6:7969.
10. Nishina T, Numata J, Nishina K, Yoshida-Tanaka K, Nitta K, Piao W, Iwata R, Ito S, Kuwahara H, Wada T, Mizusawa H, Yokota T. Chimeric antisense oligonucleotide conjugated to alpha-tocopherol. Mol Ther Nucleic Acids. 2015; 4:e220.
11. Obika S. Development of bridged nucleic acid analogues for antigene technology. Chem Pharm Bull (Tokyo). 2004; 52:1399-1404.
12. Kuwahara M, Obika S. *In vitro* selection of BNA (LNA) aptamers. Artif DNA PNA XNA. 2013; 4:39-48.
13. Baba M, Itaka K, Kondo K, Yamasoba T, Kataoka K. Treatment of neurological disorders by introducing mRNA *in vivo* using polyplex nanomicelles. J Control Release. 2015; 201:41-48.
14. Uchida S, Itaka K, Uchida H, Hayakawa K, Ogata T, Ishii T, Fukushima S, Osada K, Kataoka K. *In vivo* messenger RNA introduction into the central nervous system using polyplex nanomicelle. PLoS One. 2013; 8:e56220.
15. Murakami M, Nishina K, Watanabe C, *et al*. Enteral siRNA delivery technique for therapeutic gene silencing in the liver *via* the lymphatic route. Sci Rep. 2015; 5:17035.

(Received October 17, 2016; Accepted October 18, 2016)

Review

DOI: 10.5582/ddt.2016.01061

Smart polymeric nanocarriers for small nucleic acid delivery

Kanjiro Miyata[1,2,*]

[1] *Department of Materials Engineering, Graduate School of Engineering, The University of Tokyo, Tokyo, Japan;*
[2] *Center for Disease Biology and Integrative Medicine, Graduate School of Medicine, The University of Tokyo, Tokyo, Japan.*

Summary **In recent decades, nucleic acid therapeutics have been attracting much attention because of their potential as treatments for various diseases that require high target specificity. Nevertheless, the number of approved nucleic acid drugs is very limited due to substantially poor bioavailability, thereby generating the need for nucleic acid delivery carriers. A variety of delivery formulations have been reported so far. This review particularly describes polymer-based delivery carriers for systemic administration, highlighting the potential of biological environment-responsive chemistry for overcoming the biological barriers to nucleic acid delivery.**

Keywords: Drug delivery, antisense oligonucleotide, small interfering RNA (siRNA), block copolymer, polyion complex (PIC)

1. Introduction

Over recent decades, small nucleic acids, such as antisense oligonucleotides (ASO) and small interfering RNA (siRNA), have been extensively highlighted as potential drugs for treatment of various intractable diseases, including cancer (*1-3*). This is because they can regulate the expression of disease-related genes with high target sequence specificity. However, the arrival rate of exogenous nucleic acids from the injected site to the target cell cytoplasm or nucleus, *i.e.*, bioavailability, is substantially low, mainly due to their high susceptibility to enzymatic degradation, and negatively charged macromolecular structures that impede passive diffusion into the cytoplasm across the cell membrane. These obstacles have hampered the translation of nucleic acid-based drugs into pharmaceutical products.

To overcome the poor bioavailability of nucleic acids, various methodologies have been explored. Chemical modifications of the nucleotide backbone are one of the most typical approaches for stabilization of nucleic acids in biological fluids with reduced immune responses (*2*). Indeed, the clinically approved ASOs, fomivirsen and mipomersen, are composed of a phosphorothioate backbone, and the approved RNA aptamer, pegaptanib, contains 2'-F and 2'-O-methyl modifications (*2*). These backbone modifications not only protect nucleic acids from enzymatic degradation, but also affect their biodistribution and cellular uptake profiles. For instance, phosphorothioate-modified ASOs are reported to bind to plasma proteins in the bloodstream, leading to enhanced accumulation in the liver (*4*).

A more direct approach for improving the biodistribution and cellular uptake profiles of nucleic acids is to combine them with delivery molecules. Of these, the simplest formulation is a nucleic acid conjugated to a ligand molecule that can bind to a specific molecule (or receptor) on the target cell surface (Figure 1A) (*5*). One of the most successful examples is siRNA conjugated with *N*-acetyl-D-galactosamine (GalNAc), which targets the asialoglycoprotein receptor (ASGPR) expressed on the hepatocyte surface (*6*). This formulation is undergoing a phase III clinical trial (*3*). Another major formulation is poly(ethylene glycol) (PEG)-coated (PEGylated) nanoparticles (Figure 1B), which can be fabricated by the self-assembly of negatively charged nucleic acids and cationic lipids or polycations bearing PEG chains (*7,8*). In this formulation, the nanoparticle core can protect nucleic acid payloads from enzymatic degradation and the

Released online in J-STAGE as advance publication October 17, 2016.

*Address correspondence to:
Dr. Kanjiro Miyata, Department of Materials Engineering, Graduate School of Engineering, The University of Tokyo, 7-3-1 Hongo, Bunkyo-ku, Tokyo 113-8656, Japan.
E-mail: miyata@bmw.t.u-tokyo.ac.jp

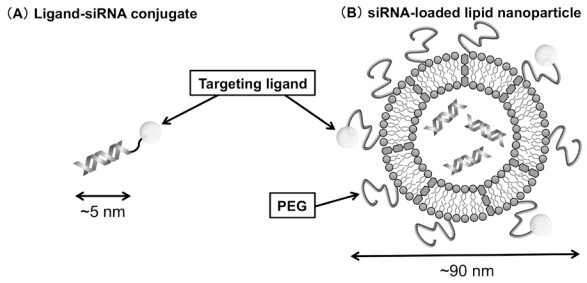

Figure 1. Examples of nucleic acid delivery formulations. (A) Ligand-siRNA conjugate and **(B)** siRNA-loaded PEGylated lipid nanoparticle.

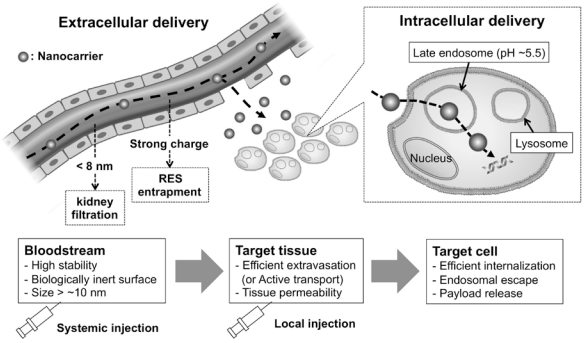

Figure 2. Schematic illustration of nucleic acid delivery and its biological barriers.

PEG shell can suppress nonspecific protein adsorption through the steric repulsion effect, permitting the longevity of nucleic acids in harsh *in vivo* conditions. Notably, PEGylated nanoparticles with a size of several tens of nanometers can preferentially accumulate in solid tumors through leaky tumor vasculature, which is termed the enhanced permeability and retention (EPR) effect (*9,10*), following systemic administration. Indeed, several formulations of anticancer drug-loaded PEGylated nanoparticles are clinically approved or undergoing clinical trials (*11-13*). It should be also noted that targeting ligand molecules can be installed onto the surface (or the PEG terminus) of PEGylated nanoparticles, generating a multivalent binding effect for enhanced target recognition (*8,11*).

Among the structural components of PEGylated nanoparticles, block copolymers comprising PEG and polycation segments are highly appealing because they can be readily functionalized by chemical modification to create multifunctional polymeric nanocarriers (*7,14*). In particular, biological environment-responsive chemistries, including redox potential- and pH-sensitive linkages, enable block copolymers to generate "smart" polymeric nanocarriers that can exhibit the desired delivery functions, such as reversible stability, targeting ability, and endosome-escaping ability, in response to a specific biological environment or signal. The present review describes the design of smart polymeric nanocarriers and recent progress toward systemic nucleic acid delivery mainly to solid tumors.

2. Biological barriers in nucleic acid delivery

Prior to the structural design of block copolymers, this chapter describes the biological barriers to nucleic acid delivery, as well as the prerequisites for nucleic acid-loaded nanocarriers. As illustrated in Figure 2, nucleic acid delivery is divided into two major stages: to the extracellular milieu, and into the intracellular compartment. In the case of systemic administration, nanocarriers need to stably circulate in the bloodstream without disintegration or distribution into non-target organs/tissues. It is known that relatively small macromolecules (or nanocarriers) with a molecular weight (MW) of less than ~40,000 (or a diameter of less than ~8 nm), *e.g.*, naked ASO and siRNA, are rapidly cleared from the bloodstream *via* renal excretion (*15,16*). On the other hand, strongly charged larger macromolecules (or nanoparticles) are more likely to be entrapped by the reticuloendothelial system (RES) *via* nonspecific protein adsorption, leading to their clearance from the blood (*7*). Thus, nanocarriers ideally have a size of over ~10 nm with a nonionic and hydrophilic (or biologically inert) surface, *i.e.*, a PEG shell, to maintain longevity in the bloodstream.

At the target organ/tissue, nanocarriers need to extravasate from the bloodstream. In the case of solid tumors (or inflammatory tissues), the vascular pores are relatively large with sizes of > 100 nm, allowing nanocarriers with a size of < 100 nm to extravasate toward the tumor tissue. This is known as the EPR effect (*9,10*). Meanwhile, the size of vascular pores in healthy organs/tissues, except for the liver and spleen, is less than 10 nm, and thus, active transport mechanisms, *e.g.*, transcytosis, may be required for nanocarriers targeting healthy organs/tissues with smaller vascular pores. After extravasation or in the case of local administration, nanocarriers need to deeply permeate the target tissue to access a wide range of target cells. Tumor tissue permeability of nanocarriers is substantially affected by tumor heterogeneity or histological characteristics (*17,18*). When a series of anticancer drug-loaded nanocarriers with varying sizes of 30, 50, 70, and 100 nm were intravenously administered into subcutaneous tumor-bearing mice, their tumor accumulation profiles were dramatically altered according to the tumor model. In the case of a hypervascular colon (C26) tumor model, all the nanocarriers showed similar, efficient tumor accumulation (~10% dose/g tissue) (Figure 3A) (*18*). In contrast, in the case of a thick fibrotic, hypovascular pancreatic (BxPC3) tumor model, the smaller nanocarriers more efficiently accumulated in the tumor tissue, compared with the larger ones, associated with

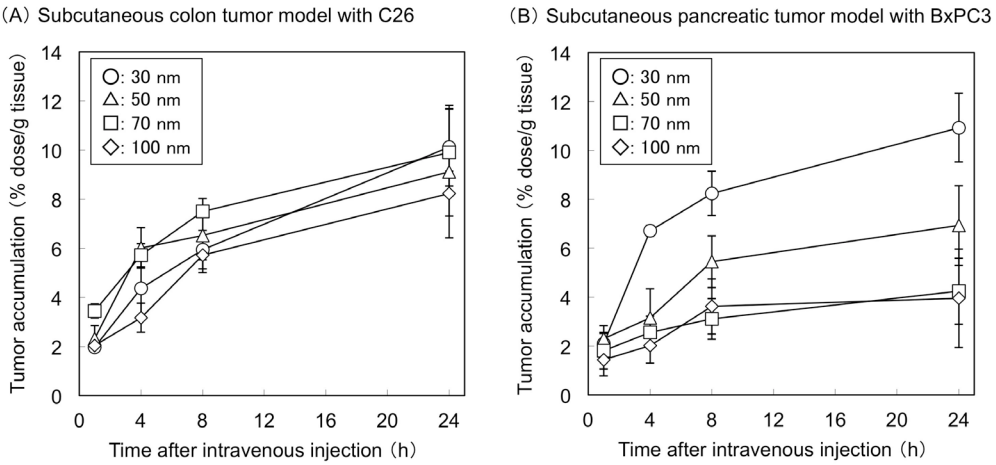

Figure 3. Tumor accumulation profiles of anticancer drug-loaded polymeric micelles after systemic administration. The polymeric micelles were prepared from a platinum anticancer drug, 1,2-diaminocyclohexane-platinum(II), and a mixture of PEG-poly(glutamic acid)/homo-poly(glutamic acid) to produce varying hydrodynamic diameters. A subcutaneous tumor model was developed using a colon cancer cell line, C26 **(A)**, and a pancreatic cancer cell line, BxPC3 **(B)**. These results were originally reported in reference 18.

an apparent size threshold of ~50 nm (Figure 3B) (*18*). These results strongly suggest that smaller nanocarriers with a size of < 50 nm are more suitable for deep permeation within heterogenous tumor environments.

After reaching the target cells, nanocarriers need to migrate to the cytoplasm (or nucleus) by overcoming cellular barriers, namely the cytoplasmic membrane and the endosomal membrane (and nuclear membrane if the target site is the nucleus). Nanocarriers are generally uptaken by cells *via* adsorptive endocytosis (*4,14*). Thus, stronger binding affinity to the target cellular surface is likely to result in more efficient cellular internalization of nanocarriers. However, a stronger binding ability conflicts with the biological inertness derived from the PEG shell that allows for avoiding RES entrapment as well as nonspecific protein adsorption. To overcome this conflicting issue, the so-called PEG dilemma, the PEG shell can be further modified with a targeting ligand molecule for more specific binding, as aforementioned. Otherwise, the PEG shell can be designed to disintegrate from the nanocarrier by utilizing cleavable linkages at the target site. After endocytosis, nanocarriers are generally subjected to endosomal sorting toward lysosomal digestion, and thus, they must escape from the endosomal compartment into the cytoplasm, where the nucleic acid payloads must be released from the nanocarrier to access the gene silencing machinery, hybridize with the complementary messenger RNA, or form the RNA-induced silencing complex (RISC).

3. Design of block copolymers for nucleic acid delivery

This chapter describes the design of block copolymers for construction of smart polymeric nanocarriers, especially for systemic siRNA delivery to solid tumors. The first section focuses on the basic properties of polymeric nanocarriers prepared with PEG-polycation block copolymers. The following sections highlight the functionalization of block copolymers to improve the delivery of polymeric nanocarriers.

3.1. *Basics of block copolymer self-assembly*

When PEG-polycation block copolymers are mixed with nucleic acids in aqueous solutions, they can spontaneously assemble into polyion complexes (PICs) through charge neutralization. This PIC formation can be explained by a two-step assembly process, as illustrated in Figure 4A (*19*). The primary step forms a minimal charge-neutralized polyion pair between a PEG-polycation and a nucleic acid, termed a unit PIC (uPIC). Above a critical association concentration (CAC), uPICs undergo secondary assembly into micellar PICs (mPICs). This two-step self-assembly is clearly demonstrated when single-strand RNA (ssRNA) (21-mer) is combined with PEG-poly(L-lysine) (PEG-PLys) (MW of PEG (MW_{PEG}): 12,000, degree of polymerization of PLys (DP_{PLys}): ~40) (Figure 4B) (*20*). At lower concentrations (< 0.01 mg/mL), the formation of small PICs with a hydrodynamic diameter (D_H) of ~10 nm is clearly observed, corresponding to the primary assembly step, *i.e.*, uPICs. In contrast, the D_H value is obviously increased at concentrations greater than 0.01 mg/mL, ultimately reaching ~40 nm. The transmission electron microscopic (TEM) image of PIC samples prepared at higher concentration displays the spherical nanoparticles (Figure 4C). These results demonstrate the formation of micelles from uPICs through the secondary assembly step. Meanwhile, a large difference is observed for double-strand RNA (21-mer/21-mer), *i.e.*, siRNA, which maintains the uPIC structure without progressing to secondary

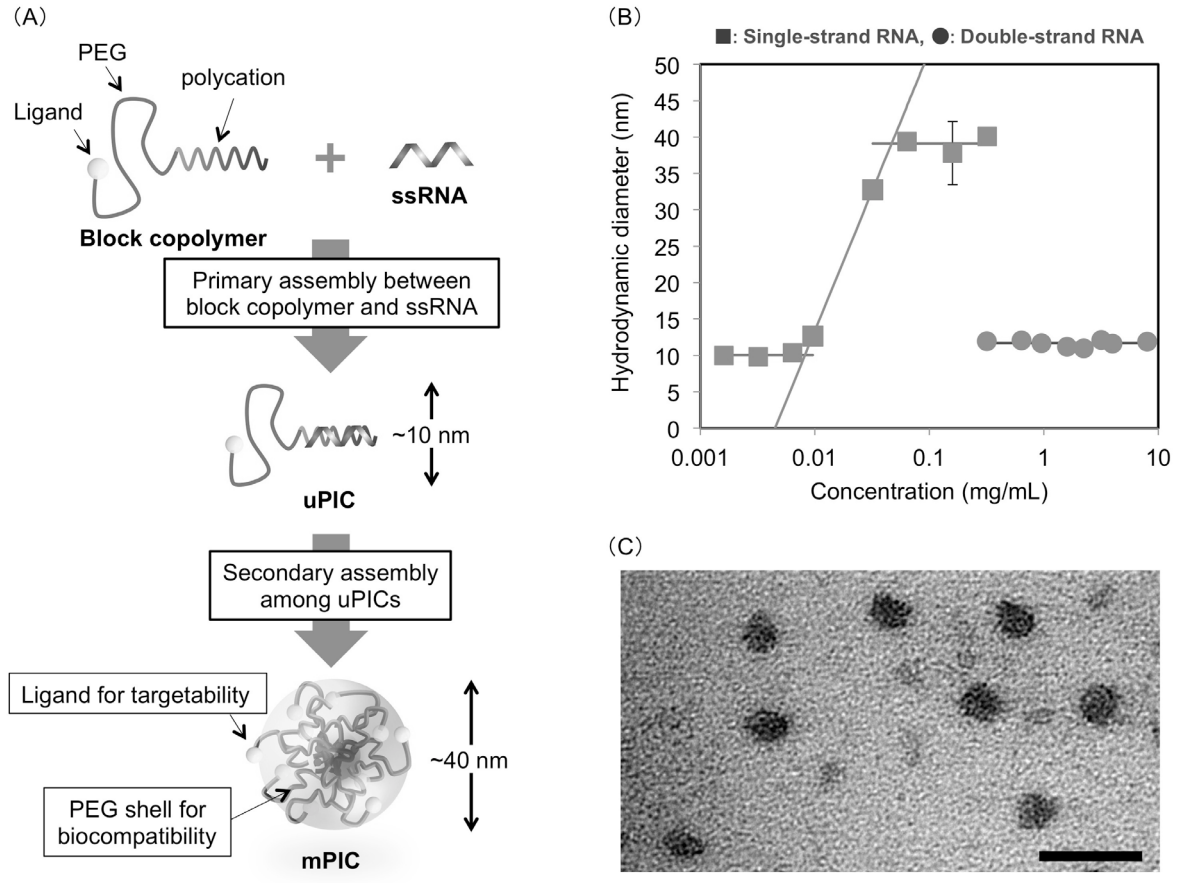

Figure 4. PIC formation between PEG-polycations and nucleic acids. (A) Schematic illustration of the two-step self-assembly from PEG-polycation and small nucleic acid. **(B)** Size of PIC samples prepared from PEG-PLys and ssRNA or siRNA at different concentrations. The hydrodynamic diameter was determined by fluorescence correlation spectroscopic analysis using fluorescently labeled RNA. **(C)** TEM image of the PIC sample prepared from PEG-PLys and ssRNA at a concentration of ~0.3 mg/mL. Scale bar indicates 50 nm. These results were originally reported in reference 20.

assembly even at much higher concentrations (Figure 4B). This difference may be explained by the difference in rigidity (or persistence length) between ssRNA and siRNA. siRNA has a persistence length of 60 nm, thereby being considered as having rigid cylindrical architecture. This rigidity potentially compromises the entropy gain that is associated with secondary assembly (or segregated core formation in a micelle), compared with flexible ssRNA with a persistence length of 1 nm, and hence inhibits mPIC formation. These results suggest that additional association forces of siRNA-loaded uPICs are crucial for construction of stable siRNA-loaded mPICs.

mPICs have a core-shell architecture, wherein the PEG shell comprises the biologically inert (or biocompatible) surface and can be further modified with ligand molecules for preferential accumulation in target tissues/cells (Figure 4A). The D_H of oligonucleotide-loaded mPICs prepared from PEG-PLys is reported to range from 40 to 80 nm with a narrow size-distribution (polydispersity index in dynamic light scattering, $\mu_2/\Gamma^2 < 0.1$) (*21,22*). The smaller mPICs were constructed using PEG-PLys with shorter PLys segments, *e.g.*, DP_{PLys} = ~20 and ~40, whereas PEG-PLys with a longer PLys segment (DP_{PLys} = ~80) generated the larger mPICs (*20,22*). Thus, the smaller mPICs are potentially highly efficient for permeation within solid tumor tissues, in contrast with lipid nanoparticles with a D_H of ~90 nm (*23*).

To fabricate more stable mPICs, the polycation segment in block copolymers can be modified with stabilizing units. In PEG-PLys, the modification of primary amines in the PLys segment with a guanidino group significantly enhances the stability of siRNA-loaded mPICs, possibly due to the hydrogen bonding (*24*). Additionally, hydrophobic groups, such as cholesteryl groups and stearoyl groups, or hydrophobic polymer segments, can be introduced into the side chains or the ω-end of the polycation segment in block copolymers for stabilization of the mPIC through hydrophobic interactions (Figure 5) (*25-27*). Conversely, hydrophobic modifications can also be applied to nucleic acids instead of the polycation segment; cholesterol-modified siRNA allowed for preparation of more stable mPICs compared with non-modified siRNA (*28*). As another stabilizing approach, mPICs can be coated with an additional outer layer, such as silica gel, which is readily prepared by simply mixing mPICs with silicate ions (*29*).

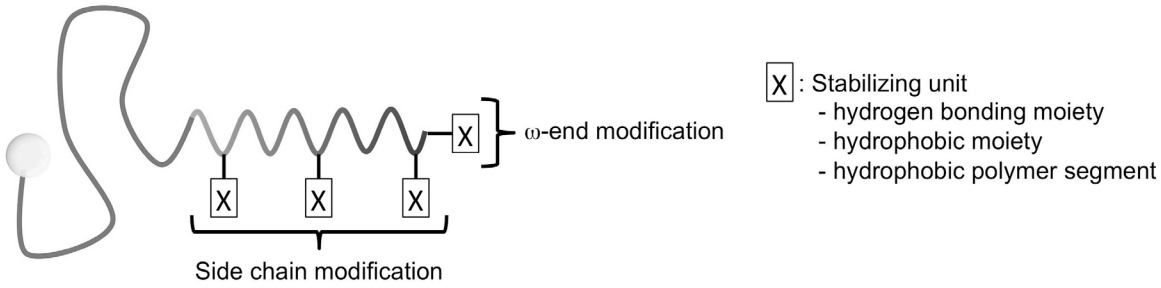

Figure 5. Modification sites of block copolymers for preparation of stable mPICs.

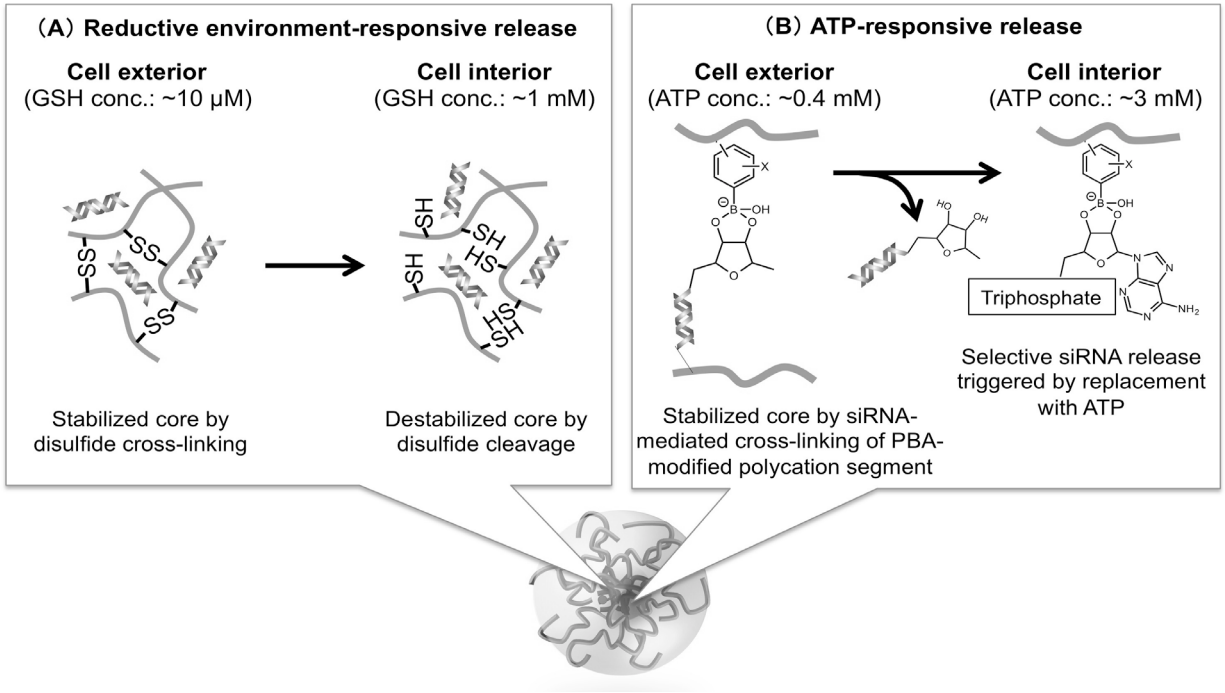

Figure 6. Design of smart polymeric nanocarriers using environment-responsive block copolymers for programmed nucleic acid release. (A) Disulfide cross-linked mPICs that can be destabilized in response to intracellular reductive conditions. **(B)** PBA-functionalized mPICs where siRNA can be released by replacement with intracellular ATP.

3.2. *Polymer design for reversible stability*

Whereas nanocarriers need to stably encapsulate nucleic acid payloads in extracellular milieu, they must ultimately release the payloads for effective gene silencing at the target site of action. To fulfill this apparently conflicting demand, block copolymers and their polymeric nanocarriers can be functionalized by environment-responsive chemistry for reversible stability or programmed payload release. Among various biological parameters, redox potential and pH have been most extensively utilized to trigger an environmental response from block copolymers because their levels are drastically altered between the interior and exterior of the cell. The cytoplasm is known to be a reductive environment, as the concentration of reduced glutathione (GSH), which acts as a reductive agent in the body, is three orders of magnitude higher in the cytoplasm compared with the extracellular milieu (*30*). Accordingly, reductive environment-responsive disulfide bonds can be utilized for stabilization of mPICs by cross-linking the polycation segments (*24,28,31-36*). In this way, the disulfide cross-linked mPICs can be stabilized in non-reductive conditions, while they are destabilized through the cleavage of disulfide bonds in reductive conditions, resulting in accelerated payload release in the cytoplasm (Figure 6A). Similarly, the pH in the late endosome (pH ~5.5) is known to be significantly lower than pH in the extracellular milieu (pH 7.4) and the cytoplasm (pH 7.2) (*37*). Therefore, cross-linking *via* acid-labile bonds, such as an acetal group (*38*), is also useful for the fabrication of acidic pH-responsive nanocarriers that can preferentially release payloads within the late endosome.

Although previous studies have reported a certain extent of stabilization from disulfide cross-linking, the stability of siRNA-loaded mPICs in the bloodstream

still requires improvement, as the blood half-life is reported to be ~10 min (*33,34*). This limitation in the longevity of siRNA-loaded mPICs may be due to significant leakage of siRNA payloads from the cross-linked polycation network in the mPIC. This leakage hypothesis is supported by fairly high stability of the mPICs, with cross-links formed between polycation and polyanion segments, allowing for a blood half-life of ~5 h (*39*). This fact suggests that direct conjugation of siRNA with the polycation segment *via* reversible linkages may be a promising strategy for increasing the longevity of mPICs in the bloodstream. To this end, a previous study highlights the characteristic moiety of siRNA, namely the *cis*-diol in the ribose ring at the 3' end of siRNA. The *cis*-diol group can make a reversible ester bond with tetravalent phenylboronic acid (PBA) groups. Accordingly, siRNA with *cis*-diol groups can act as a cross-linker between PBA-modified polycation segments through phenylboronic ester bonding, thereby generating the siRNA-mediated cross-linked mPICs (Figure 6B). Notably, this phenylboronic ester bond can be replaced with the *cis*-diol group contained in adenosine triphosphate (ATP) in a concentration-dependent manner (*40*). Particularly, whereas the mPICs cross-linked with siRNA were stable at low ATP concentrations of < 1 mM, high ATP concentrations of > 2 mM dramatically accelerated siRNA release from the mPICs. Considering that the extracellular and intracellular ATP concentrations are ~0.4 mM and 3 mM, respectively (*41*), these siRNA-mediated cross-linked mPICs are expected to selectively release the siRNA payloads in the intracellular compartment (Figure 6B), which is currently under investigation. On the other hand, the siRNA-mediated cross-linked mPICs achieved a blood half-life of > 60 min (unpublished data), demonstrating the strong potential of direct conjugation of nucleic acids to polycation segments for increasing the longevity of polymeric nanocarriers in the bloodstream.

3.3. *Polymer design for active targeting and facilitating cellular uptake*

After extravasation from the vessel into the target tissue, nanocarriers should ideally enter the target cells efficiently. In this regard, the PEG shell of mPICs significantly suppresses their cellular internalization through the steric repulsion effect (PEG dilemma). One of the most promising approaches to overcome this dilemma is active targeting using ligand molecules. Indeed, a variety of ligand molecules, including GalNAc, can be installed onto the nanocarrier surface, as reviewed elsewhere (*8,42*). In this way, multiple ligand-installed nanocarriers permit multivalent binding to target cellular surfaces for enhanced target recognition, which is in sharp contrast with the single ligand-mediated monovalent binding. As a representative ligand, transferrin (Tf), which is a glycoprotein with a MW of ~80 kDa, has been used as a cancer cell-targeting ligand over several decades (*43*) and has been clinically tested in the siRNA-loaded cyclodextrin nanoparticle (*44*). It should be noted that the Tf ligand is also available for active targeting to brain endothelial cells to elicit transcytosis toward the brain parenchyma across the blood-brain barrier (BBB) (*45*). In detail, the effect of Tf ligand density on nanoparticles was extensively examined for effective transcytosis across the BBB. Interestingly, the optimized ligand density (or avidity) was observed to cause accumulation of nanoparticles in the brain parenchyma, whereas nanoparticles with a higher density of ligands showed stronger binding to the brain endothelial cellular surface.

Peptide molecules that can be designed with a high selectivity are also promising ligand candidates. For example, a short peptide derived from rabies virus glycoprotein (RVG) (29-mer) is reported to enable the transvascular delivery of siRNA to the brain and specifically bind to the acetylcholine receptor overexpressed on the neuronal cell surface (*46*). In addition, the cyclic RGD (arginine-glycine-aspartic acid) peptide (cRGD) has been extensively tested for active targeting of $\alpha_v\beta_3$ and $\alpha_v\beta_5$ integrins overexpressed on the surface of various cancer cells and cancer-related endothelial cells (*47-49*). cRGD-installed mPICs are demonstrated to more efficiently accumulate in subcutaneous tumor models, *i.e.*, $\alpha_v\beta_5$-overexpressing cervical cancer cells (HeLa and SiHa cells) and lung cancer cells (A549 cells), compared with non-ligand-installed mPICs. Ultimately, the cRGD-installed/siRNA-loaded mPICs achieved significant antitumor activity against these tumor models by intravenously delivering therapeutic siRNAs targeted to vascular endothelial growth factor (VEGF) and its type-2 receptor (VEGF-R2) in the HeLa model (Figure 7A) (*34*), papilloma virus-derived oncogene E6/E7 in the SiHa model (Figure 7B) (*36*), and polo-like kinase 1 (PLK1) in the A549 model (Figure 7C) (*26*), associated with sequence-specific gene silencing in the tumor tissues.

An additional important feature of ligand-mediated active targeting is the critical effect of the range of ligand motion on multivalent binding. Although multiple ligand-installed mPICs have a large capacity for multivalent binding to the target molecules, a high density of PEG chains reduces their mobility, as well as the range of ligand motion, because of the steric repulsive (or crowding) effect derived from neighboring PEG chains (Figure 8A). This reduction in the PEG mobility and ligand motion makes it difficult to generate effective multivalent binding to target molecules. As an alternative, cocktail PEGylation of nanoparticles with ligand-installed longer PEG and non-ligand-installed shorter PEG demonstrated dramatically enhanced affinity to the target molecule-

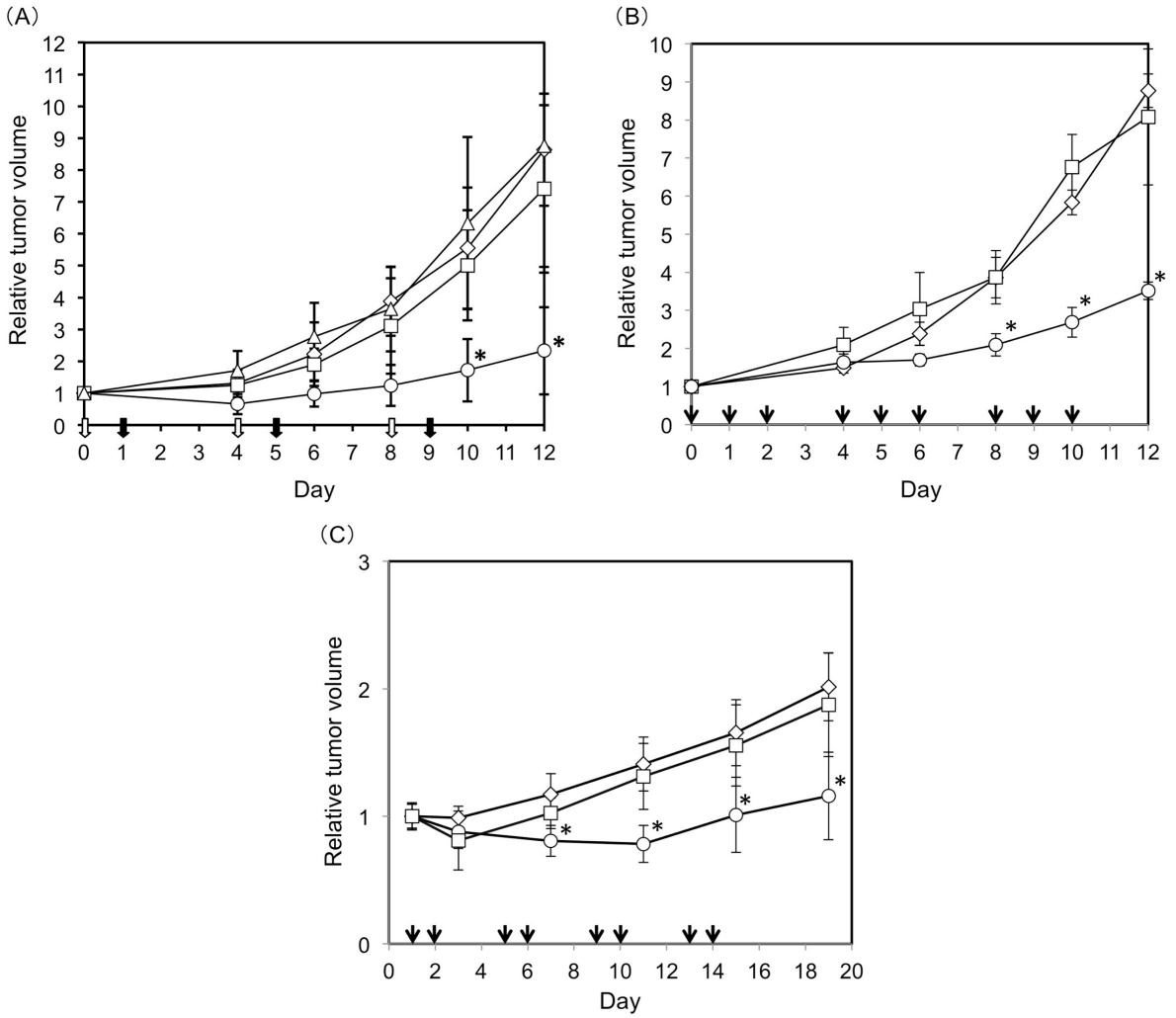

Figure 7. Antitumor activities of cRGD-installed/siRNA-loaded mPICs against subcutaneous cancer models developed from HeLa cells (A), SiHa cells (B), and A549 cells (C). siRNA-loaded mPICs were intravenously injected into the tail vein of tumor-bearing mice (~25 μg siRNA/mouse/shot) on the designated day as indicated by arrows. Open diamond: buffer-treated controls, open square: cRGD-installed/non-therapeutic control siRNA-loaded mPIC-treated mice, open triangle: non-cRGD-installed/therapeutic siRNA-loaded mPIC-treated mice, and open circle: cRGD-installed/therapeutic siRNA-loaded mPIC-treated mice. Therapeutic siRNAs were designed for targeting human VEGF (white arrow) and mouse VEGF-R2 (black arrow) **(A)**, papilloma virus-derived E6/E7 **(B)**, and human PLK1 **(C)**. *$p < 0.05$ for buffer-treated control. These results **(A)**, **(B)**, and **(C)** were originally reported in references 34, 36, and 26, respectively.

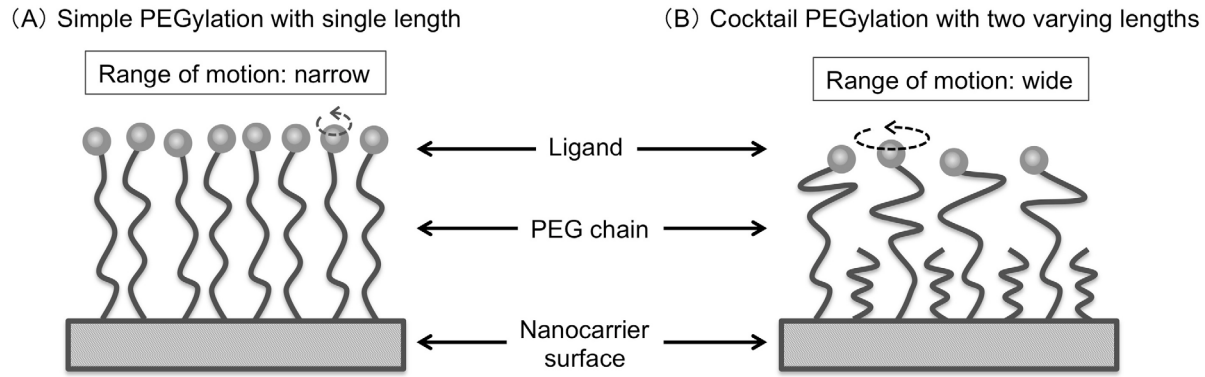

Figure 8. Design of ligand-installed PEGylated nanocarriers for enhanced target recognition. (A) Nanocarrier surface decorated with a single length of PEG, where the range of ligand motion is narrow due to the steric repulsive effect derived from neighboring PEG chains. **(B)** Enlarged range of ligand motion by cocktail PEGylation using ligand-installed longer PEG, and non-ligand-installed shorter PEG as a filler molecule.

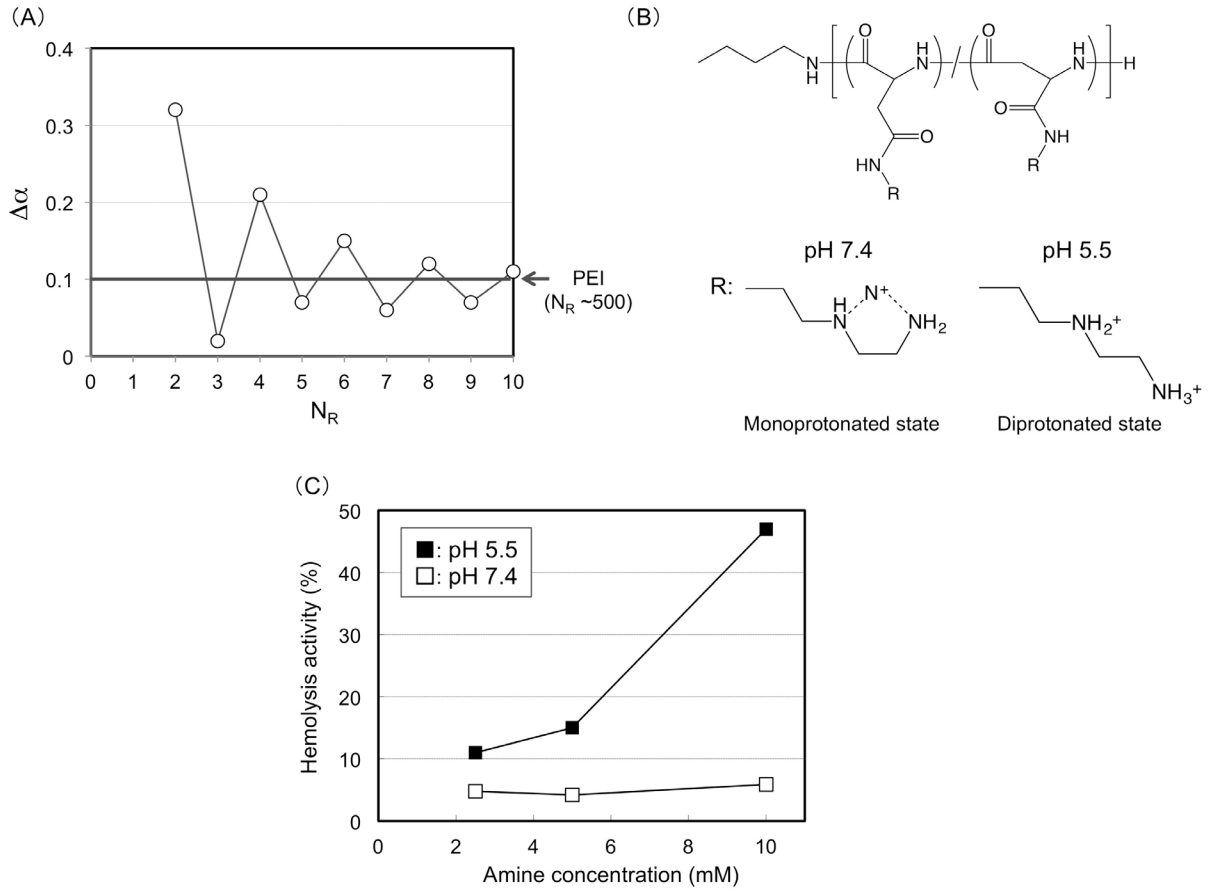

Figure 9. Acidic pH-responsiveness of aminoethylene units and PAsp(DET). (A) Relationship between the repeating number of aminoethylene units (N_R) and change in the protonation degree between pH 7.4 and 5.5 (Δα). **(B)** Protonated structures of PAsp(DET) at pH 7.4 and 5.5. **(C)** Erythrocyte hemolysis activity of PAsp(DET) determined at pH 7.4 and pH 5.5 plotted against amine concentration. This result was originally reported in reference 59.

immobilized surface, presumably due to the enlarged range of ligand motion (or mobility of PEG chains) produced by the spacer effect of shorter PEG fillers for effective multivalent binding (Figure 8B) (*50*).

3.4. *Polymer design for endosomal escape*

Once nucleic acid-loaded nanocarriers are endocytosed by cells, they generally undergo endosomal sorting and ultimately lysosomal degradation. Thus, endosomal escape toward the cytoplasm has been a much-discussed issue in nucleic acid delivery. For enabling endosomal escape of nanocarriers, a major approach is endosomal membrane disruption (or destabilization) using membrane-disrupting polycations or peptides. One of the most widely used polycations is polyethylenimine (PEI). PEI contains low pKa amines, which can protonate in response to the endosomal acidic pH of ~5.5 (*51*). This amine protonation is hypothesized to induce the influx of protons and chloride ions into the endosomal compartment, resulting in increased osmotic pressure and ultimately endosome disruption. This is termed the proton sponge effect (*52,53*). Concurrently, amine protonation provides PEI with greater cationic charge, allowing for stronger binding to the negatively charged endosomal membrane and facilitating destabilization (*14,53*).

On the other hand, the considerable cytotoxicity of PEI is always a matter of debate around its pharmaceutical application, and thus, many researchers have focused on reducing its cytotoxicity. Generally, the cytotoxicity of polycations is elicited by cationic charges that allow for nonspecific binding to the cytoplasmic and/or mitochondrial membrane. Therefore, more cationic charges/higher cationic charge densities result in greater cytotoxicity (*14,54,55*). A typical approach to reduce cytotoxicity is the preparation of biodegradable polycations *via* intracellularly cleavable bonds, such as disulfide bonds and acid-labile bonds (*56,57*). Low toxicity oligoethylenimines with MW of ~2 kDa have been conjugated with each other *via* acid-labile imine linkers for preparation of biodegradable PEI, resulting in significantly reduced cytotoxicity associated with a high level of transfection efficiency (*56*). Another approach for preparation of low toxic endosome-disrupting polycations is the spatial rearrangement of cationic moieties on the polycation segment for controlled protonation behavior (or cationic charge density). The protonation behavior of the aminoethylene unit, $-NHCH_2CH_2-$, which is the repeating unit of PEI,

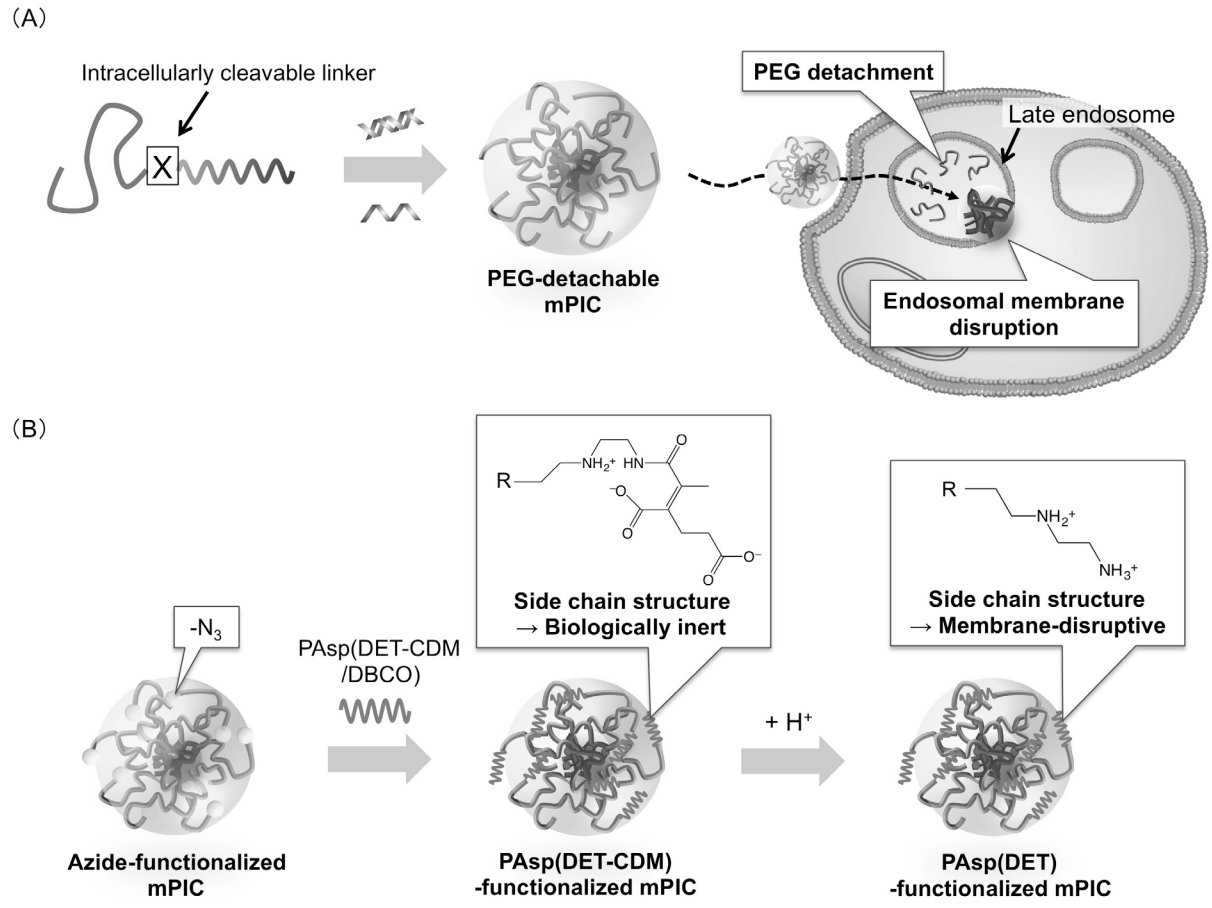

Figure 10. Design of smart polymeric nanocarriers for selective membrane disruption within the acidic endosomal compartment. (A) PEG-detachable mPICs prepared from PEG-polycation, where the PEG and the polycation are connected through intracellularly cleavable linkages, such as acid-labile bonds. **(B)** Surface-functionalized mPICs using the endosome-disrupting polymer that can become active toward the cell membrane after being unmasked at acidic pH.

is substantially altered by the repeat number (N_R); increase in N_R progressively reduces the change in the protonation degree ($\Delta\alpha$) of aminoethylene units between extracellular neutral pH and endosomal acidic pH with a simple harmonic motion (Figure 9A) (*14,58*). This finding suggests that the aminoethylene unit at N_R = 2 possesses higher endosomal pH-responsiveness, compared with the others. When the twice-repeated aminoethylene moieties were introduced into the side chain of polyaspartamide, the obtained polymer, termed PAsp(DET), maintained high $\Delta\alpha$ (= 0.31), which is significantly higher than that of PEI with a DP of ~500 ($\Delta\alpha$ = ~0.1) (*14,59*). In detail, the protonation state of side chains in PAsp(DET) is the monoprotonated state with a relatively low cationic charge density at neutral pH, which is distinctly converted to the diprotonated state at endosomal acidic pH (Figure 9B). Interestingly, this change in the protonated state of PAsp(DET) was associated with altered membrane disruption (or hemolysis) activity; hemolysis activity was negligible at neutral pH but dramatically elevated at endosomal acidic pH (Figure 9C), demonstrating acidic pH-responsive membrane disruptive functionality. Indeed, PAsp(DET) was confirmed to exhibit high transfection efficiency with much lower cytotoxicity, compared with PEI (*59*).

As expected, the PEG shell of mPICs considerably compromises endosomal membrane-disruptivity of polycations. Thus, biological environment-responsiveness is still required to render the nanocarrier surface biologically inert in the extracellular milieu but membrane-active within the endosome. One reasonable approach is PEG-detachable formulations, wherein the PEG segment and the polycation segment are connected *via* intracellularly cleavable bonds, *e.g.*, disulfide (-SS-) bonds and acid-labile bonds (Figure 10A) (*60,61*). In this way, systemic delivery of VEGF siRNA by mPICs prepared from PEG-SS-PAsp(DET) featuring stearoyl moieties in the PAsp(DET) side chains exhibits significant antitumor activity in a subcutaneous pancreatic (BxPC3) tumor model (*25*). Another sophisticated approach is the installation of endosome-disrupting polymers onto the mPIC surface (or PEG terminus). In this case, the polycations need additional chemical modifications to mask their cationic charges (or amines). A successful example of amine-masking is the use of amide linkages derived from maleic acid derivatives, including *cis*-aconitic acid and

carboxylated dimethyl maleic acid (CDM), which are relatively stable at neutral pH yet degradable at acidic pH, regenerating the parent amine moiety (Figure 10B) (*62-64*). The CDM-modified PAsp(DET) (PAsp(DET-CDM)) was successfully conjugated to the PEG terminus of mPIC through copper-free click chemistry between a dibenzocyclooctyne (DBCO) group and an azide group (Figure 10B) (*35*). The demasking of PAsp(DET-CDM) was verified by an increase in zeta-potential of mPICs at acidic pH, presumably due to the regeneration of cationic PAsp(DET) on the mPIC surface. Ultimately, the PAsp(DET-CDM)-installed mPICs achieved fairly high gene silencing activity in cultured cancer cells, compared with non-installed control mPICs.

4. Conclusion and perspectives

This review describes the design of polymeric nanocarriers and recent progress regarding their use in small nucleic acid delivery by highlighting methods to overcome biological barriers. To date, many published works have reported excellent therapeutic outcomes in animal disease models. Notably, multifunctional nanocarriers have elicited significant gene silencing mainly in solid tumors as well as the liver, demonstrating their promising therapeutic potential. Nevertheless, there are still limitations or gaps for translation into pharmaceutical products. One of the major reasons for disruption to translation is the limitation of animal disease models, some (or many) of which may not be good surrogates for human patients. Currently, this issue is being actively tackled by many researchers engaged in biology and drug delivery. The establishment of good surrogates can dramatically facilitate the pharmaceutical translation of oligonucleotide therapeutics.

Acknowledgements

The research described in this review was supported by the Center of Innovation (COI) program of the Japan Science and Technology Agency (JST), a Grant-in-Aid for scientific research (JSPS KAKENHI Grant number 25282141) from the Ministry of Education, Science, Sports, and Technology (MEXT), the Project for Development of Innovative Research on Cancer Therapeutics (P-DIRECT) and the Basic Science and Platform Technology Program for Innovative Biological Medicine from the Japan Agency for Medical Research and Development (AMED), and the Mochida Memorial Foundation for Medical and Pharmaceutical Research.

References

1. Burnett JC, Rossi JJ. RNA-based therapeutics: Current progress and future prospects. Chem Biol. 2012; 19:60-71.
2. Sharma VK, Sharma RK, Singh SK. Antisense oligonucleotides: Modifications and clinical trials. Med Chem Comm. 2014; 5:1454-1471.
3. Wittrup A, Lieberman J. Knocking down disease: A progress report on siRNA therapeutics. Nat Rev Genet. 2015; 16:543-552.
4. Juliano RL, Carver K. Cellular uptake and intracellular trafficking of oligonucleotides. Adv Drug Deliv Rev. 2015; 87:35-45.
5. Raouane M, Desmaele D, Urbinati G, Massaad-Massade L, Couvreur P. Lipid conjugated oligonucleotides: A useful strategy for delivery. Bioconjug Chem. 2012; 23:1091-1104.
6. Nair JK, Willoughby JLS, Chan A, *et al*. Multivalent N-acetylgalactosamine-conjugated siRNA localizes in hepatocytes and elicits robust RNAi-mediated gene silencing. J Am Chem Soc. 2014; 136:16958-16961.
7. Kataoka K, Harada A, Nagasaki Y. Block copolymer micelles for drug delivery: Design, characterization and biological significance. Adv Drug Deliv Rev. 2001; 47:113-131.
8. Kanasty R, Dorkin JR, Vegas A, Anderson D. Delivery materials for siRNA therapeutics. Nat Mater. 2013; 12:967-977.
9. Matsumura Y, Maeda H. A new concept for macromolecular therapeutics in cancer chemotherapy: Mechanism of tumoritropic accumulation of proteins and the antitumor agent Smancs. Cancer Res. 1986; 46:6387-6392.
10. Maeda H. Toward a full understanding of the EPR effect in primary and metastatic tumors as well as issues related to its heterogeneity. Adv Drug Deliv Rev. 2015; 91:3-6.
11. Davis ME, Chen Z, Shin DM. Nanoparticle therapeutics: An emerging treatment modality for cancer. Nat Rev Drug Discov. 2008; 7:771-782.
12. Duncan R, Vicent MJ. Polymer therapeutics-prospects for 21st century: The end of the beginning. Adv Drug Deliv Rev. 2013; 65:60-70.
13. Cabral H, Kataoka K. Progress of drug-loaded polymeric micelles into clinical studies. J Control Release. 2014; 190:465-476.
14. Miyata K, Nishiyama N, Kataoka K. Rational design of smart supramolecular assemblies for gene delivery: Chemical challenges in the creation of artificial viruses. Chem Soc Rev. 2012; 41:2562-2574.
15. Seymour LW, Duncan R, Strohalm J, Kopecek J. Effect of molecular weight of N-(2-hydroxypropyl) methacrylamide copolymers on body distribution and rate of excretion after subcutaneous, intraperitoneal, and intravenous administration to rats. J Biomed Mater Res. 1987; 21:1341-1358.
16. Choi HS, Liu W, Misra P, Tanaka E, Zimmer JP, Ipe BI, Bawendi MG, Frangioni JV. Renal clearance of quantum dots. Nat Biotechnol. 2007; 25:1165-1170.
17. Kano MR, Bae Y, Iwata C, Morishita Y, Yashiro M, Oka M, Fujii T, Komuro A, Kiyono K, Kaminishi M, Hirakawa K, Ouchi Y, Nishiyama N, Kataoka K, Miyazono K. Improvement of cancer-targeting therapy, using nanocarriers for intractable solid tumors by inhibition of TGF-β signaling. Proc Natl Acad Sci U S A. 2007; 104:3460-3465.
18. Cabral H, Matsumoto Y, Mizuno K, Chen Q, Murakami M, Kimura M, Terada Y, Kano MR, Miyazono K, Uesaka M, Nishiyama N, Kataoka K. Accumulation of sub-100 nm polymeric micelles in poorly permeable tumours depends on size. Nat Nanotechnol. 2011; 6:815-823.

19. Harada A, Kataoka K. Chain length recognition: Core-shell supramolecular assembly from oppositely charged block copolymers. Science. 1999; 283:65-67.
20. Hayashi K, Chaya H, Fukushima S, Watanabe S, Takemoto H, Osada K, Nishiyama N, Miyata K, Kataoka K. Influence of RNA strand rigidity on polyion complex formation with block catiomers. Macromol Rapid Commun. 2016; 37:486-493.
21. Kataoka K, Togawa H, Harada A, Yasugi K, Matsumoto T, Katayose S. Spontaneous formation of polyion complex micelles with narrow distribution from antisense oligonucleotide and cationic block copolymer in physiological saline. Macromolecules. 1996; 29:8556-8557.
22. Harada A, Togawa H, Kataoka K. Physicochemical properties and nuclease resistance of antisense oligodeoxynucleotides entrapped in the core of polyion complex micelles composed of poly(ethylene glycol)-poly(L-lysine) block copolymers. Eur J Pham Sci. 2001; 13:35-42.
23. Tabernero J, Shapiro GI, LoRusso PM, *et al*. First-in-humans trial of an RNA interference therapeutic targeting VEGF and KSP in cancer patients with liver involvement. Cancer Discov. 2013; 3:406-417.
24. Matsumoto S, Christie RJ, Nishiyama N, Miyata K, Ishii A, Oba M, Koyama H, Yamasaki Y, Kataoka K. Environment-responsive block copolymer micelles with a disulfide cross-linked core for enhanced siRNA delivery. Biomacromolecules. 2009; 10:119-127.
25. Kim HJ, Oba M, Pittella F, Nomoto T, Cabral H, Matsumoto Y, Miyata K, Nishiyama N, Kataoka K. PEG-detachable cationic polyaspartamide derivatives bearing stearoyl moieties for systemic siRNA delivery toward subcutaneous BxPC3 pancreatic tumor. J Drug Target. 2012; 20:33-42.
26. Kim HJ, Ishii T, Zheng M, Watanabe S, Toh K, Matsumoto Y, Nishiyama N, Miyata K, Kataoka K. Multifunctional polyion complex micelle featuring enhanced stability, targetability, and endosome escapability for systemic siRNA delivery to subcutaneous model of lung cancer. Drug Deliv Transl Res. 2014; 4:50-60.
27. Kim HJ, Miyata K, Nomoto T, Zheng M, Kim A, Liu X, Cabral H, Christie RJ, Nishiyama N, Kataoka K. siRNA delivery from triblock copolymer micelles with spatially-ordered compartments of PEG shell, siRNA-loaded intermediate layer, and hydrophobic core. Biomaterials 2014; 35:4548-4556.
28. Oe Y, Christie RJ, Naito M, Low SA, Fukushima S, Toh K, Miura Y, Matsumoto Y, Nishiyama N, Miyata K, Kataoka K. Actively-targeted polyion complex micelles stabilized by cholesterol and disulfide cross-linking for systemic delivery of siRNA to solid tumors. Biomaterials. 2014; 35:7887-7895.
29. Gouda N, Miyata K, Christie RJ, Suma T, Kishimura A, Fukushima S, Nomoto T, Liu X, Nishiyama N, Kataoka K. Silica nanogelling of environment-responsive PEGylated polyplexes for enhanced stability and intracellular delivery of siRNA. Biomaterials 2013; 34:562-570.
30. Saito G, Swanson JA, Lee KD. Drug delivery strategy utilizing conjugation *via* reversible disulfide linkages: Role and site of cellular reducing activities. Adv Drug Deliv Rev. 2003; 55:199-215.
31. Kakizawa Y, Harada A, Kataoka K. Environment-sensitive stabilization of core-shell structured polyion complex micelle by reversible cross-linking of the core through disulfide bond. J Am Chem Soc. 1999; 121:11247-11248.
32. Kakizawa Y, Harada A, Kataoka K. Glutathione-sensitive stabilization of block copolymer micelles composed of antisense DNA and thiolated poly(ethylene glycol)-*block*-poly(L-lysine): A potential carrier for systemic delivery of antisense DNA. Biomacromolecules. 2001; 2:491-497.
33. Christie RJ, Miyata K, Matsumoto Y, Nomoto T, Menasco D, Lai TC, Pennisi M, Osada K, Fukushima S, Nishiyama N, Yamasaki Y, Kataoka K. Effect of polymer structure on micelles formed between siRNA and cationic block copolymer comprising thiols and amidines. Biomacromolecules. 2011; 12:3174-3185.
34. Christie RJ, Matsumoto Y, Miyata K, Nomoto T, Fukushima S, Osada K, Halnaut J, Pittella F, Kim HJ, Nishiyama N, Kataoka K. Targeted polymeric micelles for siRNA treatment of experimental cancer by intravenous injection. ACS Nano. 2012; 6:5174-5189.
35. Tangsangasaksri M, Takemoto H, Naito M, Maeda Y, Sueyoshi D, Kim HJ, Miura Y, Ahn J, Azuma R, Nishiyama N, Miyata K, Kataoka K. siRNA-loaded polyion complex micelle decorated with charge-conversional polymer tuned to undergo stepwise response to intra-tumoral and intra-endosomal pHs for exerting enhanced RNAi efficacy. Biomacromolecules. 2016; 17:246-255.
36. Nishida H, Matsumoto Y, Kawana K, *et al*. Systemic delivery of siRNA by actively targeted polyion complex micelles for silencing the E6 and E7 human papillomavirus oncogenes. J Control Release. 2016; 231:29-37.
37. Pillay CS, Elliott E, Dennison C. Endolysosomal proteolysis and its regulation. Biochem J. 2002; 363:417-429.
38. Knorr V, Russ V, Allmendinger L, Ogris M, Wagner E. Acetal linked oligoethylenimines for use as pH-sensitive gene carriers. Bioconjug Chem. 2008; 19:1625-1634.
39. Anraku Y, Kishimura A, Kobayashi A, Oba M, Kataoka K. Size-controlled long-circulating PICsome as a ruler to measure critical cut-off disposition size into normal and tumor tissues. Chem Commun. 2011; 47:6054-6056.
40. Naito M, Ishii T, Matsumoto A, Miyata K, Miyahara Y, Kataoka K. A phenylboronate-functionalized polyion complex micelle for ATP-triggered release of siRNA. Angew Chem Int Ed Engl. 2012; 51:10751-10755.
41. Traut TW. Physiological concentrations of purines and pyrimidines. Mol Cell Biochem. 1994; 140:1-22.
42. Jeong JH, Kim SW, Park TG. Molecular design of functional polymers for gene therapy. Prog Polym Sci. 2007; 32:1239-1274.
43. Wagner E, Cotten M, Foisner R, Birnstiel ML. Transferrin-polycation-DNA complexes: The effect of polycations on the structure of the complex and DNA delivery to cells. Proc Natl Acad Sci U S A. 1991; 88:4255-4259.
44. Davis ME, Zuckerman JE, Choi CHJ, Seligson D, Tolcher A, Alabi CA, Yen Y, Heidel JD, Ribas A. Evidence of RNAi in humans from systemically administered siRNA *via* targeted nanoparticles. Nature. 2010; 464:1067-1070.
45. Wiley DT, Webster P, Gale A, Davis ME. Transcytosis and brain uptake of transferrin-containing nanoparticles

by tuning avidity to transferrin receptor. Proc Natl Acad Sci U S A. 2013; 110:8662-8667.
46. Kumar P, Wu H, McBride JL, Jung KE, Kim MH, Davidson BL, Lee SK, Shankar P, Manjunath N. Transvascular delivery of small interfering RNA to the central nervous system. Nature. 2007; 448:39-43.
47. Arap W, Pasqualini R, Ruoslahti E. Cancer treatment by targeted drug delivery to tumor vasculature in a mouse model. Science. 1998; 279:377-380.
48. Schiffelers RM, Ansari A, Xu J, Zhou Q, Tang Q, Storm G, Molema G, Lu PY, Scaria PV, Woodle MC. Cancer siRNA therapy by tumor selective delivery with ligand-targeted sterically stabilized nanoparticle. Nucleic Acids Res. 2004; 32:e149.
49. Shayakhmetov DM, Eberly AM, Li ZY, Lieber A. Deletion of penton RGD motifs affects the efficiency of both the internalization and the endosome escape of viral particles containing adenovirus serotype 5 or 35 fiber knobs. J Virol. 2005; 79:1053-1061.
50. Ishii T, Miyata K, Anraku Y, Naito M, Yi Y, Jinbo T, Takae S, Fukusato Y, Hori M, Osada K, Kataoka K. Enhanced target recognition of nanoparticles by cocktail PEGylation with chains of varying lengths. Chem Commun. 2016; 52:1517-1519.
51. Smits RG, Koper GJM, Mandel M. The influence of nearest- and next-nearest-neighbor interactions on the potentiometric titration of linear poly(ethylenimine). J Phys Chem. 1993; 97:5745-5751.
52. Boussif O, Lezoualch F, Zanta MA, Mergny MD, Scherman D, Demeneix B, Behr JP. A versatile vector for gene and oligonucleotide transfer into cells in culture and in-vivo – polyethylenimine. Proc Natl Acad Sci U S A. 1995; 92:7297-7301.
53. Neu M, Fischer D, Kissel T. Recent advances in rational gene transfer vector design based on poly(ethylene imine) and its derivatives. J Gene Med. 2005; 7:992-1009.
54. Fischer D, Li Y, Ahlemeyer B, Krieglstein J, Kissel T. *In vitro* cytotoxicity testing of polycations: Influence of polymer structure on cell viability and hemolysis. Biomaterials. 2003; 24:1121-1131.
55. Moghimi SM, Symonds P, Murray JC, Hunter AC, Debska G, Szewczyk A. A two-stage poly(ethylenimine)-mediated cytotoxicity: Implications for gene transfer/therapy. Mol Ther. 2005; 11:990-995.
56. Kim YH, Park JH, Lee M, Kim YH, Park TG, Kim SW. Polyethylenimine with acid-labile linkages as a biodegradable gene carrier. J Control Release. 2005; 103:209-219.
57. Lee Y, Mo H, Koo H, Park JY, Cho MY, Jin GW, Park JS. Visualization of the degradation of a disulfide polymer, linear poly(ethylenimine sulfide), for gene delivery. Bioconjug Chem. 2007; 18:13-18.
58. Miyata K, Christie RJ, Suma T, Takemoto H, Uchida H, Nishiyama N, Kataoka K. Fine-tuning of repeating aminoethylene units in poly(aspartamide) side chains for enhanced siRNA delivery. In: Tailored Polymer Architectures for Pharmaceutical and Biomedical Applications (Scholz C, Kressler J, eds.). American Chemical Society, USA, 2013; pp. 189-196.
59. Miyata K, Oba M, Nakanishi M, Fukushima S, Yamasaki Y, Koyama H, Nishiyama N, Kataoka K. Polyplexes from poly(aspartamide) bearing 1,2-diaminoethane side chains induce pH-selective, endosomal membrane destabilization with amplified transfection and negligible cytotoxicity. J Am Chem Soc. 2008; 130:16287-16294.
60. Walker GF, Fella C, Pelisek J, Fahrmeir J, Boeckle S, Ogris M, Wagner E. Toward synthetic viruses: Endosomal pH-triggered deshielding of targeted polyplexes greatly enhances gene transfer *in vitro* and *in vivo*. Mol Ther. 2005; 11:418-425.
61. Takae S, Miyata K, Oba M, Ishii T, Nishiyama N, Itaka K, Yamasaki Y, Koyama H, Kataoka K. PEG-detachable polyplex micelles based on disulfide-linked block catiomers as bioresponsive nonviral gene vectors. J Am Chem Soc. 2008; 130:6001-6009.
62. Rozema DB, Ekena K, Lewis DL, Loomis AG, Wolff JA. Endosomolysis by masking of a membrane-active agent (EMMA) for cytoplasmic release of macromolecules. Bioconjug Chem. 2003; 14:51-57.
63. Lee Y, Miyata K, Oba M, Ishii T, Fukushima S, Han M, Koyama H, Nishiyama N, Kataoka K. Charge-conversion ternary polyplex with endosome disruption moiety: A technique for efficient and safe gene delivery. Angew Chem Int Ed Engl. 2008; 47:5163-5166.
64. Maeda Y, Pittella F, Nomot T, Takemoto H, Nishiyama N, Miyata K, Kataoka K. Fine-tuning of charge-conversion polymer structure for efficient endosomal escape of siRNA-loaded calcium phosphate hybrid micelles. Macromol Rapid Commun. 2014; 35:1211-1215.

(Received September 14, 2016; Revised September 28, 2016; Accepted October 7, 2016)

Review

DOI: 10.5582/ddt.2016.01063

Gene delivery systems by the combination of lipid bubbles and ultrasound

Yoichi Negishi[2], Yoko Endo-Takahashi[2], Kazuo Maruyama[1,*]

[1] *Department of Drug and Gene Delivery Research, Faculty of Pharma-Sciences, Teikyo University, Itabashi, Tokyo, Japan;*
[2] *Department of Drug Delivery and Molecular Biopharmaceutics, School of Pharmacy, Tokyo University of Pharmacy and Life Sciences, Hachioji, Tokyo, Japan.*

Summary **Gene therapy is promising for the treatment of many diseases including cancers and genetic diseases. From the viewpoint of safety, ultrasound (US)-mediated gene delivery with nano/microbubbles was recently developed as a novel non-viral vector system. US-mediated gene delivery using nano/microbubbles are able to produce transient changes in the permeability of the cell membrane after US-induced cavitation while reducing cellular damage and enables the tissue-specific or the site-specific intracellular delivery of gene both *in vitro* and *in vivo*. We have recently developed novel lipid nanobubbles (Lipid Bubbles). These nanobubbles can also be used to enhance the efficacy of the US-mediated genes (plasmid DNA, siRNA, and miRNA *etc*.) delivery. In this review, we describe US-mediated delivery systems combined with nano/microbubbles and discuss their feasibility as non-viral vector systems.**

Keywords: Ultrasound, lipid bubbles, gene delivery, cavitation

1. Introduction

Gene therapy has potential for treating genetic diseases and cancer. Viral vector-directed gene transfers show high gene transfer efficiency but are deficient in several areas. For example, some viral vectors could randomly integrate DNA into host genomes, which poses potential risks, including neoplastic transformation (*1-3*). Delivery vectors that are highly efficient for gene transduction must also be safe and easy to use. Non-viral vectors have recently received attention as gene carriers, but their transduction efficiency is very low, although efforts have been made to address this (*4-6*). Towards this end, ultrasound (US) has been investigated for improving the efficiency of transgene delivery and holds promise as a means of generating a non-invasive gene delivery system.

US has been utilized as useful tool for *in vivo* imaging, destruction of renal calculus and treatment of fibroid. Recently, it was reported that US was proved to increase permeability of the plasma membrane and reduces the thickness of the unstirred layer of the cell surface, which encourage the DNA entry into cells (*7,8*). The first studies applying US for gene delivery used frequencies in the range of 20-50 kHz. However, these frequencies, along with cavitation, are also known induce tissue damage if not properly controlled. To improve this problem, many studies using therapeutic US for gene delivery, which operates at frequencies of 1-3 MHz, intensities of 0.5-2.5 W/cm^2 and pulse-mode have emerged. In addition, it has been reported that microbubbles, used as US contrast agents, play an important role in enhancing the efficiency of gene delivery without causing cell damage (*9*). In general, cell damage is dependent on the US intensity, the exposure time, the concentration of microbubbles, and the cell type, with US intensity and exposure time being particularly important. Therefore, effective US-mediated gene delivery requires optimization of the US exposure conditions (*10-13*). Some researchers studied about the cell damage by the disruption of microbubbles with US exposure (*14-19*).

Microbubbles are cavitated by exposure to US, generating microstreams or microjets which result in

Released online in J-STAGE as advance publication October 28, 2016.

*Address correspondence to:
Dr. Kazuo Maruyama, Department of Drug and Gene Delivery Research, Faculty of Pharma-Sciences, Teikyo University, 2-11-1 Kaga, Itabashi, Tokyo 173-8605, Japan.
E-mail: maruyama@pharm.teikyo-u.ac.jp

shear stress to cells and the generation of transient holes in the cell membrane (*20*). Since this approach can be used to deliver extracellular material such as genes into cells, microbubbles could facilitate US-mediated gene delivery. In addition, submicron-sized bubbles (nanobubbles), which are smaller than conventional microbubbles, were recently reported (*21,22*), and we have developed novel lipid nanobubbles (Lipid Bubbles) (*13,23-31*). These nanobubbles can also be used to enhance the efficiency of US-mediated gene delivery. In this review, we describe US-mediated delivery systems combined with nano/microbubbles and discuss their feasibility as non-viral vector systems.

2. Microbubbles and US

The behavior of microbubbles depends on the amplitude of the US used. Very low acoustic pressure (mechanical index (MI) < 0.05-0.1) induces linear oscillation of the microbubble, and the reflected frequency is equal to the transmitted frequency (Figure 1a). An increase in acoustic pressure (0.1 < MI < 0.3), referred to as low-power imaging, causes non-linear expansion and compression of the microbubble (Figure 1b). The bubble is somewhat more resistant to compression than to expansion, a phenomenon known as stable or non-inertial cavitation, and results in the emission of non-linear harmonic signals at multiples of the transmitted frequency (*32*). Harmonic imaging with microbubbles enhances the bubble-to-tissue backscatter signal ratio due to insignificant harmonic backscatter from tissue in this range of MI. Therefore, this technique can improve the signal-noise ratio and be useful in left ventricular pacification imaging (*33*). In addition, stable or non-inertial cavitation can enhance transient cell membrane permeability (Figure 2a) (*34*). Machluf *et al*. reported that the exposure of cells to US (0.16 MI, 1 MHz) in the presence of microbubbles resulted in the delivery of plasmid DNA (pDNA) into the cells (*35,36*).

Higher acoustic pressure (MI > 0.3-0.6) causes forced expansion and compression of the microbubble and results in bubble disruption (collapse) (Figure 1c). Bubble disruption by this inertial cavitation is utilized as flash-replenishment in reperfusion study of diagnosis (*37*). This inertial cavitation induces microstreams/microjets around the bubbles. These microstreams/microjets can enhance the permeability of the cell membrane due to the formation of transient pores (Figure 2b) (*20*). In the presence of nano-/microbubbles, the threshold for cavitation decreases, allowing the destruction of the microbubbles at lower US energies.

3. Lipid bubbles

As mentioned above, there are many important information for US-mediated gene delivery utilizing

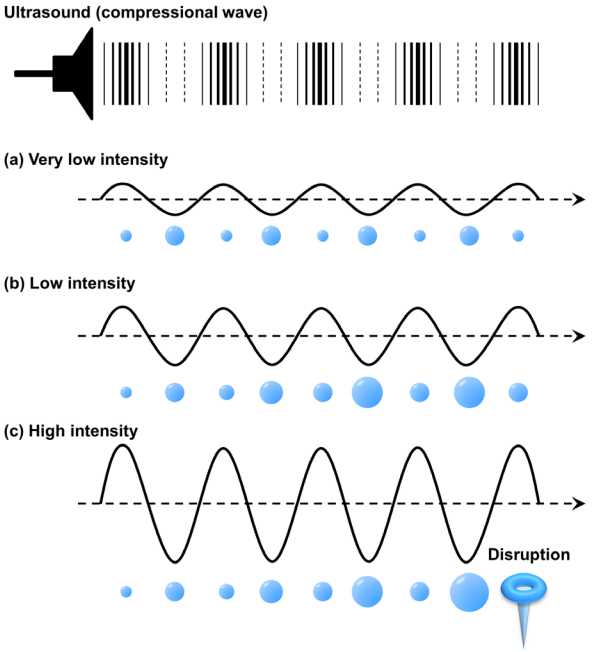

Figure 1. Schematics showing microbubble behavior in acoustic fields. (a) Very low intensity ultrasound induces linear oscillation of the microbubble. **(b)** Low intensity ultrasound induces oscillation of the microbubble, with a gradual increase in the diameter of the microbubble. Stable oscillation occurs when the microbubble reaches its resonant diameter. **(c)** High intensity ultrasound causes a rapid increase in the diameter of the microbubble for a few cycles, which induces bubble disruption.

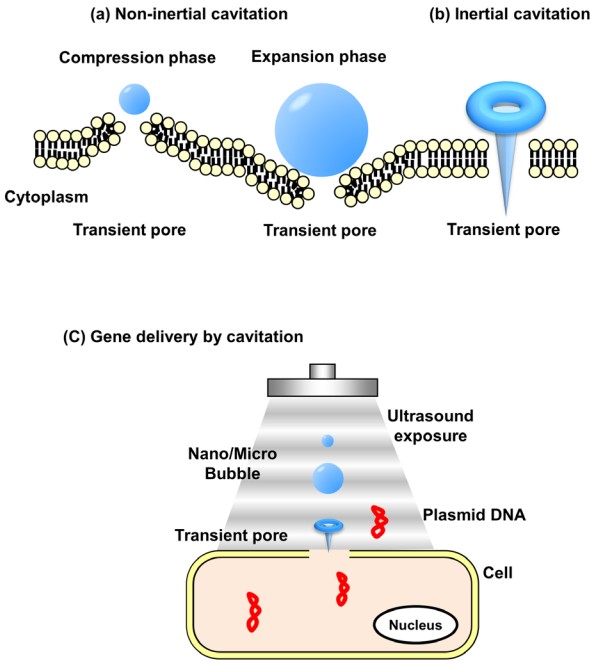

Figure 2. Schematics showing pore formation in the cell membrane by oscillating or disrupting microbubbles. (a) The pushing and pulling behavior (non-inertial cavitation) of microbubbles and **(b)** the collapse of microbubbles (inertial cavitation) rupturing the cell membrane and creating pores allowing trans-membrane flux of fluid and macromolecules such as plasmid DNA and oligonucleotides **(c)**.

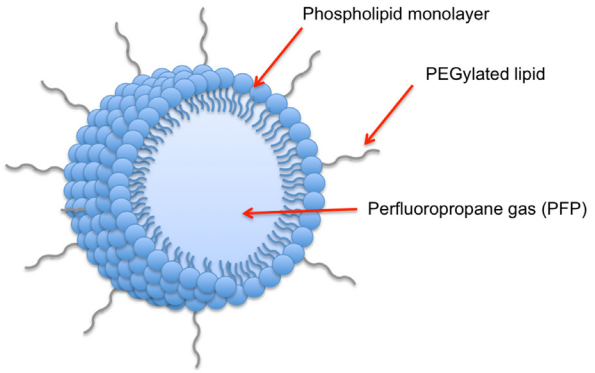

Figure 3. Illustration of a Lipid Bubble.

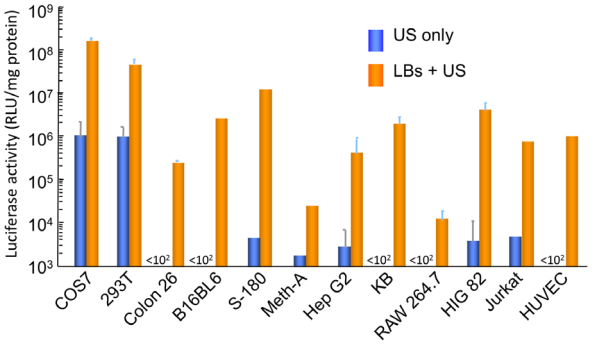

Figure 4. pDNA delivery with LBs and US *in vitro*. Luciferase activities in various types of cells transfected with LBs and US.

microbubbles. Microbubbles are contrast agents used in US imaging. Microbubbles can also be used to improve transfection efficiency when combined with US. Microbubbles are generally unstable and have a mean diameter of between 1-6 μm, making them too large for intravascular applications (*38*). Moreover, it is difficult to modify their surface with functional molecules. Therefore, microbubbles should be small and stable, and their surface should be easily modified with functional molecules for targeting.

Liposomes have several advantages as drug, antigen and gene delivery carriers as their size can be easily controlled, and they can be modified with targeting molecules. Therefore, we used liposome technology to develop novel lipid bubbles (LBs) containing the US gas, perfluoropropane (Figure 3). LBs are about 600-800 nm in diameter, making them smaller than Sonazoid® which is US contrast agent (about 2 μm).

4. *In vitro* pDNA delivery with LBs

We investigated *in vitro* whether the combination of LBs and US could provide a gene delivery tool. First, we attempted to transfect pDNA encoding firefly luciferase (pCMV-Luc) into COS-7 and 293T cells with LBs and US. Luciferase activity in COS-7 and 293T cells treated with LBs and US was higher than in cells treated with LBs or US alone (Figure 4). The gene expression efficiency was very high with the US exposure for 10 seconds though it was so short. We also confirmed that LBs could effectively deliver plasmid DNA into cells even for 1 second of US exposure (Data not shown). Thus, LBs were novel gene delivery tools that could instantaneously transfect extracellular plasmid DNA into cells. Heat and jet streams are generally induced with cavitation, which might damage cells. We therefore examined the effects of US on cells with or without LBs. Ultrasound did not damage COS-7 cells in the absence of LBs and only slightly affected the cells even when the amount of US was sufficient to induce cavitation of LBs. Though it was natural, we also confirmed that the cavitation induced with LBs did not damage plasmid DNA (data not shown).

Next, we demonstrated that LBs and US could be used to transfect pDNA into various cell lines such as Colon 26, B16BL6, S-180, Meth-A, Hep G2, KB cells, mouse macrophase-like cell line RAW 264.7 cells, Jurkat cells derived from T cell lines, and human umbilical vein endothelial cells (HUVEC) (Figure 4). Since it is difficult to transfect lymphocytes with pDNA using non-viral vectors, the combination of LBs and US hold promise as tools for gene transfection *in vitro*. Considering *in vivo* gene delivery with Bubble liposomes, it is necessary to deliver plasmid DNA into cells in presence of serum. Then, we examined about the effect of serum on gene delivery with LBs. Gene expression with LBs was not affected even in the presence of serum.

5. *In vivo* pDNA delivery with LBs

Cancer gene therapy requires the delivery of genes into tumor tissue with high efficiency, safety and minimal invasiveness. We attempted to deliver pDNA into tumor tissue using LBs and US. B6C3F1 tumor model mice were intradermally inoculated with OV-HM cells in the flank. After 7 days, a mixture of LBs (2.5 μg of lipid) and pCMV-Luc (10 μg) was injected into the tumor, then US (1 MHz, 0.7 W/cm^2, 1 min) was transdermally applied to the tumor tissue. Transfection efficiency using a conventional lipofection method was also investigated. Complexes of Lipofectamine 2000 (20 μg) and pCMV-Luc (10 μg) were injected into the tumors. Luciferase activity was measured two days after LBs with US or conventional transfection. Tumors treated with LBs and US showed higher luciferase activity compared to tumors treated with LBs or US alone, or with conventional lipofection. This result indicates that LBs and US can efficiently deliver pDNA into tumor tissue *in vivo*, and motivated us to examine whether LBs and US could be used for cancer gene therapy. Interleukin-12 (IL-12) exhibits immunomodulatory antitumor effects and is considered an effective antitumor agent (*39,40*), but its short

half-life and systemic toxicity following intravenous injection are major obstacles to its therapeutic use (*41,42*). Therefore, we transfected pDNA encoding the IL-12 gene (pCMV-IL-12) into tumor tissue using LBs and US with the aim of achieving high local expression of IL-12. When pCMV-IL-12 was transfected using LBs, US or Lipofectamine 2000, tumor growth was not suppressed. In contrast, transfection of pCMV-IL-12 with LBs and US suppressed tumor growth significantly (Figure 5). To investigate the mechanism behind the anti-tumor effects of pCMV-IL-12 transfected using LBs and US, we assessed the involvement of $CD4^+$ and $CD8^+$ T cells and NK cells. The depletion of $CD8^+$ T cells effectively blocked the anti-tumor effect of pCMV-IL-12 transfected using LBs and US. These results suggest that the combination of LBs and US can effectively induce sufficient IL-12 expression to cause anti-tumor immune responses.

Systemic gene delivery techniques are ideal for cancer therapy because they can deliver genes to tumors deep in the body. We confirmed that LBs act as US imaging agents for several minutes following intravascular administration. We attempted to deliver genes into tumor tissue using LBs and US by intravascular administration. S-180 cells were inoculated into the left footpad of ddY mice; after 4 days, 100 μL of pCMV-Luc (10 μg) and LBs (100 μg) were injected into the femoral artery and US (0.7 MHz, 1.2 W/cm^2, 2 min) was immediately applied transdermally to the tumor tissue. Transfection with LBs, US or Lipofectamine 2000 alone was also conducted. Two days following transfection, the luciferase activity of the tumor tissues was measured. The luciferase activity of tumors treated with LBs and US was higher than that of tumors treated with LBs, US, or Lipofectamine 2000, suggesting that LBs and US can efficiently deliver genes into tumor tissue following intravascular administration. Thus, LBs and US hold promise for cancer gene delivery by local or intravenous administration.

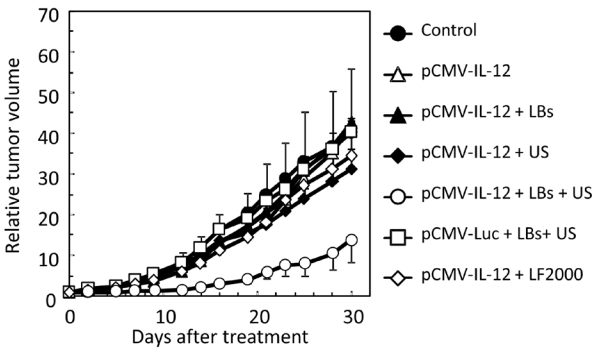

Figure 5. Antitumor effect of IL-12 gene delivery with LBs and US. Antitumor effect was evaluated by measuring tumor volume. BL: Lipid Bubbles, US: Ultrasound, LF2000: Lipofectamine 2000, pCMV-IL-12: pDNA encoding the IL-12 gene, pCMV-Luc: pDNA encoding the Luciferase gene.

6. *In vitro*/*In vivo* siRNA delivery with LBs

Small interfering RNA (siRNA) can silence specific gene expression. Therefore, siRNA is expected to be a novel therapeutic drug, however, efficient and robust delivery systems have been required for its clinical application. Recently, we have developed novel polyethyleneglycol modified liposomes (Lipid bubbles; LBs) entrapping an US (US) imaging gas, which can function as a gene delivery tool in the combination of US exposure. So, we tried to know the ability of LBs in the combination of US to deliver siRNA *in vitro* and *in vivo* (*23*). We first examined to transfect pDNA and siRNA into COS-7 cells. Cells were cotransfected with pDNA encoding firefly luciferase (pCMV-GL3) and a nontargeting control or luciferase-targeting siRNA (siCont or siGL3). The luciferase activity was downregulated even in the presence of a high serum concentration. This is in accordance with our previous data concerning pDNA delivery with LBs and US (*44*). These results might be owing to the mechanism of transfection enabling siRNA to be directly and instantaneously delivered into the cytoplasm. In fact, the intracellular localization of fluorescence labeling siRNA just behind the transfection was homogeneously dispersed, primarily in the cytoplasm. The intracellular localization of pDNA transfected with LBs and US also showed the same tendency. These results differed from an observation made regarding the endosomal pathway of the lipoplex. Furthermore, the gene-silencing efficiency of the transfected siRNA using LBs and US was independent of the culture conditions (4°C or 37°C) and the presence of an endosomolytic agent. Thus, endocytosis minimally participates in the transfection process with LBs and US and siRNA is able to be directly and instantaneously delivered into the cytoplasm. Recent studies have reported that siRNAs are capable of activating innate immunity in mammalian cells and the immune response was mainly caused *via* Toll-like receptors (TLRs) in the endosome (*44-46*). It may be possible that the transfection method with Lipid bubbles and US ignores the activation of an immune response *via* TLRs. Therefore, the combination method of LBs and US enabling siRNA delivery directly into the cytoplasm of target cells may be suitable for siRNA delivery.

When pDNA encoding luciferase and its siRNA were cotransfected into the muscles of mice using LBs and US, the suppression of luciferase expression was observed, and the effect persisted for up to 7 days, suggesting that LBs could also be a useful tool *in vivo*. Furthermore, when the siRNA targeted to the endogenous gene (GSK-3β) was transfected into the muscle using LBs and US, protein suppression could be observed in US exposed area. As a result, gene-silencing effect was also observed in the skin. In contrast, in kidney, gene-silencing effect was not observed and

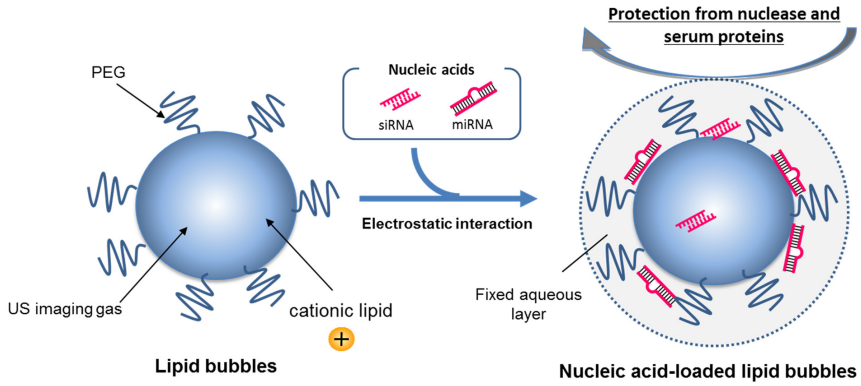

Figure 6. Scheme of nucleic acid-loaded lipid bubbles.

the luciferase expression was not even observed in the group not transfected with siRNA. These results were assumed to be due to the direct injection into the parenchymal tissue of kidney, the excretory organ of pDNA and siRNA (*47,48*). Therefore, by the application of intravascular administration or other methods suited for target tissue, LBs and US might be a useful tool for the delivery of siRNA into widespread tissue (*49*).

7. siRNA-loaded lipid bubbles

LBs as referred to above are composed neutral lipid; therefore, it is difficult to colocalize LBs in blood vessels after intravenous administration. In addition, if siRNA is delivered *via* systemic injection, it suffers from nuclease degradation, plasma protein interaction, and rapid removal from circulation, leading to a reduction in transfection efficiency *in vivo*. To solve these issues, we next tried to load siRNA to LBs by two methods in an attempt to make a more effective delivery tool for systemic injections (Figure 6).

7.1. *SiRNA-loaded LBs using the electrostatic interaction between cationic lipid and siRNA*

To load siRNA to LBs, cationic lipids are also useful because the lipids are able to interact with siRNA possessing negative electric charges. We initially attempted to prepare LBs containing 1,2-dioleoyl-3-trimethylammonium-propane (DOTAP), a cationic lipid often used for gene delivery (*50*). This LBs was composed of DPPC, DOTAP, PEG2000, and PEG750 in a 79:15:3:3 (molar ratio). Using a high-frequency US imaging system, we confirmed that LBs containing DOTAP could function as an echo-contrast reagent (*51*). By flow cytometry, we also confirmed that siRNA could interact with LBs, the interaction was due to the cationic charge of DOTAP, and LBs containing DOTAP, PEG_{750}, and PEG_{2000} could be loaded with much more siRNA compared to that of LBs containing DOTAP and PEG_{2000}. We considered that the structural changes in the PEG chain by the presence of both short and long PEG chains facilitated interaction between the cationic lipid and anionic siRNA. These results suggested that siRNA could be loaded not only by the electrostatic interaction but also by the fixed aqueous layer formed with PEG. We also showed that siRNA held by LBs showed increased stability in 50% serum compared with free siRNA. We next attempted to transfect siRNA to cells previously transfected luciferase gene using si-LBs and US exposure. The gene-silencing effect of siRNA was comparable to those of siRNA transfected using conventional LBs and US. Therefore, it appears that the exposure to US induced cavitation, the release of siRNA from LBs, and the delivery of siRNA into the cytoplasm. The siRNA could be bound to only outside of LBs containing cationic lipids; therefore, the loadable amount of siRNA might be fewer than that by chol-si-LBs. However, the preparation method of si-LBs was easier than that of chol-si-LBs, and si-LBs had the advantage because there was no need to reprepare LBs whenever siRNA was changed. For these reasons, LBs containing DOTAP could be a convenient siRNA carrier. Furthermore, LBs containing cationic lipid are expected to have widespread application to delivery tools of various molecules possessing negative electric charges. Indeed, we showed that LBs containing DOTAP were also useful delivery tool of pDNA *in vitro* and *in vivo* study (*50,51*). It is known that short-chain and unsaturated fatty acids increase membrane fluidity (*52*). DOTAP is unsaturated fatty acid and is thought to destabilize the membrane of LBs. In fact, the increased DOTAP content made it difficult to entrap the gas (*9*). We therefore expected that LBs using other saturated cationic lipids would improve the stability of the liposomal membrane. Indeed, LBs containing other three types of saturated cationic lipids (DSTAP, DSDAP, DDAB) were more effective as a contrast agent compared to LBs containing DOTAP (*53*). Especially, LBs containing DSDAP could work well in the US imaging ability and transfection efficacy. These results suggested that changing of the cationic lipid led to membrane stabilization and improvement of gas retention ability.

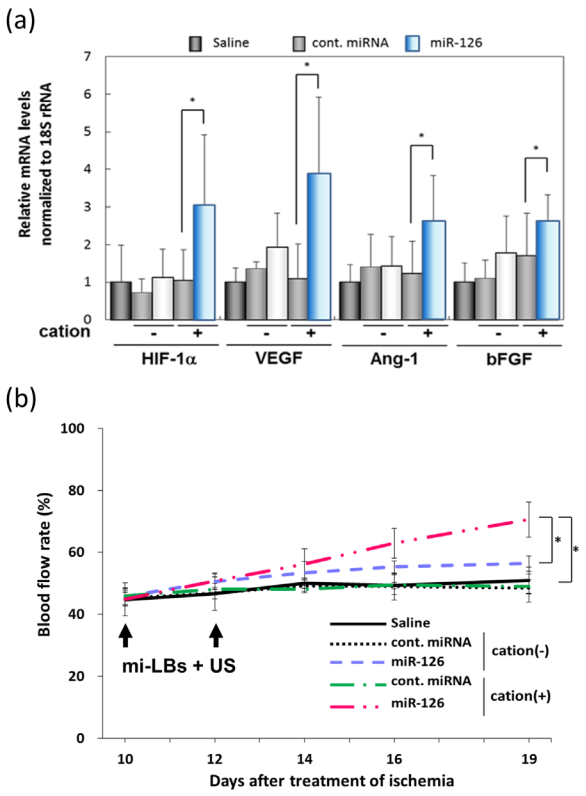

Figure 7. The therapeutic effects of miR-126 transfer by mi-LBs and US exposure on mice with hindlimb ischemia. Ten days after femoral artery ligation, mice were treated with mi- LBs and US. The treatment was administered *via* tail vein injection twice daily every two days to mice with hindlimb ischemia. We injected a solution of miRNA (40 μg of miCont or miR-126) and LBs (200 μg). **(a)** The effect of miR-126 transfer by mi- LBs and US on mRNA expression for angiogenic genes. Seven days after the second transfection, RNA was isolated from the thigh muscle and analyzed using real-time PCR. **(b)** The effect of miR-126 transfer using mi- LBs and US on the recovery of blood flow. After the second transfection, blood flow was measured using a laser Doppler blood flow meter. All data are reported as the mean ± S.D. (n = 4-6). *indicates $p < 0.05$ using a one-way ANOVA with Tukey's post-hoc test. Reprinted from Endo-Takahashi *et al*. with permission (*57*).

The combination of LBs and US is effective tool *via* local injection. However, it is useful that siRNA are transfected using novel efficient siRNA carrier like chol-si-LBs or si-LBs *via* systemic injection to kidney in which gene-silencing effects were not observed *via* local injection or to deep tissues which were difficult for directly injection. Taken together, it is expected that tissue- or organ-specific delivery of siRNA and the specific gene-silencing effect may be achieved by the destruction technologies of LBs combined with targeted US exposure leading to clinical applications for various diseases.

7.2. *microRNA-loaded lipid Bubbles*

MicroRNAs (miRNAs) are involved in biological functions and their dysregulations often lead to human diseases (*54*). Recently, a large number of miRNAs have been identified as a key target for therapeutic intervention. However, the efficient delivery vehicle of a therapeutic RNA to its target tissue is required to develop miRNA-based therapeutics (*55*). So, we attempted to prepare miRNA-loaded LBs (mi-LBs) and evaluated the utility of mi-LBs using a hindlimb ischemia model and miR-126 (*56*), which promotes angiogenesis *via* the cancellation of negative regulators of VEGF signaling (*57-59*). Before *in vivo* transfection experiments, we confirmed the interaction between miRNA and LBs containing the cationic lipid, which was previously reported to be an effective cationic lipid for the preparation of pDNA loaded- LBs (*53*). We found that the amount of miRNA bound to the LBs increased in the presence of cationic lipid. Next, the delivery of mi-LBs to the hindlimb ischemia mouse model was performed *via* intravascular injection. The mi-LBs reached an ischemic site after intravascular injection, were visualized by diagnostic US, and delivered miR-126 following therapeutic US. The delivery of miR-126 led to the increase of angiogenic gene expressions and followed by the improvement of blood flow (Figure 7). Thus, the combination of mi-LBs and US exposure may serve as a theranostic agent with combined properties of a diagnostic and therapeutic system (*56*).

8. Conclusions

US has long been used as a useful diagnostic tool. Therapeutic US was recently developed and is being used in clinical settings. The combination of therapeutic US and nano/microbubbles is an interesting and important system for establishing a novel and non-invasive gene delivery system. Genes are delivered more efficiently using this system compared with a conventional non-viral vector system such as the lipofection method, resulting in higher gene expression. This higher efficiency is due to the gene being delivered into the cytosol and bypassing the endocytosis pathway. Many *in vivo* studies have demonstrated US-mediated gene delivery with nano/microbubbles, and several gene therapy feasibility studies for various diseases have been reported. In addition, nano/microbubbles can deliver genes site-specifically by the control of US exposure site. Therefore, it is expected that this technology could be used clinically as a novel gene delivery system.

Acknowledgements

This study was supported by MEXT-Supported Program for the Strategic Research Foundation at Private Universities 2013-2016.

References

1. Check E. Safety panel backs principle of gene-therapy trials. Nature. 2002; 420:595.
2. Check E. Second cancer case halts gene-therapy trials.

Nature. 2003; 421:305.
3. Marshall E. Gene therapy death prompts review of adenovirus vector. Science. 1999; 286:2244-2245.
4. Itaka K, Ohba S, Miyata K, Kawaguchi H, Nakamura K, Takato T, Chung UI, Kataoka K. Bone regeneration by regulated *in vivo* gene transfer using biocompatible polyplex nanomicelles. Mol Ther. 2007; 15:1655-1662.
5. Kogure K, Akita H, Yamada Y, Harashima H. Multifunctional envelope-type nano device (MEND) as a non-viral gene delivery system. Adv Drug Deliv Rev. 2008; 60:559-571.
6. Liu F, Conwell CC, Yuan X, Shollenberger LM, Huang L. Novel nonviral vectors target cellular signaling pathways: Regulated gene expression and reduced toxicity, The Journal of pharmacology and experimental therapeutics. J Pharmacol Exp Ther. 2007; 321:777-783.
7. Miller MW, Miller DL, Brayman AA. A review of *in vitro* bioeffects of inertial ultrasonic cavitation from a mechanistic perspective. Ultrasound Med Biol. 1996; 22:1131-1154.
8. Fechheimer M, Boylan JF, Parker S, Sisken JE, Patel GL, Zimmer SG. Transfection of mammalian cells with plasmid DNA by scrape loading and sonication loading. Proc Natl Acad Sci U S A. 1987; 84:8463-8467.
9. Greenleaf WJ, Bolander ME, Sarkar G, Goldring MB, Greenleaf JF. Artificial cavitation nuclei significantly enhance acoustically induced cell transfection. Ultrasound Med Biol. 1998; 24:587-595.
10. Feril LB Jr, Ogawa R, Tachibana K, Kondo T. Optimized ultrasound-mediated gene transfection in cancer cells. Cancer Sci. 2006; 97:1111-1114.
11. Li T, Tachibana K, Kuroki M, Kuroki M. Gene transfer with echo-enhanced contrast agents: Comparison between Albunex, Optison, and Levovist in mice – initial results. Radiology. 2003; 229:423-428.
12. Pislaru SV, Pislaru C, Kinnick RR, Singh R, Gulati R, Greenleaf JF, Simari RD. Optimization of ultrasound-mediated gene transfer: Comparison of contrast agents and ultrasound modalities. Eur Heart J. 2003; 24:1690-1698.
13. Suzuki R, Takizawa T, Negishi Y, Utoguchi N, Sawamura K, Tanaka K, Namai E, Oda Y, Matsumura Y, Maruyama K. Tumor specific ultrasound enhanced gene transfer *in vivo* with novel liposomal bubbles. J Control Release. 2008; 125:137-144.
14. Feril LB, Kondo T, Zhao QL, Ogawa R, Tachibana K, Kudo N, Fujimoto S, Nakamura S. Enhancement of ultrasound-induced apoptosis and cell lysis by echo-contrast agents. Ultrasound Med Biol. 2003; 29:331-337.
15. Guo DP, Li XY, Sun P, Tang YB, Chen XY, Chen Q, Fan LM, Zang B, Shao LZ, Li XR. Ultrasound-targeted microbubble destruction improves the low density lipoprotein receptor gene expression in HepG2 cells. Biochem Biophys Res Commun. 2006; 343:470-474.
16. Hassan MA, Buldakov MA, Ogawa R, Zhao QL, Furusawa Y, Kudo N, Kondo T, Riesz P. Modulation control over ultrasound-mediated gene delivery: Evaluating the importance of standing waves. J Control Release. 2010; 141:70-76.
17. Hassan MA, Feril LB Jr, Suzuki K, Kudo N, Tachibana K, Kondo T. Evaluation and comparison of three novel microbubbles: Enhancement of ultrasound-induced cell death and free radicals production. Ultrason Sonochem. 2009; 16:372-378.
18. Kudo N, Okada K, Yamamoto K. Sonoporation by single-shot pulsed ultrasound with microbubbles adjacent to cells. Biophys J. 2009; 96:4866-4876.
19. Wells DJ. Electroporation and ultrasound enhanced non-viral gene delivery *in vitro* and *in vivo*. Cell Biol Toxicol. 2010; 26:21-28.
20. Taniyama Y, Tachibana K, Hiraoka K, Namba T, Yamasaki K, Hashiya N, Aoki M, Ogihara T, Yasufumi K, Morishita R. Local delivery of plasmid DNA into rat carotid artery using ultrasound. Circulation. 2002; 105:1233-1239.
21. Gao Z, Kennedy AM, Christensen DA, Rapoport NY. Drug-loaded nano/microbubbles for combining ultrasonography and targeted chemotherapy. Ultrasonics. 2008; 48:260-270.
22. Wang Y, Li X, Zhou Y, Huang P, Xu Y. Preparation of nanobubbles for ultrasound imaging and intracelluar drug delivery. Int J Pharm. 2010; 384:148-153.
23. Negishi Y, Endo Y, Fukuyama T, Suzuki R, Takizawa T, Omata D, Maruyama K, Aramaki Y. Delivery of siRNA into the cytoplasm by liposomal bubbles and ultrasound. J Control Release. 2008; 132:124-130.
24. Suzuki R, Maruyama K. Effective *in vitro* and *in vivo* gene delivery by the combination of liposomal bubbles (bubble liposomes) and ultrasound exposure. Methods Mol Biol. 2010; 605:473-486.
25. Suzuki R, Namai E, Oda Y, Nishiie N, Otake S, Koshima R, Hirata K, Taira Y, Utoguchi N, Negishi Y, Nakagawa S, Maruyama K. Cancer gene therapy by IL-12 gene delivery using liposomal bubbles and tumoral ultrasound exposure. J Control Release. 2010; 142:245-250.
26. Suzuki R, Oda Y, Utoguchi N, Namai E, Taira Y, Okada N, Kadowaki N, Kodama T, Tachibana K, Maruyama K. A novel strategy utilizing ultrasound for antigen delivery in dendritic cell-based cancer immunotherapy. J Control Release. 2009; 133:198-205.
27. Suzuki R, Takizawa T, Kuwata Y, Mutoh M, Ishiguro N, Utoguchi N, Shinohara A, Eriguchi M, Yanagie H, Maruyama K. Effective anti-tumor activity of oxaliplatin encapsulated in transferrin-PEG-liposome. Int J Pharm. 2008; 346:143-150.
28. Suzuki R, Takizawa T, Negishi Y, Hagisawa K, Tanaka K, Sawamura K, Utoguchi N, Nishioka T, Maruyama K. Gene delivery by combination of novel liposomal bubbles with perfluoropropane and ultrasound. J Control Release. 2007; 117:130-136.
29. Suzuki R, Takizawa T, Negishi Y, Utoguchi N, Maruyama K. Effective gene delivery with liposomal bubbles and ultrasound as novel non-viral system. J Drug Target. 2007; 15:531-537.
30. Un K, Kawakami S, Suzuki R, Maruyama K, Yamashita F, Hashida M. Enhanced transfection efficiency into macrophages and dendritic cells by a combination method using mannosylated lipoplexes and bubble liposomes with ultrasound exposure. Hum Gene Ther. 2010; 21:65-74.
31. Yamashita T, Sonoda S, Suzuki R, Arimura N, Tachibana K, Maruyama K, Sakamoto T. A novel bubble liposome and ultrasound-mediated gene transfer to ocular surface: RC-1 cells *in vitro* and conjunctiva *in vivo*. Exp Eye Res. 2007; 85:741-748.
32. Unger EC, Hersh E, Vannan M, Matsunaga TO, McCreery T. Local drug and gene delivery through microbubbles. Prog Cardiovasc Dis. 2001; 44:45-54.
33. Mulvagh SL, DeMaria AN, Feinstein SB, Burns PN, Kaul S, Miller JG, Monaghan M, Porter TR, Shaw LJ,

Villanueva FS. Contrast echocardiography: Current and future applications. J Am Soc Echocardiogr. 2000; 13:331-342.
34. Mulvagh SL, DeMaria AN, Feinstein SB, Burns PN, Kaul S, Miller JG, Monaghan M, Porter TR, Shaw LJ, Villanueva FS. Vibrating microbubbles poking individual cells: Drug transfer into cells *via* sonoporation. J Am Soc Echocardiogr. 2000; 13:331-342.
35. Duvshani-Eshet M, Adam D, Machluf M. The effects of albumin-coated microbubbles in DNA delivery mediated by therapeutic ultrasound. J Control Release. 2006; 112:156-166.
36. Duvshani-Eshet M, Baruch L, Kesselman E, Shimoni E, Machluf M. Therapeutic ultrasound-mediated DNA to cell and nucleus: Bioeffects revealed by confocal and atomic force microscopy. Gene Ther. 2006; 13:163-172.
37. Kalantarinia K, Belcik JT, Patrie JT, Wei K. Real-time measurement of renal blood flow in healthy subjects using contrast-enhanced ultrasound. Am J Physiol Renal Physiol. 2009; 297:F1129-1134.
38. Lindner JR. Microbubbles in medical imaging: Current applications and future directions. Nat Rev Drug Discov. 2004; 3:527-532.
39. Brunda MJ. Interleukin-12. J Leukoc Biol. 1994; 55:280-288.
40. Nastala CL1, Edington HD, McKinney TG, Tahara H, Nalesnik MA, Brunda MJ, Gately MK, Wolf SF, Schreiber RD, Storkus WJ, Lotze MT. Recombinant IL-12 administration induces tumor regression in association with IFN-gamma production. J Immunol. 1994; 153:1697-1706.
41. Atkins MB, Robertson MJ, Gordon M, Lotze MT, DeCoste M, DuBois JS, Ritz J, Sandler AB, Edington HD, Garzone PD, Mier JW, Canning CM, Battiato L, Tahara H, Sherman ML. Phase I evaluation of intravenous recombinant human interleukin 12 in patients with advanced malignancies. Clin Cancer Res. 1997; 3:409-417.
42. Colombo MP, Vagliani M, Spreafico F, Parenza M, Chiodoni C, Melani C, Stoppacciaro A. Amount of interleukin 12 available at the tumor site is critical for tumor regression. Cancer Res. 1996; 56:2531-2534.
43. Suzuki R, Takizawa T, Negishi Y, Utoguchi N, Sawamura K, Tanaka K, Namai E, Oda Y, Matsumura Y, Maruyama K. Tumor specific ultrasound enhanced gene transfer *in vivo* with novel liposomal bubbles. J Control Release. 2008; 125:137-144.
44. Elbashir SM, Harborth J, Lendeckel W, Yalcin A, Weber K, Tuschl T. Duplexes of 21-nucleotide RNAs mediate RNA interference in cultured mammalian cells. Nature. 2001; 411:494-498.
45. Sledz CA, Holko M, de Veer MJ, Silverman RH, Williams BR. Activation of the interferon system by short-interfering RNAs. Nat Cell Biol. 2003; 5:834-839.
46. Sioud M. RNA interference and innate immunity. Adv Drug Deliv Rev. 2007; 59:153-163.
47. Kobayashi N, Kuramoto T, Yamaoka K, Hashida M, Takakura Y. Hepatic uptake and gene expression mechanisms following intravenous administration of plasmid DNA by conventional and hydrodynamics-based procedures. J Pharmacol Exp Ther. 2001; 297:853-860.
48. Lu PY, Xie F, Woodle MC. *In vivo* application of RNA interference: From functional genomics to therapeutics. Adv Genet. 2005; 54:117-142.
49. Chen S, Ding JH, Bekeredjian R, Yang BZ, Shohet RV, Johnston SA, Hohmeier HE, Newgard CB, Grayburn PA. Efficient gene delivery to pancreatic islets with ultrasonic microbubble destruction technology. Proc Natl Acad Sci U S A. 2006; 103:8469-8474.
50. Endo-Takahashi Y, Negishi Y, Kato Y, Suzuki R, Maruyama K, Aramaki Y. Efficient siRNA delivery using novel siRNA-loaded Bubble liposomes and ultrasound. Int J Pharm. 2012; 422:504-509.
51. Negishi Y, Endo-Takahashi Y, Matsuki Y, Kato Y, Takagi N, Suzuki R, Maruyama K, Aramaki Y. Systemic delivery systems of angiogenic gene by novel bubble liposomes containing cationic lipid and ultrasound exposure. Mol Pharm. 2012; 9:1834-1840.
52. Lian T, Ho RJ. Trends and developments in liposome drug delivery systems. J Pharm Sci. 2001; 90:667-680.
53. Endo-Takahashi Y, Negishi Y, Nakamura A, Suzuki D, Ukai S, Sugimoto K, Moriyasu F, Takagi N, Suzuki R,Maruyama K, Aramaki Y. pDNA-loaded Bubble liposomes as potential ultrasound imaging and gene delivery agents. Biomaterials. 2013; 34:2807-2813.
54. McManus MT, Sharp PA. Gene silencing in mammals by small interfering RNAs. Nat Rev Genet. 2002; 3:737-747.
55. Zhang Y, Wang Z, Gemeinhart RA. Progress in microRNA delivery. J Control Release. 2013; 172:962-974.
56. Endo-Takahashi Y, Negishi Y, Nakamura A, Ukai S, Ooaku K, Oda Y, Sugimoto K, Moriyasu F, Takagi N, Suzuki R, Maruyama K, Aramaki Y. Systemic delivery of miR-126 by miRNA-loaded Bubble liposomes for the treatment of hindlimb ischemia. Sci Rep. 2014; 4:3883.
57. Wang S, Aurora AB, Johnson BA, Qi X, McAnally J, Hill JA, Richardson JA, Bassel-Duby R, Olson EN. The endothelial-specific microRNA miR-126 governs vascular integrity and angiogenesis. Dev Cell. 2008; 15:261-271.
58. Fish JE, Santoro MM, Morton SU, Yu S, Yeh RF, Wythe JD, Ivey KN, Bruneau BG, Stainier DY, Srivastava D. miR-126 regulates angiogenic signaling and vascular integrity. Dev Cell. 2008; 15:272-284.
59. van Solingen C, Seghers L, Bijkerk R, Duijs JM, Roeten MK, van Oeveren-Rietdijk AM, Baelde HJ, Monge M, Vos JB, de Boer HC, Quax PH, Rabelink TJ, van Zonneveld AJ. Antagomir-mediated silencing of endothelial cell specific microRNA-126 impairs ischemia-induced angiogenesis. J Cell Mol Med. 2008; 13:1577-1585.

(Received September 27, 2016; Revised October 24, 2016; Accepted October 25, 2016)

Mini-Review

DOI: 10.5582/ddt.2016.01065

Drug delivery system of therapeutic oligonucleotides

Yutaro Asami, Kotaro Yoshioka, Kazutaka Nishina, Tetsuya Nagata, Takanori Yokota*

Department of Neurology and Neurological Science, Graduate School, Tokyo Medical and Dental University, Tokyo, Japan.

Summary **Therapeutic oligonucleotides are promising technologies. Nevertheless, improvement of their efficacy is an important issue. Introducing this drug delivery system (DDS) makes for a great enhancement for delivery of oligonucleotides to targeted tissue or cells. The strategy of DDS for therapeutic oligonucleotides is divided into four categories, A) single piece of oligonucleotide, B) oligonucleotide-ligand conjugate, C) oligonucleotide-polymer conjugate, and D) nanoparticle. In this review we will describe those basic concepts, especially for the technology of conjugating ligand. In addition, we developed a new technology, heteroduplex oligonucleotide (HDO), binding ligand-molecule to antisense oligonucleotide indirectly. We also outline α-tocopherol (a natural isomer of vitamin E) conjugated HDO.**

Keywords: Ligand conjugate, siRNA, antisense oligonucleotide, heteroduplex oligonucleotide

1. Introduction

Therapeutic oligonucleotides have rapidly progressed during the last decade and pipelines targeting a variety of disorders are now going to clinical trials (*1,2*). Despite the promising progress, improvement of efficacy *in vivo* remains a major challenge.

A variety of chemical modifications have been developed, and introducing drug delivery system (DDS) leads to greater improvement for delivery of oligonucleotides to targeted organs and cells (*3*). Especially effective delivery of small interfering RNA (siRNA) *in vivo* is difficult by itself, and needs some DDS. Strategy of therapeutic oligonucleotides is divided into four categories, as follows (Figure 1).

A) *Single piece of oligonucleotide*

Chemical modification improves stability against nuclease degradation. However, oligonucleotides are immediately egested by the kidney or accumulated in the liver and retention in blood circulation is not adequate (*4*).

Antisense oligonucleotides (ASOs) and siRNAs have a phosphorothioate (PS) backbone modification, which has two advantages. One is improvement of stability to nucleases in the body, another is improvement of binding affinity to serum proteins like albumin or others so that excretion from the kidney is delayed (*5,6*).

The first systemic ASO drug, Kynamro® targeting the liver with systemic administration was approved by U.S. Food and Drug Administration (FDA) (*7*). Targeting tissues other than the liver, however, is rather difficult and drugs for local administration have been mainly developed, for example intraocular or intrathecal administration (*8-11*).

B) *Oligonucleotide-ligand conjugate*

An approach to conjugate a ligand molecule to an oligonucleotide has been taken. Ligand conjugation improved retention of the oligonucleotide in blood and transition to the targeted organ or cell (Figure 2), as we describe later (*12*).

C) *Oligonucleotide-polymer conjugate*

Conjugating polymer to oligonucleotide can also improve retention in blood circulation. Several types of oligonucleotide can be conjugated as one particle with polymer, the size of the molecule is approximately 10 nm, compared to 5 nm for a single oligonucleotide (*3*).

D) *Nanoparticle*

There are two better-known nanoparticles, lipid

**Address correspondence to:*
Dr. Takanori Yokota, Department of Neurology and Neurological Science, Graduate School, Tokyo Medical and Dental University, 1-5-45 Yushima, Bunkyo-ku, Tokyo 113-8519, Japan.
E-mail: tak-yokota.nuro@tmd.ac.jp

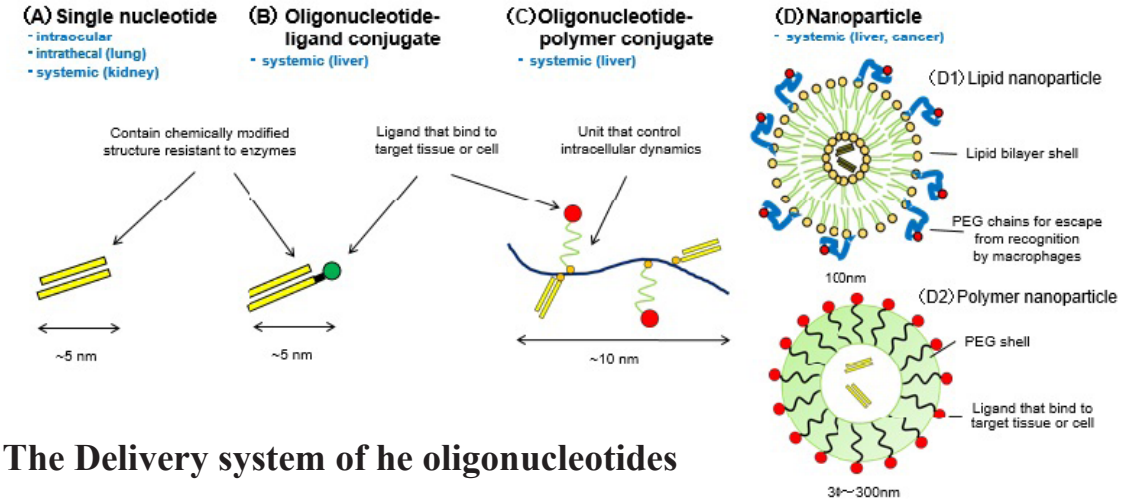

Figure 1. Delivery system of oligonucleotides. Four strategies of therapeutic oligonucleotides are illustrated. **A)** single piece of oligonucleotide, **B)** oligonucleotide-ligand conjugate, **C)** oligonucleotide-polymer conjugate, and **D)** nanoparticle. Nanoparticle has two more categories, lipid nanoparticle and polymer nanoparticle. Illustration of chemical modifications of siRNA is simplified.

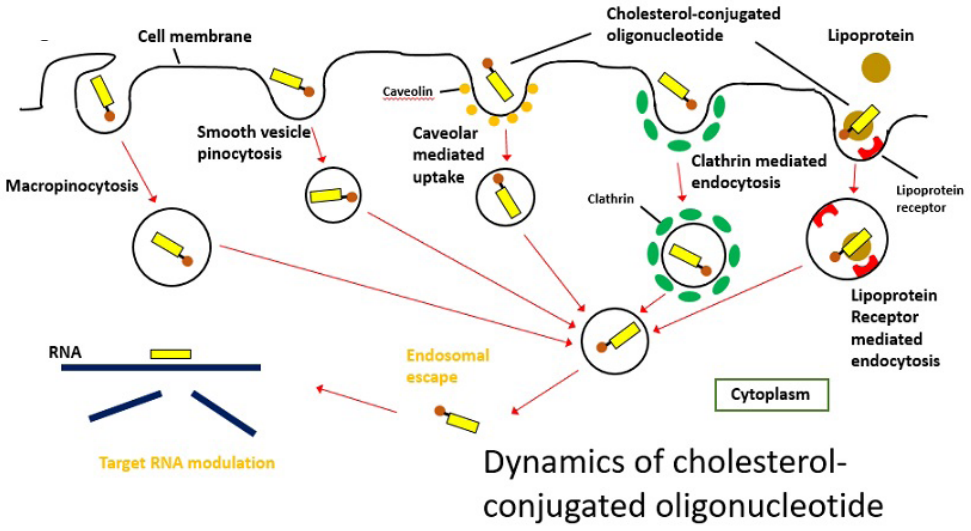

Figure 2. The intracellular and extracellular dynamics of cholesterol-conjugated oligonucleotide. Cellular uptake and intracellular trafficking of cholesterol-conjugated oligonucleotides are depicted. Cholesterol-conjugated oligonucleotide binds to lipoproteins in blood and is delivered to the liver or other tissues. Cellular uptake of the cholesterol-conjugated oligonucleotide is at least in part mediated by lipoprotein receptors. There are several endocytotic pathways other than lipoprotein receptors. Most of cholesterol-conjugated oligonucleotides are taken into early endosomes and accumulate in late endosomes and lysosomes, however, very small amount of them escape from endosome and enter into cytoplasm. Then oligonucleotides modulate the target RNA. Illustration of chemical modifications of oligonucleotides are simplified.

nanoparticle and polymer nanoparticle, in which oligonucleotides are loaded inside. Lipid nanoparticle is a small particle about a size of 100 nm, which has a shell of lipid bilayer and can load oligonucleotide in it. Polyethylene glycol (PEG) chains are able to be conjugated outside of the membrane, which help to escape recognition by macrophages. This is called a stable-nucleic-acid lipid particle (SNALP), widely used for delivery of siRNA (*13,14*). Polymer nanoparticle has a shell of PEG and oligonucleotides are loaded in it. Ligands can be conjugated on the surface. This is an aggregate of many molecules, hence the size is as large as 30 to 300 nm. Because of good retention of the nanoparticles in the blood, the development of migration to the liver and delivery to cancer tissues are now advanced (*15,16*).

In this review, we recount especially B), oligonucleotide-ligand conjugate. Conjugating ligand to siRNA has been tried since early times. Direct conjugation of ligand particle to an ASO leads to

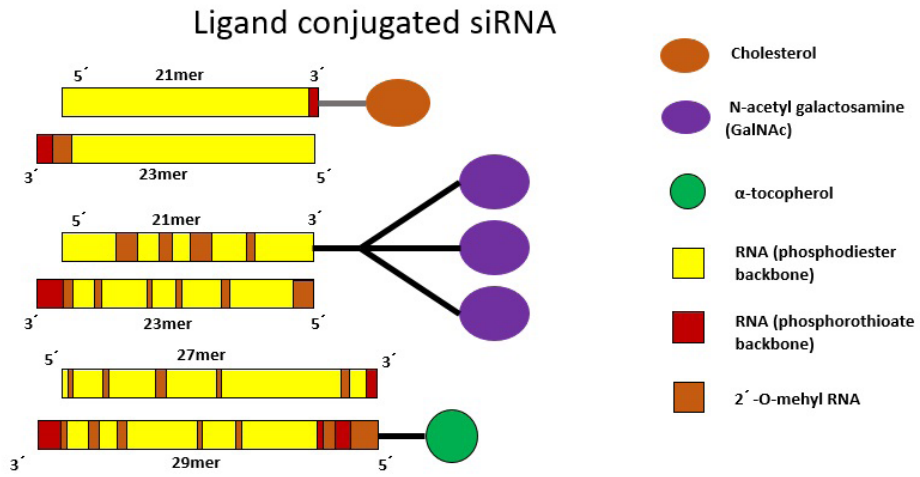

Figure 3. Schematic illustration of ligand-conjugated siRNA. Cholesterol-conjugated or N-acetyl galactosamine (GalNAc)-conjugated siRNA consists of a 21-nucleotide sense strand and a 23-nucleotide antisense strand, in which the 3' end of the antisense strand has a two-nucleotide overhang. A cholesterol or GalNAc is conjugated to the 3' end of the sense strand, respectively. Alfa-tocopherol-conjugated siRNA is a 27/29 nucleotides siRNA. The site of α-tocopherol (a natural isomer of vitamin E) conjugation is the 5' end of 29-mer antisense strand.

decrease of efficacy, and some technology to solve the problem such as using a cleavable linker is needed. Heteroduplex oligonucleotide (HDO) is a new method to indirectly bind ligand to ASO, we outline also α-tocopherol (a natural isomer of vitamin E) conjugated HDO (Toc-HDO).

2. Ligand-conjugated siRNA

siRNA is a double-stranded short RNA which can effectively downregulate a target gene that is complementary to its sequence. siRNA is recognized by Dicer and cleaved to 21/21 nucleotides double-stranded RNA in the cell. In the case of ligand-conjugated siRNA, the ligand is also cleaved by Dicer in this process so that the ligand does not negatively affect the efficacy. siRNA is then taken into an RNA induced silencing complex (RISC) *via* RISC-loading complex (RLC). The main component of RISC is argonaute (Ago) family protein (especially Ago2) that has slicer activity, RISC recognizes target messenger RNA (mRNA) that is complementary to the guide chain of the siRNA, then the target mRNA is cleaved with Ago2 (*3,17,18*). There are three examples of ligand-conjugated siRNA (Figure 3).

2.1. *Cholesterol-conjugated siRNA*

A conjugation oligonucleotide with cholesterol was one of the earliest successes in the conjugation of ligand to oligonucleotides (*19,20*). This siRNA consisted of a 21-nucleotide sense strand and a 23-nucleotide antisense strand, in which the 3' end of the antisense strand had a two-nucleotide overhang. A cholesterol was conjugated to the 3' end of the sense strand. This 21/23-mer siRNA would be cleaved by Dicer to 21/21-mer mature siRNA in the cell, which has gene silencing activity. The cholesterol conjugated siRNA targeting *apolipoprotein B* (*ApoB*) mRNA had an approximately two fold silencing effect in liver tissue compared to unconjugated using intravenous administration (*19*). In serum, cholesterol-conjugated siRNAs were found in the fraction with high density lipoprotein (HDL), low density lipoprotein (LDL) cholesterol and albumins. This meant the Cholesterol-conjugated siRNAs seemed to interact with HDL, LDL cholesterol and albumins in the serum (*12*).

2.2. *N-acetyl galactosamine-conjugated siRNA*

N-acetyl galactosamine (GalNAc) is an oligosaccharide, which has high affinity for asialoglycoprotein receptor (ASGPR). The ASGPR is a C-type lectin which is expressed abundantly on hepatocytes (500 thousand copies/cell), and its physiological function is the clearance of glycoproteins (*21*).

Triantennary GalNAc would be the best ligand for ASGPR, and the oligonucleotide is delivered much more to hepatocytes than non-parenchymal cells. The structure of siRNA was a 21/23-mer primary structure and triantennary GalNAc was conjugated at the 3' end of the sense strand. After binding of the ligand, the ASGPR-ligand complex was internalized into the cell. The ASGPR-GalNAc complex dissociated in the endosomal low pH, the receptor was recycled, while the ligand was taken into the lysosome (*5*). The GalNAc-siRNA conjugate was cleaved, then the mature 21/21-mer siRNA was discharged. The GalNAc-siRNA had approximately 5-fold potency in hepatocytes compared to the unconjugated siRNA with subcutaneous

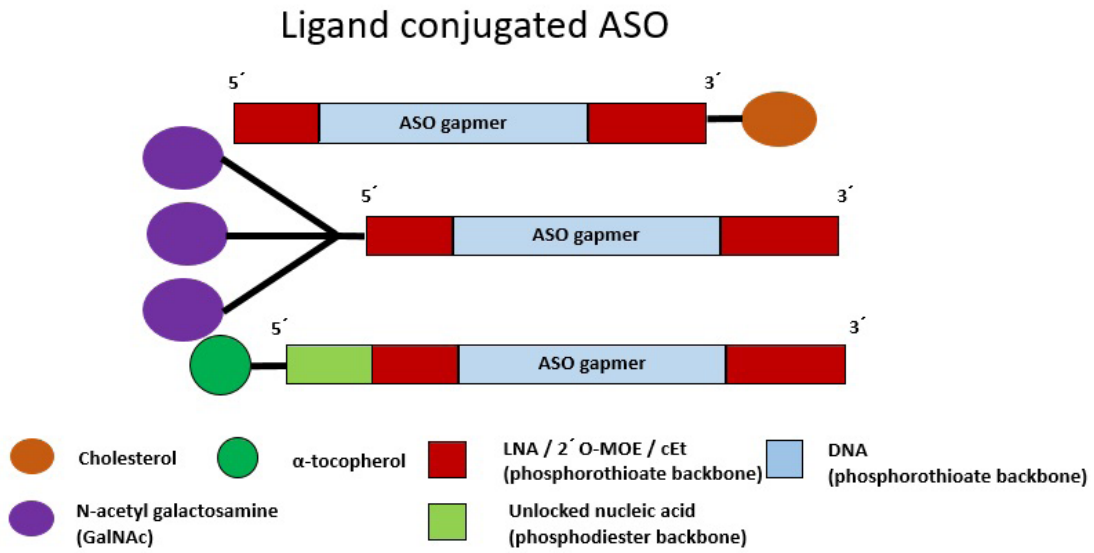

Figure 4. Schematic illustration of ligand-conjugated ASO. Cholesterol-conjugated antisense oligonucleotide (ASO) has a cleavable structure between cholesterol and ASO. GalNAc-conjugated ASO has a GalNAc ligand in its 5' end, which has a cleavable linker between the ligand and ASO. In α-tocopherol-conjugated ASO, ASO consists of 13 nucleotides. Between tocopherol and ASO are 4~7 nucleotide phosphodiester backbone unlocked nucleic acids (UNAs). LNA: locked nucleic acid, 2'-O-MOE: 2'-O-methoxyethyl RNA, cEt: constrained ethyl BNA.

administration (*22*). GalNAc-siRNA bound to plasma proteins at the rate of 94% in whole mouse plasma (*23*).

2.3. *Tocopherol-conjugated siRNA*

Ideal features of ligand molecules are essential for target organs or cells, and the target tissue cannot create the molecule. Vitamin E seemed to be most suitable for the vector because of safety and well known physiological movements (*24,25*). Hence α-tocopherol (a natural isomer of vitamin E) was conjugated to 27/29 nucleotides siRNA (Toc-siRNA). The site of α-tocopherol conjugation was the 5'end of 29-mer antisense strand. This Toc-siRNA was cleaved to the mature form 21/21-mer siRNA in the cell by Dicer. Subsequently the RISC loading and target RNA cleavage occurred. With Toc-siRNA, the gene silencing effect was much higher than the cholesterol-conjugated siRNA in liver. Only 2 mg/kg of Toc-siRNA were needed to reduce efficiently *ApoB* mRNA compared to 50-100 mg/kg of cholesterol-conjugated siRNA in the mouse liver when administered intravenously (*26*). Intestinal infusion is another way to deliver Toc-siRNA to the liver. Toc-siRNA administered as a lipid nanoparticle to the mouse large intestine in a postprandial state at a dose of 30 mg/kg reduced *ApoB* mRNA level in the liver by approximately 40% compared to the unconjugated siRNA (*27*).

3. Ligand-conjugated antisense oligonucleotide

Antisense oligonucleotide (ASO) is a single-stranded short oligonucleotide, which is chemically modified, especially 2'-O-methoxyethyl (2'-O-MOE), locked nucleic acids (LNAs) and constrained ethyl BNA (cEt). These structures improve binding affinity of the ASO to the target mRNA. Recently, gapmer ASO is predominantly used that contains two to five chemically modified nucleotides as wings at each terminal. The center of the gapmer ASO consists of a 5-10 base gap of DNA. The gapmer binds to the target mRNA and forms a DNA/RNA heteroduplex, that is recognized by RNase H and enables it to cleave the target mRNA (*5,28*). There are three examples of ligand-conjugated ASO (Figure 4).

3.1. *Cholesterol-conjugated ASO*

Cholesterol was also conjugated to ASO, not only to siRNA. Mukai *et al*. reported that a cholesterol-conjugated ASO accumulated in the liver approximately at three times a higher amount than that of unconjugated (*29*). Wada *et al*. designed a Triethylenglycol (TEG)-disulfate linker as a cleavable spacer between cholesterol and ASO. In a comparison between 5' and 3' for binding site of the cholesterol, 3'-cholesterol-conjugated ASOs accumulated more in the liver than 5'-cholesterol-conjugated ASOs. It reduced target mRNA approximately 60% in the liver with intravenous administration. Cholesterol-conjugated ASO interacted with some circulating proteins in serum, probably lipoproteins (*30*).

3.2. *GalNAc-conjugated ASO*

GalNAc was also conjugated to ASO. Until the process of endocytosis, GalNAc-conjugated ASO seemed to act similarly to the GalNAc-conjugated siRNA described above. It was suggested that the ASO escaped from endosomal compartments, and the GalNAc-ASO

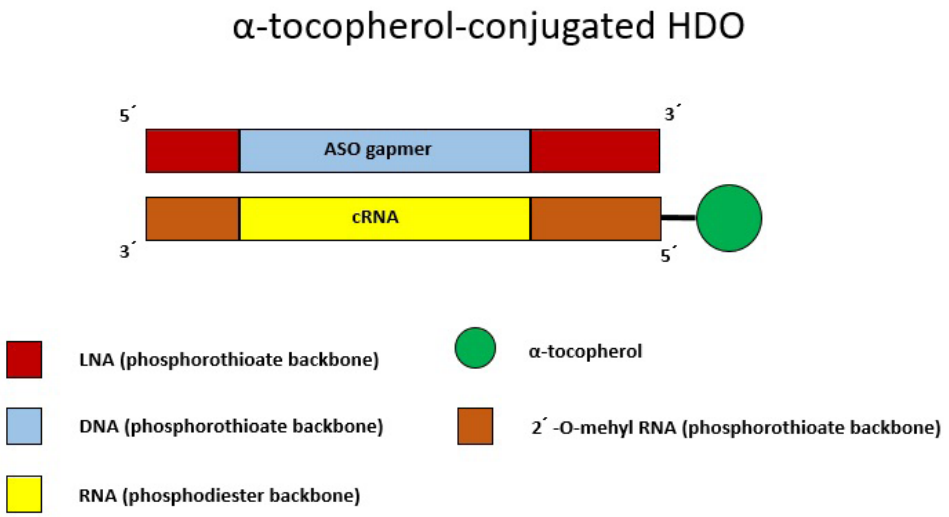

Figure 5. Ligand conjugated heteroduplex oligonucleotide. Schematic illustration of heteroduplex oligonucleotide (HDO). A HDO consists of a DNA strand gapmer which has phosphorothioate backbone and RNA strand that is complementary to the ASO (cRNA). In the cRNA strand, the nucleotides complementary to the DNA strand in the center portion are unmodified RNAs, while the nucleotides complementary to LNA in the DNA strand are phosphorothioate-modified 2'-O-methyl RNA. Alfa-tocopherol is conjugated to the 5' end of the cRNA strand. LNA: locked nucleic acid, cRNA: complementary RNA.

conjugate was cleaved at the cleavable site of the linker, then the parent ASO was discharged.

The triantennary GalNAc conjugated antisense oligonucleotide was considered to work as an hepatocyte targeting prodrug. With subcutaneous injection, it had approximately 10-fold gene silencing potency compared to the unconjugated ASO (*21,23*).

3.3. *Tocopherol-conjugated ASO*

Alpha-tocopherol (Toc)-siRNA, that was directly conjugated α-tocopherol, enhanced downregulation of endogenous genes in mouse liver compared to not conjugated. However, α-tocopherol directly conjugated ASO did not have a gene silencing effect. It was speculated that conjugation of tocopherol interfered with the gene silencing effect, then a spacer was used between ASO and tocopherol. Toc-ASO using PEG or nucleotides with phosphorothioate linkages as a spacer (second wing) also had no effect. Toc-ASO introduced nucleotides with phosphodiester linkages as second wing had reduced target gene expression.

As a length effect, Toc-13-mer (direct conjugation) and Toc-14-mer ASO had no effect, but Toc-17-mer and 20-mer ASO reduced gene expression and Toc-17-mer had an especially better effect. This was because a single nucleic acid might not be recognized by nucleases. When it was longer than a 17-mer ASO, a shorter second wing seemed to be better.

These effective Toc-ASOs were considered to reach mouse liver with full length, after that cleaved to 13-mer ASO and showed a gene silencing effect. Toc-ASO in mouse liver was more than 3.5 fold compared to tocopherol unconjugated ASO with intravenous administration. Alfa-tocopherol also improved the pharmacokinetics of the ASO (*31*).

Though Toc-ASO had a better gene silencing effect than previous ASO, its efficacy could be reduced if the "linker nucleotide" was not effectively cleaved. Hence a method to conjugate tocopherol indirectly to the ASO is desired. We discuss tocopherol-conjugated heteroduplex oligonucleotide (Toc-HDO), which we have newly created.

4. Tocopherol-conjugated HDO

HDO consists of DNA/RNA double-stranded oligonucleotide.

The DNA strand is gapmer ASO and its internucleotide linkages have phosphorothioate modifications. The RNA strand is complementary to the ASO (cRNA). In the cRNA strand, the nucleotides complementary to the LNA nucleotides of the ASO have 2'-O-methyl modifications, which are linked with phosphorothioate substitution. However, the nucleotides complementary to the DNA strand are unmodified RNAs. Alfa-tocopherol is conjugated to the 5' end of the cRNA strand (Figure 5).

The Toc-HDO targeting *ApoB* mRNA achieved great downregulation of targeted mRNA in liver tissue and also reduced serum LDL cholesterol much more than the Toc-unconjugated single strand ASO.

The Toc-HDO was accumulated approximately 5 times selectively in the liver compared to single strand ASO measured by fluorescence-label assay and quantitative real-time polymerase chain reaction (PCR) assay. However, the silencing effect of the Toc-HDO was 22.2-fold higher than the ASO at effective dose (ED) 50, we consider that the Toc-HDO was delivered much better to the hepatocytes than to the parenchymal

cells, or that the silencing effect was increased after the uptake by hepatocytes.

Serum alanine amino transferase (ALT) level was lower in the Toc-HDO injected mouse than in the ASO injected mouse with same silencing effect when targeting ApoB mRNA. Serum interferon (IFN)-γ and tumor necrosis factor (TNF)-α also did not increase.

The carrier molecule of the Toc-HDO in mouse serum was lipoprotein. Hepatocyte uptake of the Toc-HDO was at least in part mediated through the LDL receptor (*32*).

5. Conclusion

We described the outline of DDS for oligonucleotides, especially ligand-conjugated oligonucleotide. DDS is essential technology for therapeutic oligonucleotides, and further improvements are expected.

References

1. Ozcan G, Ozpolat B, Coleman RL, Sood AK, Lopez-Berestein G. Preclinical and clinical development of siRNA-based therapeutics. Adv Drug Deliv Rev. 2015; 87:108-119.
2. Mansoor M, Melendez AJ. Advances in antisense oligonucleotide development for target identification, validation, and as novel therapeutics. Gene Regul Syst Bio. 2008; 2:275-295.
3. Hong CA, Nam YS. Functional nanostructures for effective delivery of small interfering RNA therapeutics. Theranostics. 2014; 4:1211-1232.
4. Juliano RL, Alam R, Dixit V, Kang HM. Cell-targeting and cell-penetrating peptides for delivery of therapeutic and imaging agents. Wiley Interdiscip Rev Nanomed Nanobiotechnol. 2009; 1:324-335.
5. Juliano RL. The delivery of therapeutic oligonucleotides. Nucleic Acids Res. 2016; 44:6518-6548.
6. Piao W, Nishina K, Yoshida-Tanaka K, Kuwahara H, Nishina T, Sakata M, Mizusawa H, Yokota T. Efficient *in vivo* delivery of antisense oligonucleotide to choroid plexus. J Med Dent Sci. 2013; 60:9-16.
7. Geary RS, Baker BF, Crooke ST. Clinical and preclinical pharmacokinetics and pharmacodynamics of mipomersen (kynamro®): A second-generation antisense oligonucleotide inhibitor of apolipoprotein B. Clin Pharmacokinet. 2015; 54:133-146.
8. Azad RF, Driver VB, Tanaka K, Crooke RM, Anderson KP. Antiviral activity of a phosphorothioate oligonucleotide complementary to RNA of the human cytomegalovirus major immediate-early region. Antimicrob. Agents Chemother. 1993; 37:1945-1954
9. Fujita Y, Takeshita F, Kuwano K, Ochiya T. RNAi Therapeutic Platforms for Lung Diseases. Pharmaceuticals (Basel). 2013; 6:223-250.
10. Anderson KP, Fox MC, Brown-Driver V, Martin MJ, Azad RF. Inhibition of human cytomegalovirus immediate-early gene expression by an antisense oligonucleotide complementary to immediate-early RNA. Antimicrob. Agents Chemother. 1996; 40:2004–2011
11. Ng EW, Shima DT, Calias P, Cunningham ET, Jr., Guyer DR, Adamis AP. Pegaptanib, a targeted anti-VEGF aptamer for ocular vascular disease. Nat Rev Drug Discov. 2006; 5:123-132.
12. Wolfrum C, Shi S, Jayaprakash KN, Jayaraman M, Wang G, Pandey RK, Rajeev KG, Nakayama T, Charrise K, Ndungo EM, Zimmermann T, Koteliansky V, Manoharan M, Stoffel M. Mechanisms and optimization of *in vivo* delivery of lipophilic siRNAs. Nat Biotechnol. 2007; 25:1149-1157.
13. Semple SC, Akinc A, Chen J, *et al*. Rational design of cationic lipids for siRNA delivery. Nat Biotechnol. 2010; 28:172-176.
14. Jayaraman M, Ansell SM, Mui BL, *et al*. Maximizing the potency of siRNA lipid nanoparticles for hepatic gene silencing *in vivo*. Angew Chem Int Ed Engl. 2012; 51:8529–8533.
15. Davis ME, Zuckerman JE, Choi CH, Seligson D, Tolcher A, Alabi CA, Yen Y, Heidel JD, Ribas A. Evidence of RNAi in humans from systemically administered siRNA *via* targeted nanoparticles. Nature. 2010; 464:1067-1670.
16. Cabral H, Matsumoto Y, Mizuno K, Chen Q, Murakami M, Kimura M, Terada Y, Kano MR, Miyazono K, Uesaka M, Nishiyama N, Kataoka K. Accumulation of sub-100 nm polymeric micelles in poorly permeable tumours depends on size. Nat Nanotechnol. 2011; 6:815-823.
17. Sibley CR, Seow Y, Wood MJ. Novel RNA-based strategies for therapeutic gene silencing. Mol Ther. 2010; 18:466-476.
18. Liu J, Carmell MA, Rivas FV, Marsden CG, Thomson JM, Song JJ, Hammond SM, Joshua-Tor L, Hannon GJ. Argonaute2 is the catalytic engine of mammalian RNAi. Science. 2004; 305:1437-1441.
19. Soutschek J, Akinc A, Bramlage B, *et al*. Therapeutic silencing of an endogenous gene by systemic administration of modified siRNAs. Nature. 2004; 432:173-178.
20. Lorenz C, Hadwiger P, John M, Vornlocher HP, Unverzagt C. Steroid and lipid conjugates of siRNAs to enhance cellular uptake and gene silencing in liver cells. Bioorg Med Chem Lett. 2004; 14:4975-4977.
21. Prakash TP, Graham MJ, Yu J, *et al*. Targeted delivery of antisense oligonucleotides to hepatocytes using triantennary N-acetyl galactosamine improves potency 10-fold in mice. Nucleic Acids Res. 2014; 42:8796-8807.
22. Nair JK, Willoughby JL, Chan A, *et al*. Multivalent N-acetylgalactosamine-conjugated siRNA localizes in hepatocytes and elicits robust RNAi-mediated gene silencing. J Am Chem Soc. 2014; 136:16958-16961.
23. Yu RZ, Graham MJ, Post N, Riney S, Zanardi T, Hall S, Burkey J, Shemesh CS, Prakash TP, Seth PP, Swayze EE, Geary RS, Wang Y, Henry S. Disposition and Pharmacology of a GalNAc3-conjugated ASO Targeting Human Lipoprotein (a) in Mice. Mol Ther Nucleic Acids. 2016; 5:e317.
24. Schmölz L, Birringer M, Lorkowski S, Wallert M. Complexity of vitamin E metabolism. World J Biol Chem. 2016; 7:14-43.
25. Albahrani AA, Greaves RF. Fat-Soluble Vitamins: Clinical Indications and Current Challenges for Chromatographic Measurement. Clin Biochem Rev. 2016; 37:28-47
26. Nishina K, Unno T, Uno Y, Kubodera T, Kanouchi T, Mizusawa H, Yokota T. Efficient *in vivo* delivery of siRNA to the liver by conjugation of alpha-tocopherol. Mol Ther. 2008; 16:734-740.

27. Murakami M, Nishina K, Watanabe C, Yoshida-Tanaka K, Piao W, Kuwahara H, Horikiri Y, Miyata K, Nishiyama N, Kataoka K, Yoshida M, Mizusawa H, Yokota T. Enteral siRNA delivery technique for therapeutic gene silencing in the liver *via* the lymphatic route. Sci Rep. 2015; 5:17035.
28. Kasuya T, Hori S, Watanabe A, Nakajima M, Gahara Y, Rokushima M, Yanagimoto T, Kugimiya A. Ribonuclease H1-dependent hepatotoxicity caused by locked nucleic acid-modified gapmer antisense oligonucleotides. Sci Rep. 2016; 6:30377.
29. Mukai H, Ozaki D, Cui Y, Kuboyama T, Yamato-Nagata H, Onoe K, Takahashi M, Wada Y, Imanishi T, Kodama T, Obika S, Suzuki M, Doi H, Watanabe Y. Quantitative evaluation of the improvement in the pharmacokinetics of a nucleic acid drug delivery system by dynamic PET imaging with (18)F-incorporated oligodeoxynucleotides. J Control Release. 2014; 180:92-99.
30. Wada S, Yasuhara H, Wada F, Sawamura M, Waki R, Yamamoto T, Harada-Shiba M, Obika S. Evaluation of the effects of chemically different linkers on hepatic accumulations, cell tropism and gene silencing ability of cholesterol-conjugated antisense oligonucleotides. J Control Release. 2016; 226:57-65.
31. Nishina T, Numata J, Nishina K, Yoshida-Tanaka K, Nitta K, Piao W, Iwata R, Ito S, Kuwahara H, Wada T, Mizusawa H, Yokota T. Chimeric Antisense Oligonucleotide Conjugated to alpha-Tocopherol. Mol Ther Nucleic Acids. 2015; 4:e220.
32. Nishina K, Piao W, Yoshida-Tanaka K, *et al*. DNA/RNA heteroduplex oligonucleotide for highly efficient gene silencing. Nat Commun. 2015; 6:7969.

(Received September 28, 2016; Revised October 25, 2016; Accepted October 26, 2016)

Original Article

DOI: 10.5582/ddt.2016.01055

In vitro and *in vivo* biophysical properties of oligonucleotides containing 5'-thio nucleosides

Md Ariful Islam[1,*], Reiko Waki[1,*], Aki Fujisaka[1,2,*], Kosuke Ramon Ito[1], Satoshi Obika[1,]**

[1] *Graduate School of Pharmaceutical Sciences, Osaka University, Osaka, Japan;*
[2] *Faculty of Pharmacy, Osaka Ohtani University, Osaka, Japan.*

Summary **Phosphorothioate modification is one of the most widely investigated and promising chemical modifications in oligonucleotide (ON) based therapeutics. Structurally similar 5'-thio or phosphorothiolate-modified nucleotides, in which a 5'-bridging oxygen is replaced with a sulfur atom, are gaining importance for ON-based research. Several reports have been published describing the synthesis of 5'-thio-modified ONs but no detailed *in vitro* and *in vivo* data are available. Here, we report the synthesis of 5'-thio-modified 2'-deoxy-5-methylcytidine. 5'-Thio-modified thymidine and 2'-deoxy-5-methylcytidine were incorporated into target ONs, then we evaluated their binding affinity, nuclease stability, RNase H mediated scission, stability in blood serum, and *in vitro* and *in vivo* activity. This is the first report showing the influence of 5'-thio-modified antisense ONs in *in vitro* and *in vivo* experiments.**

Keywords: Phosphorothiolate, methylcytosine, RNase H activity, *in vitro* and *in vivo* antisense activity

1. Introduction

Nucleic acid analogues are widely used in biochemical research and oligonucleotide (ON) based therapy. The phosphorothioate modification (Figure 1A), in which a non-bridging oxygen covalently bound to phosphorus is replaced by a sulfur atom, is of considerable interest in ON-based therapy because of its ease of synthesis and the improved pharmacological properties of the modified ONs (*1-3*). However, these modified ONs contain chiral center at the phosphorus atom, resulting two stereoisomers referred to as Sp and Rp. Those stereoisomers have distinct physical and biochemical properties (*4,5*), and are very difficult to purify.

The 5'-thio modification (or phosphorothiolate modification) is structurally similar to the phosphorothioate modification, with a sulfur atom replacing the 5'-bridged oxygen connected to the ribofuranose sugar moiety (Figure 1B). The 5'-thio modification provides important biochemical probes for investigating fundamental features of enzyme catalysis and is a potential candidate for therapeutic applications (*6*). In addition, phosphorothiolates affect the ON sugar conformation, making them ideal for fine-tuning the potency of antisense DNA and small interfering RNAs (siRNAs). Furthermore, unlike phosphorothioates, phosphorothiolates do not have a chiral center at the phosphorous atom (*7,8*). The importance of the 5'-thio modification is reflected in the large number of synthetic chemical and enzymatic approaches reported to date, yet significant synthetic challenges remain for the fully automated solid-phase synthesis of 5'-thio phosphorothiolates (*9,10*). Recently Hofmann and Engels described a very convenient method for the synthesis of 5'-thio-modified ONs using an automated solid support DNA synthesizer (*11*). However, to our knowledge, despite the large body of work conducted on the chemical synthesis of 5'-thio-modified ONs such as a report describing ribozyme catalytic action on the phosphorothiolate linkage (*9*), there are no comprehensive studies on the *in vitro* and *in vivo* properties of 5'-thio-modified ONs yet. Given the potential of the 5'-thio modification to improve pharmacokinetic and pharmacodynamic properties, there is considerable interest in identifying new ON analogs exhibiting high *in vivo* efficacy and low toxicity (*12*). Here we describe the synthesis of ONs containing a 5'-thio-modified monomer using a fully automated

*These authors contributed equally to this works.
***Address correspondence to:*
Dr. Satoshi Obika, Graduate School of Pharmaceutical Sciences, Osaka University, 1-6 Yamadaoka, Suita, Osaka 565-0871, Japan.
E-mail: obika@phs.osaka-u.ac.jp

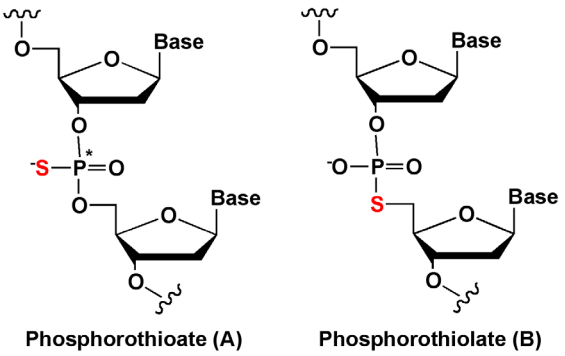

Figure 1. Chemical structure of a phosphorothioate (A) and a phosphorothiolate (B) linkage. *Chiral center.

solid support DNA synthesizer, as well as evaluation of their hybridizing ability with complementary strands, nuclease resistance, *in vitro* and *in vivo* bioassay, ribonuclease H (RNase H) mediated scission properties, and stability in blood serum.

2. Materials and Methods

2.1. *Materials*

All starting materials and reactants were purchased and used without further purification. Moisture-sensitive reactions were conducted in dried glassware under argon gas. All NMR spectrums were measured using JEOL-JNM (JEOL Resonance Inc., Tokyo, Japan) instruments. ^{1}H-NMR spectra were recorded at 300, 400 and 500 MHz. ^{13}C-NMR spectra were recorded at 75 and 100 MHz. ^{31}P-spectra were recorded at 202 MHz. IR spectrum and optical rotation data for all new compounds were measured using FT/IR-4200 (JASCO Corporation, Tokyo, Japan) and P-2200 (JASCO Corporation) respectively. Silica gel PSQ 60B (Fuji Silysia Chemical Ltd., Kasugai, Japan) was used for column chromatography. The progress of the reactions was monitored by analytical thin layer chromatography (TLC) on pre-coated aluminum sheets (Silica gel 60 F254-sheet, Merck KGaA, Darmstadt, Germany), and the products were visualized under UV light.

2.2. *Oligonucleotide synthesis*

ONs containing 5'-thio monomers were synthesized on an automated DNA synthesizer (ns-8, GeneDesign Inc., Ibaraki, Japan) using a conventional phosphoramidite method. 1.0 M *tert*-Butyl hydroperoxide in acetonitrile (Sigma-Aldrich Co. LLC, St. Louis, US) was used as an oxidizer instead of commonly used iodine. 5'-thio amidite monomers were successfully coupled using an extended coupling (8 min), detritrylation (26.5 min) and oxidation (5 min) times for the modified positions. The synthesized ONs were purified by reverse-phase HPLC (RP-HPLC, Shimadzu Inc., Kyoto, Japan) with Xbridge™ OST C18 column 2.5 µm (4.6 × 50 mm) (Waters Corporation, Milford, US) using 0.1M TEAA (triethylammonium acetate) buffer (pH 7.0) containing 50% MeCN (gradient: 5-17.5% MeCN over 20 min). Composition and purity were characterized by MALDI-TOF mass spectrometry (Autoflex II TOF/TOF mass spectrometer, Bruker Daltonics K.K., Yokohama, Japan) and RP-HPLC. Complementary RNA, DNA, and antisense oligonucleotides (ASOs) incorporated with 5'-thio-modified thymidine and 2'-deoxy-5-methylcytidine were synthesized by GeneDesign, Inc.

2.3. T_m *measurements*

UV melting experiments (*13*) were conducted using a SHIMADZU UV-1800 spectrometer (Shimadzu Inc., Kyoto, Japan) equipped with a T_m analysis accessory. The UV melting profiles were recorded by dissolving the oligonucleotide at 4 µM in 10 mM sodium phosphate buffer (pH 7.2) containing 100 mM NaCl, then scanning at 0.5°C/min and detecting at 260 nm. The temperature at which half the duplex dissociated was considered the T_m. The final T_m values were determined by averaging three independent measurements.

2.4. *Exonuclease stability assay*

Nuclease degradation experiments (*13*) were conducted by hydrolyzing ONs (750 pmol) at 37°C in buffer (100 µL) containing 50 mM Tris-HCl (pH 8.0), 10 mM $MgCl_2$, and 1 µg/mL phosphodiesterase I (GE Healthcare UK Ltd., Buckinghamshire, UK). Aliquots were removed at timed intervals (0, 2.5, 10, 20 and 40 min) and heated to 90°C for more than 2 min to deactivate the nuclease. The collected samples were analyzed by RP-HPLC (6-13% MeCN over 15 min) to evaluate the amount of intact ONs remaining (Figure S22, *http://ddtjournal.com/docindex.php?year=2016&kanno=5*). The percentage of intact ON in each sample was calculated and plotted against the digestion time to obtain a degradation curve.

2.5. *In vitro assay*

NMuLi cells (ATCC®, Manassas, VA), a cell line derived from mouse liver epithelium, were seeded at 3 × 10^3 cells/well in a 96-well plate and incubated in Dulbecco's Modified Eagle's Medium (DMEM, Nakalai Tesque, Kyoto, Japan) containing 10% heat-inactivated fetal bovine serum (FBS) without antibiotics in a 5% CO_2 incubator for 24 h. ASOs were transfected into cells using Lipofectamine 3000 (Thermo Fisher Scientific, Waltham, MA) without changing the medium according to the manufacturer's protocol. After 24 h, the cells were washed with phosphate buffered saline (PBS) once, then cell lysates were produced using the Lysis reagent in a SuperPrep® kit (TOYOBO, Osaka, Japan).

Reverse transcription (RT) was performed using the RT reagent in a SuperPrep® kit (TOYOBO) according to the manufacturer's procedure. The resulting cDNA template was used for quantitative PCR (qPCR) using TaqMan® Fast Universal PCR Master Mix (Thermo Fisher Scientific) and TaqMan® probe targeting phosphatase and tensin homolog (*Pten*) gene (Mm00477208_m1, Thermo Fisher Scientific) or *Gapdh* gene (Mm03302249_g1, Thermo Fisher Scientific). The expression level of each target gene was quantified using the ΔΔCt method, and the level of *Pten* mRNA was normalized to that of *Gapdh* mRNA. IC_{50} of each ASO was calculated by a sigmoidal curve fitting using Igor Pro software.

2.6. *In vivo assay*

All animal experiments were approved by the Institutional Animal Care and Use Committee of Osaka University. 7-week-old male C57BL/6J mice were obtained from Clea Japan (Tokyo, Japan) and were maintained on a 12-h light/12-h dark cycle and fed *ad libitum*. ASOs were intraperitoneally (*i.p.*) administered into individual mouse at 35 mg/kg (n = 4). After 72 h, all mice were sacrificed after anesthetization with isoflurane, perfused with PBS, and the livers were harvested, snap frozen, and the total RNA was isolated using a QuickGene RNA tissue kit SII (Wako, Tokyo, Japan) according to the manufacturer's protocol. Total RNA (1 μg) was reverse transcribed using a High Capacity cDNA Reverse Transcription kit (Thermo Fisher Scientific), then qPCR was performed as described above. Relative expression levels of *Pten* mRNA were evaluated against those of *Gapdh* mRNA. Aspartate aminotransferase (AST) and alanine aminotransferase (ALT) levels were analyzed in blood serum separated using a Microtainer brand tubes (#365967, Becton Dickinson, Franklin Lakes, NJ) from blood collected from the postcaval vein. AST and ALT levels in the blood serum were examined using a FUJI DRI-CHEM7000 clinical chemistry analyzer (Fujifilm, Tokyo, Japan) and FUJI DRI-CHEM slides: GOT/AST-PIII and GPT/ALT-PIII (Fujifilm).

2.7. *RNase H Digestion assay* (*13*)

5'-Cy3-labeled complementary RNA (0.5 μM) and individual antisense ONs (10 μM) were pre-mixed in 55 μL reaction buffer containing 40 mM Tris-HCl (pH 7.2), 150 mM NaCl, 4 mM $MgCl_2$, and 1 mM dithiothreitol (DTT). After incubation for 10 min at 37°C, 0.01 U/μL of *Escherichia coli* RNase H (Takara Bio Inc., Kusatsu, Japan) was added and the mixture was incubated at 37°C. Aliquots were removed at timed intervals and the reaction was terminated by mixing the aliquot with stop solution containing 35 mM EDTA and 2.5 M urea, followed by heating at 95°C for 5 min. The reaction samples were analyzed on 25% denaturing polyacrylamide gels containing 7 M urea, and 5'-Cy3-labeled RNA and digested products were visualized using Image Quant (LAS 4010, GE Healthcare) with a 20 s exposure time.

2.8. *Serum stability assay*

5'-Cy3-labeled ASOs were added to the serum separated from the 8-week-old C57BL/6J mouse blood as described in *in vivo* experiment procedure and the mixtures were incubated at 37°C. Aliquots were removed at timed intervals and the reaction was terminated at 95°C, then the 5'-Cy3-labeled ASOs and digested products were analyzed on 25% denaturing polyacrylamide gels containing 7 M urea. 5'-Cy3-labeled ASOs and digested products were visualized using Image Quant with a 20 s exposure time.

2.9. *Statistical analysis*

Pharmacological studies were performed using 4 mice per treatment group. All data are expressed as means ± S.D. $p < 0.01$ was considered to be statistically significant in all cases. Statistical comparisons of results were performed by Student's multiple comparison *t*-tests.

3. Results and Discussion

3.1. *Phosphoramidite monomer synthesis*

The 5'-thio thymidine phosphoramidite monomer **2a** was obtained as a previously described report (*11*). Then, from known nucleoside **2**, we synthesized the 2',5'-dideoxy-5'-thio-5-methylcytidine amidite monomer **5** (Scheme 1). Briefly, compound **2** was treated with acetic anhydride to obtain 3'-*O*-acetyl protected compound **3** in 84% yield. Benzyl protected 2'-deoxy-5-methylcytidine derivative **4** was obtained from compound **3** using known procedures (*14*) in 56% yield over three steps. Subsequent 3'-*O*-phosphitylation of **4** with 2-cyanoethyl-*N,N,N',N'*-tetraisopropylphosphorodiamidite provided the respective desired phosphoramidites **5** in 79% yield.

3.2. *T_m measurements*

The effect of the 5'-thio modification on duplex forming ability was estimated by measuring the melting temperature of the duplexes between **ON-2-5** and complementary DNA (cDNA) or RNA (cRNA) strands and comparing with those of the corresponding unmodified duplexes with **ON-1**/cDNA or **ON-1**/cRNA as described in Table 1. Single or multiple incorporation of the 5'-thio-modified monomer into different positions of the ONs showed acceptable differences in binding affinity following annealing to cDNA and cRNA (−2 to 1°C/modification).

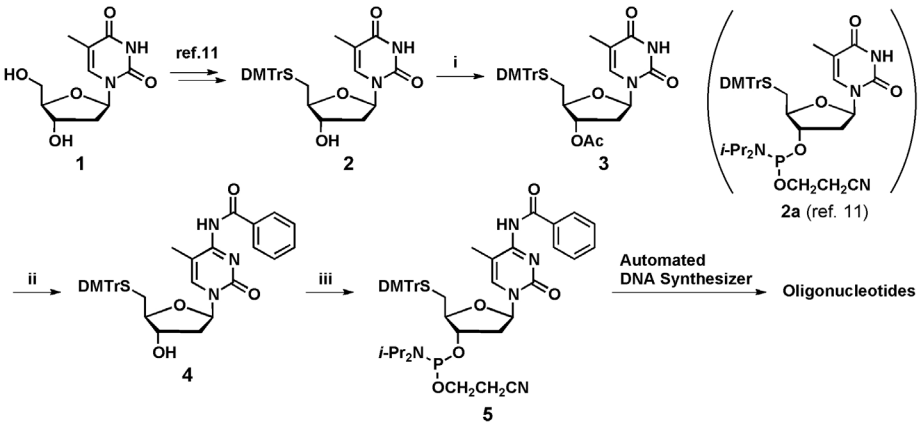

Scheme 1. Reagents and conditions. i. Ac_2O, pyridine, rt, 84%; ii. a. 1,2,4-triazole, $POCl_3$, TEA, MeCN, 0 °C to rt; b. Aq. NH_3, 1,4-dioxane, rt; c. benzoic anhydride, DMF, rt, 56% over 3 steps; iii. diisopropylammonium tetrazolide, 2-cyanoethyl-*N,N,N′,N′*-tetraisopropylphosphorodiamidite, MeCN, THF, rt, 79%.

Table 1. The sequences of 5'-thio modified oligonucleotides using T_m analysis or exonuclease resistance

Abbreviation	Sequences[b]	T_m (ΔT_m/modification) °C[a]	
		DNA[b]	RNA[b]
ON-1	5'-gcgtttttttgct-3'	50	45
ON-2	5'-gcgttt^{S}tttgct-3'	48 (-2.0)	45 (±0)
ON-3	5'-gcgtt^{S}t^{S}t^{S}ttgct-3'	44 (-2.0)	42 (-1)
ON-4	5'-gcgt^{S}tt^{S}tt^{S}tgct-3'	46 (-1.3)	43 (-0.7)
ON-5	5'-gcgttttttg^{Sm}ct-3'	50 (±0)	46 (+1)
ON-6	5'-ttttttttt-3'	N.D.	
ON-7	5'-ttttttttt$_{S}$t-3'	N.D.	
ON-8	5'-ttttttttt^{S}t-3'	N.D.	
ON-9	5'-ttttttttt^{m}c-3'	N.D.	
ON-10	5'-ttttttttt^{Sm}c-3'	N.D.	

ND: Not determined.
[a] UV melting profiles measured in 10 mM phosphate buffer (pH 7.2) containing 100 mM NaCl at a scan rate of 0.5°C/min at 260 nm.
[b] The concentration of oligonucleotide used was 4 μM for each strand. The sequence of complementary DNA or RNA is 5'-AGCAAAAAACGC-3'.
The black case represents natural DNA, and the red case represents as follows: ^{S}t, 5'-thio-t; ^{Sm}c, 5'-thio-^{m}c. The inferior case $_{S}$ indicates a phosphorothioate linkage.

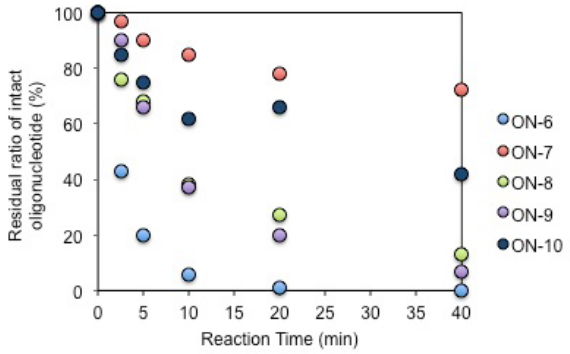

Figure 2. The ability of exonuclease resistance. Hydrolysis of ONs (750 pmol) conducted at 37°C in buffer (100 μL) containing 50 mM Tris-HCl (pH 8.0), 10 mM $MgCl_2$, and phosphodiesterase I (1.0 μg/mL). Sequences: 5′-d(TTTTTTTTTT)-3'; T = thymidine (light blue, **ON-6**), Phosphorothioate thymidine (red, **ON-7**), 5'-thio-thymidine (green, **ON-8**), 2'-deoxy-5-methycytidine (purple, **ON-9**), 2',5'-dideoxy-5'-thio-5-methycytidine (deep blue, **ON-10**).

3.3. *Exonuclease stability assay*

The enzymatic stability of the modified ONs was evaluated using phosphodiesterase I. Comparisons of the exonuclease stabilities of a series of oligonucleotides (**ON-6-10**) are shown in Figure 2. Under the conditions used in this experiment, oligonucleotide containing 2'-deoxy-5-methycytidine (**ON-9**) was more stable than oligonucleotide containing thymidine (**ON-6**). As expected, 5'-thio-modified oligonucleotides **ON-8** and **ON-10** had higher nuclease resistance compared to **ON-6** and **ON-9**, respectively. In contrast, phosphorothioate-modified oligonucleotide (**ON-7**) exhibited more enhanced stability against 3′-exonuclease compared to **ON-6** and **ON-9**.

3.4. *Design of antisense oligonucleotides for in vitro and in vivo assay*

We designed phosphorothioate antisense oligonucleotides (**ASO-1**, Table 2) targeting mouse *Pten* mRNA (NCBI ref: NM_008960.2), an LNA-DNA-LNA (2-8-2) gapmer containing a toxif motif (tgc) in the gap region (*15*). Gapmer design of two LNAs in each wing side with a ten natural nucleotide gap is believed to be sufficient to activate RNase H mediated cleavage of the target mRNA (*16*). Additionally, we prepared other antisense containing a 5'-thio-modified nucleoside, designated **ASO-2-4** as described in Table 2. Except for the 5'-thio modification sites, all those ASOs had a phosphorothioate backbone. In **ASO-2**, the 5'-thio modification was incorporated at the fourth and eighth positions from the 5'-end, whereas in **ASO-3** and **ASO-4**, a single 5'-thio modification was incorporated at the fourth or eighth position from the 5'-end, respectively. The potencies and toxicity characteristics of **ASO-2**, **ASO-3** and **ASO-4** were compared with the positive

Table 2. T_m values of 5'-thio modified oligonucleotides with complementary RNA[a]

Abbreviation	Sequences[b]	T_m (°C)[a]	IC_{50} (nM)[c]
ASO-1	5'-$T_s{}^mC_sa_st_sg_sg_sc_st_sg_sc_sa_sg_s{}^mC_sT$-3'	63.0	9.11
ASO-2	5'-$T_s{}^mC_sa_o{}^{St}t_sg_sg_sc_o{}^{St}t_sg_sc_sa_sg_s{}^mC_sT$-3'	61.5	15.3
ASO-3	5'-$T_s{}^mC_sa_o{}^{St}t_sg_sg_sc_st_sg_sc_sa_sg_s{}^mC_sT$-3'	61.0	6.99
ASO-4	5'-$T_s{}^mC_sa_st_sg_sg_sc_o{}^{St}t_sg_sc_sa_sg_s{}^mC_sT$-3'	61.1	32.2
ASO-5	5'-Cy3$_sT_s{}^mC_sa_st_sg_sg_sc_st_sg_sc_sa_sg_s{}^mC_sT$-3'	N.D.	N.D.
ASO-6	5'-Cy3$_sT_s{}^mC_sa_o{}^{St}t_sg_sg_sc_o{}^{St}t_sg_sc_sa_sg_s{}^mC_sT$-3'	N.D.	N.D.

ND: Not determined.
[a] UV melting profiles measured in 10 mM phosphate buffer (pH 7.2) containing 100 mM NaCl at a scan rate of 0.5°C/min at 260 nm.
[b] The concentration of oligonucleotide was 2 μM for each strand. The sequence of complementary RNA is 5'-AGCUGCAGCCAUGA-3'.
The black lower or upper case represents natural DNA or LNA, and the red case represents as follows: Stt, 5'-thio-t. The inferior case $_S$ or $_O$ indicates a phosphorothioate or a phosphodiester linkage, respectively.
[c] Each ASO was transfected into NMuLi cells using a lipofection method at the concentration of 0.25-200 nM.

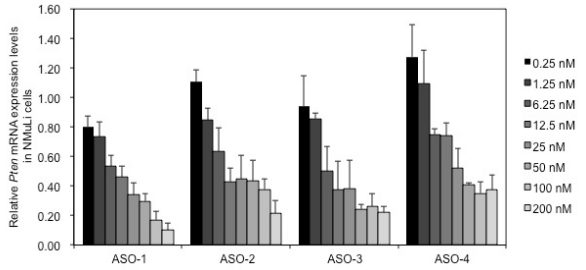

Figure 3. *In vitro* antisense efficiency of ASO-1, -2, -3, and ASO-4. Each ASO was transfected into NMuLi cells at the concentration of 0.25 nM to 200 nM using Lipofectamine3000. After 24 h, the cells were retrieved and the relative expression levels of *Pten* mRNA were determined.

control ASO-1. A thermal melting study was carried out and the T_m values of the ASOs with complementary RNA were determined. As expected, the affinity of all 5'-thio-modified ASOs (**ASO-2-4**) was essentially identical to that of **ASO-1** (Table 2).

3.5. *In vitro assay*

We evaluated the *in vitro* gene silencing properties of the ASOs in mice hepatic NMuLi cells (Figure 3) treated with 0.25-200 nM of each **ASO** in Table 2 using a lipofection method. A dose-dependent reduction of the *Pten* mRNA expression level was observed using qRT-PCR. Furthermore, 5'-thio-modified ASO at the fourth position from the 5'-end (**ASO-3**) showed very good *in vitro* gene silencing activity (Figure 3) with a high IC_{50} (7 nM). In contrast, 5'-thio-modified ASO at the fourth and eighth positions (**ASO-2**) or at the eighth position (**ASO-4**) had a low IC_{50} (13 nM or 28 nM), while the control **ASO-1** showed IC_{50} value of 9 nM.

3.6. *In vivo assay*

The *in vitro* results inspired us to evaluate the mRNA silencing activity of 5'-thio-modified ASO in an *in vivo* model. LNA-modified **ASO-1** (positive control) or 5'-thio-modified ASOs (**ASO-2**, **ASO-3**) were single-dose administered (*i.p.*) to 8-week-old male C57BL/6J mice at 35 mg/kg. After 72 h, all mice were sacrificed and the expression levels of *Pten* mRNA in the liver were analyzed. Figure 4A shows that the antisense oligonucleotide with a 5'-thio modification at the fourth and eighth positions from the 5'-end (**ASO-2**) exhibited almost no antisense activity and no reduction of mRNA expression, similar to that of the saline administered group, whereas LNA-modified **ASO-1** reduced the mRNA expression level by over 60%. On the other hand, **ASO-1** exhibited higher hepatotoxicity compared to **ASO-2** (Figure 4B). A single 5'-thio modification at the fourth position from the 5'-end (**ASO-3**) resulted in somewhat improved antisense activity (Figure 4C) but similar hepatotoxicity to that of **ASO-1** (Figure 4D). An ideal antisense oligonucleotide should exhibit high antisense activity with very low toxicity. These *in vivo* data showed that increasing the number of 5'-thio modifications reduced hepatotoxicity but unexpectedly reduced antisense activity as well.

3.7. *RNase H digestion assay*

RNase H activity provides important information for understanding the mechanism underlying the *in vivo* activity of ASOs. As described above, the *in vivo* activity was not as expected from the *in vitro* data and thus we conducted an RNase H mediated scission assay. Heteroduplexes of complementary RNA with the positive control gapmer antisense oligonucleotide (**ASO-1**) or with the 5'-thio-modified gapmer antisense oligonucleotide (**ASO-2-4**) were examined in the presence of RNase H (Figure 5). The degradation levels of 5'-Cy3-labeled complementary RNA (Cy3-RNA) in the heteroduplexes were analyzed as described above using denaturing-PAGE (Figure 5A). The residual ratios of Cy3-RNA were quantitated by calibrating the fluorescence intensity of Cy3-RNA, and the data were plotted against RNase H digestion time as shown in Figure 5B. The cleavage activity of each ASO against the Cy3-RNA is represented as the half-life ($t_{1/2}$) and the data are summarized in Figure 5C. Compared with **ASO-1**/RNA heteroduplex degradation activity ($t_{1/2}$ = 4.5 min), 5'-thio-modified ASOs more slowly

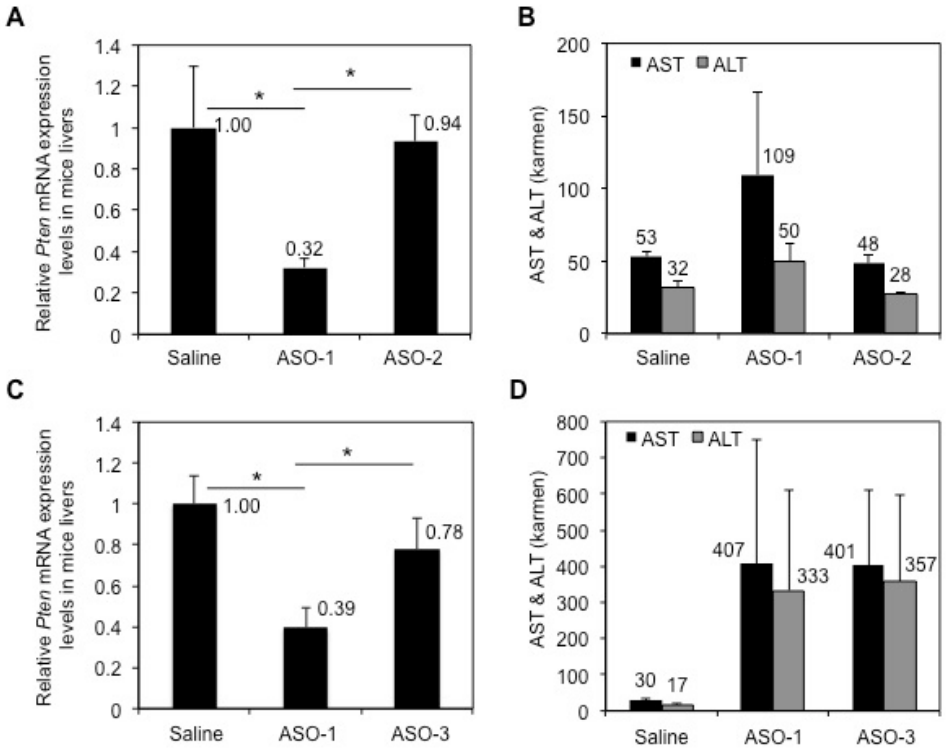

Figure 4. ***In vivo*** **antisense efficiency of ASO-1, -2, -3, and ASO-4 in mice liver.** Each ASO was intraperitoneally administered at 35 mg/kg. Mice were sacrificed after 72 h, and then, the relative expression levels of *Pten* mRNA in livers **(A**, **C)** and the AST, ALT levels in serum were calculated **(B**, **D)**. **p* < 0.01.

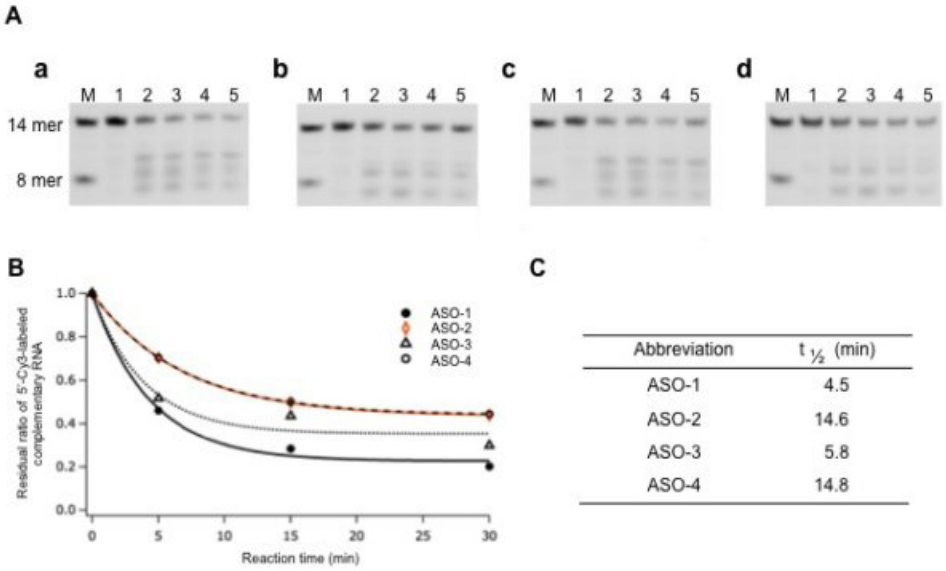

Figure 5. ***E. coli*** **RNase H activity analysis of ASO-1, -2, -3, and ASO-4. (A)** Denaturing PAGE analysis of 5'-Cy3-labeled complementary RNA forming duplexes with **ASO-1 (a)**, **ASO-2 (b)**, **ASO-3 (c)**, or **ASO-4 (d)** after *E. coli* RNase H reaction. M indicates the marker of 5'-Cy3-labeled of 14-mer RNA (5'-Cy3-AGCUGCAGCCAUGA-3') and 8-mer RNA (5'-Cy3-AGCUGCAG-3'). Lines 1-5 represent digestion time at 0, 5, 15, 30, and 60 min, respectively. Conditions of cleavage reaction: 5'-Cy3-labeled RNA (0.5 μM) and 19-22 (10 μM) in reaction buffer containing 40 mM Tris-HCl (pH 7.2), 150 mM NaCl, 4 mM $MgCl_2$, and 1 mM DTT at 37°C with 0.01 U/μL of *E. coli* RNase H. **(B)** Residual ratio of 5'-Cy3-labeled complementary RNA plots after *E. coli* RNase H reaction. **(C)** The half-life periods of 5'-Cy3-labeled complementary RNA forming duplexes with each ASO after *E. coli* RNase H reaction.

but effectively activated RNase H mediated scission. More specifically, **ASO-3** had almost the same half-life ($t_{1/2}$ = 5.8 min) compared with the positive control **ASO-1**. However, the RNase H activity of 5'-thio-modified ASOs at the eighth position or the fourth and eighth position from the 5'-end (**ASO-2**, **ASO-4**) was approximately three times weaker than that of **ASO-3**, indicating that an increase in the number of 5'-thio modifications or changing their position in the sequence was significant for the RNase H activity.

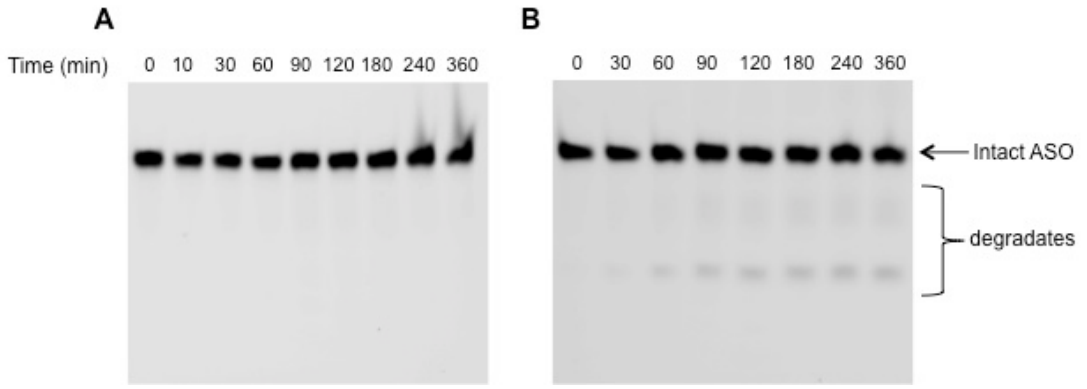

Figure 6. Serum stability assay of ASO-5 and ASO-6 in mouse blood serum. Denaturing PAGE analysis of 5'-Cy3-labeled ASO-1 **(ASO-5**, **A)** and **ASO-2 (ASO-6**, **B)** after adding to mouse serum at 37°C. The serum stability assay was examined up to 360 min.

The RNase H cleavage cascade has been previously reported as follows. First, RNase H binds to the 5' site of the target RNA, forming heteroduplexes with a gap region at the 3' site of the ASO (*17*). Next, the binding domain of RNase H recognizes the phosphorodiester or phosphorothioate linkages of the ASO at the 3' site of the gap region, then the catalytic domain of RNase H interacts with the target RNA at the gap region of the ASO (*17*). Gapmer ASO must contain successive 4-7 natural DNA nucleotides in gap region for the target RNA to be efficiently digested (*18,19*). Consequently, 5'-thio modification of the ASO at the fourth or at the fourth and eighth positions from the 5'-end site would influence RNase H digestion of the target RNA.

3.8. *Serum stability assay*

Chemically modified ASOs are generally more stable in blood serum than is natural DNA (*12*). However, our *in vivo* data suggested that the antisense activity of 5'-thio-modified ASOs may depend on the stability of the ASOs in serum. To confirm whether 5'-thio-modified ASO is stable in serum, we evaluated the blood serum stability of the ASO bearing the 5'-thio-modification at the fourth and eighth positions from the 5'-end (**ASO-2**) and compared it to LNA gapmer antisense oligonucleotide (**ASO-1**). 5'-Cy3 labeled **ASO-1** and **ASO-2** (**ASO-5**, **ASO-6**) was added to the serum collected from an 8-week-old C57BL/6J mouse and reacted for various lengths of time, then analyzed using denaturing-PAGE. As shown in Figure 6A, 5'-Cy3-labeled LNA gapmer ASO (**ASO-5**) was not degraded at all for 360 min. Fluorescently labeled 5'-thio-modified ASO (**ASO-6**) was essentially stable and little degradation was observed (Figure 6B). These results indicate that 5'-thio-modified ASO exhibits very good stability in blood serum and thus should reach the liver after ASO administration.

The *in vitro*, *in vivo*, RNase H activity and serum stability assay data showed discrepancies: the *in vitro* data showed that 5'-thio-modified ASO looked promising whereas the *in vivo* data did not. Initially, we thought that 5'-thio-modified ASO is not facilitated the RNase H mediated scission or is not stable at blood serum, but 5'-thio-modified ASO showed slow but significant RNase H activation as well as high stability in blood serum. Alternatively, it is possible that the sulfur atom at the 5' position alters pharmacokinetic properties such as protein binding and distribution, resulting in lower activity in the *in vivo* model.

4. Conclusion

In conclusion, we incorporated 5'-thio-modified derivatives into a series of ONs and evaluated their *in vitro* and *in vivo* biophysical properties. Inconsistencies between the *in vitro* and *in vivo* data remain unresolved and will be addressed in future studies.

Acknowledgements

One of us (Md Ariful Islam) would like to thank The Ministry of Education, Culture, Sports, Science and Technology (MEXT) of Japan for a research scholarship.

References

1. Matsukura M, Shinozuka K, Zon G, Mitsuya H, Reitz M, Cohen JS, Broder S. Phosphorothioate analogs of oligodeoxynucleotides: Inhibitors of replication and cytopathic effects of human immunodeficiency virus. Proc Natl Acad Sci U S A. 1987; 84:7706-7710.
2. Eckstein F. Nucleoside phosphorothioates. Annu Rev Biochem. 1985; 54:367-402.
3. Yamamoto T, Nakatani M, Narukawa K, Obika S. Antisense drug discovery and development. Future Med Chem. 2011; 3:339-365.
4. Oka N, Wada T. Stereocontrolled synthesis of oligonucleotide analogs containing chiral internucleotidic phosphorus atoms. Chem Soc Rev. 2011; 40:5829-5843.
5. Jahns H, Roos M, Imig J, Baumann F, Wang Y, Gilmour R, Hall J. Stereochemical bias introduced during RNA

synthesis modulates the activity of phosphorothioate siRNAs. Nat Commun. 2015; 6:6317.
6. Li NS, Tuttle N, Staley JP, Piccirilli JA. Synthesis and incorporation of the phosphoramidite derivative of 2′-*O*-photocaged 3′-*S*-thioguanosine into oligoribonucleotides: Substrate for probing the mechanism of RNA catalysis. J Org Chem. 2014; 79:3647-3652.
7. Li NS, Frederiksen JK, Piccirilli JA. Synthesis, properties, and applications of oligonucleotides containing an RNA dinucleotide phosphorothiolate linkage. Acc Chem Res. 2011; 44:1257-1269.
8. Gaynor JW, Cosstick R. Synthesis, properties and application of nucleic acids containing phosphorothiolate linkages. Curr Org Chem. 2008; 12:291-308.
9. Li NS, Tuttle N, Staley JP, Piccirilli JA. Synthesis and incorporation of the phosphoramidite derivative of 2′-O-photocaged 3′-S-thioguanosine into oligoribonucleotides: Substrate for probing the mechanism of RNA catalysis. J Org Chem. 2014; 79:3647-3652.
10. Connolly BA, Rider P. Chemical synthesis of oligonucleotides containing a free sulphydryl group and subsequent attachment of thiol specific probes. Nucleic Acids Res. 1985; 13:4485-4502.
11. Hofmann KJ, Engels JW. Efficient solid phase synthesis of cleavable oligodeoxynucleotides based on a novel strategy for the synthesis of 5'-S-(4,4'-dimethoxytrityl)-2'-deoxy-5'-thionucleoside phosphoramidites. Helv Chim Acta. 2004; 87:2812-2828.
12. Wahlestedt C, Salmi P, Good L, *et al*. Potent and nontoxic antisense oligonucleotides containing locked nucleic acids. Proc Natl Acad Sci U S A. 2000; 97:5633-5638.
13. Mitsuoka Y, Fujimura Y, Waki R, Kugimiya A, Yamamoto T, Hari Y, Obika S. Sulfonamide-bridged nucleic acid: Synthesis, high RNA selective hybridization, and high nuclease resistance. Org Lett. 2014; 16:5640-5643.
14. Koshkin AA. Conformationally restricted triplex-forming oligonucleotides (TFOs) binding properties of α-L-LNA and introduction of the N^7-glycosylated LNA-guanosine. Tetrahedron. 2006; 62:5962-5972.
15. Burdick AD, Sciabola S, Mantena SR, Hollingshead BD, Stanton R, Warneke JA, Zeng M, Martsen E, Medvedev A, Makarov SS, Reed LA, Davis JW, Whiteley LO. Sequence motifs associated with hepatotoxicity of locked nucleic acid–modified antisense oligonucleotides. Nucleic Acids Res. 2014; 42:4882-4891.
16. Yamamoto T, Harada-Shiba M, Nakatani M, Wada S, Yasuhara H, Narukawa K, Sasaki K, Shibata MA, Torigoe H, Yamaoka T, Imanishi T, Obika S. Cholesterol-lowering action of BNA-based antisense oligonucleotides targeting PCSK9 in atherogenic diet-induced hypercholesterolemic mice. Mol Ther Nucleic Acids. 2012; 1:e22.
17. Lima WF, Rose JB, Nichols JG, Wu H, Migawa MT, Wyrzkiewicz TK, Siwkowski AM, Crooke ST. Human RNase H1 discriminates between subtle variations in the structure of the heteroduplex substrate. Mol Pharmacol. 2007; 71:83-91.
18. Kurreck J, Wyszko E, Clemens G, Erdmann V. Design of antisense oligonucleotides stabilized by locked nucleic acids. Nucleic Acids Res. 2002; 30:1911-1918.
19. Crooke ST, Lemonidis KM, Neilson L, Griffey R, Lesnik EA, Monia BP. Kinetic characteristics of *Escherichia coli* RNase H1: Cleavage of various antisense oligonucleotide-RNA duplexes. Biochem J. 1995; 312:599-608.

(Received August 30, 2016; Revised October 22, 2016; Accepted October 24, 2016)

Commentary

DOI: 10.5582/ddt.2016.01056

Nucleic acid drugs and DNA-based delivery systems

Makiya Nishikawa*

Department of Biopharmaceutics and Drug Metabolism, Graduate School of Pharmaceutical Sciences, Kyoto University, Kyoto, Japan.

Summary **Nucleic acids are biologically active materials, and chemically modified nucleic acids are now being used in nucleic acid drugs. DNA, one of the two types of nucleic acids, can also be used as a material to construct DNA-based delivery systems, such as DNA hydrogel, for therapeutic compounds. Use of chemically modified nucleic acids would greatly increase the therapeutic potency of such DNA-based delivery systems. However, attention should be paid to the differences in the physicochemical properties of natural and chemically modified nucleic acids. Another, more important concern for chemically modified nucleic acids is the high cost of their synthesis. Reducing the cost of synthesizing oligonucleotides, and especially ones with chemically modified nucleic acids, is crucial to the expanded use of both nucleic acid drugs and DNA-based delivery systems.**

Keywords: Nucleic acid drug, DNA-based delivery system

Amplification of specific sequences of DNA is now widely performed in many laboratories all over the world. This polymerase chain reaction process requires pairs of primers, which are short DNA or oligodeoxynucleotides (ODNs). Therefore, huge amounts of ODNs are being commercially synthesized and used every single day. This large-scale synthesis of ODNs has greatly reduced the cost of this process. The cost of ODNs depends on oligo companies, but the most inexpensive ones are about ¥1,000 Japanese yen (about $10 US dollar) for each milligram of ODN of about 90 nucleotides or shorter. Oligoribonucleotides and oligonucleotides with chemical modifications are generally much more expensive than natural phosphodiester ODNs. The process of purifying oligonucleotides increases their quality but also their cost.

Nucleic acid drugs, including antisense oligonucleotides, aptamer, small interfering RNA, and immunomodulatory oligonucleotides, have attracted considerable attention over the past years. There are only a few clinically approved nucleic acid drugs worldwide, but numerous candidates are being developed. Mipomersen, an antisense oligonucleotide targeting human apolipoprotein B100 mRNA, is a 20-mer oligonucleotide (*1*). It is one of the "second-generation" antisense oligonucleotides, in which the nucleotides are linked with phosphorothioate linkages, and the sugar parts of the both ends are 2'-O-methoxyethyl-modified ribose. These chemical modifications are necessary for nucleic acid drugs because degradation by enzymes precludes them from displaying pharmacological activity *in vivo*. A pioneer study that systemically administered antisense oligonucleotides to mice found that ODNs with a few modifications were very quickly degraded and eliminated from the circulation (*2*). Chemical modification, however, will also significantly alter the physicochemical properties of nucleic acid drugs. A typical example of such alterations is the high protein binding capacity of phosphorothioate oligonucleotides, which greatly regulates their plasma protein binding and tissue distribution (*3*). Therefore, oligonucleotides with specific chemical modifications may have identical base sequences but they do, in fact, differ from one another.

The current authors have developed self-gelatinizable nucleic acid technology (*4*), by which injectable DNA hydrogels are obtained using two or more ODNs in a very simple process. This DNA hydrogel is a promising

Released online in J-STAGE as advance publication October 23, 2016.

**Address correspondence to:*
Dr. Makiya Nishikawa, Department of Biopharmaceutics and Drug Metabolism, Graduate School of Pharmaceutical Sciences, Kyoto University, Sakyo-ku, Kyoto 606-8501, Japan.
E-mail: makiya@pharm.kyoto-u.ac.jp

DNA-based delivery system for bioactive compounds. The current authors have shown that DNA hydrogel is useful for sustained delivery of doxorubicin (an anticancer agent), peptides, and proteins (*5,6*). The physicochemical and biological properties of this DNA hydrogel can be modulated through the use of chemically modified nucleotides, which would greatly increase its therapeutic potency and, inevitably, the cost of its synthesis. Therefore, reducing the cost of synthesizing oligonucleotides is crucial to the development and expanded use of both nucleic acid drugs and DNA-based delivery systems, such as DNA hydrogel.

References

1. Raal FJ, Santos RD, Blom DJ, Marais AD, Charng MJ, Cromwell WC, Lachmann RH, Gaudet D, Tan JL, Chasan-Taber S, Tribble DL, Flaim JD, Crooke ST. Mipomersen, an apolipoprotein B synthesis inhibitor, for lowering of LDL cholesterol concentrations in patients with homozygous familial hypercholesterolaemia: A randomised, double-blind, placebo-controlled trial. Lancet. 2010; 375:998-1006.
2. Miyao T, Takakura Y, Akiyama T, Yoneda F, Sezaki H, Hashida M. Stability and pharmacokinetic characteristics of oligonucleotides modified at terminal linkages in mice. Antisense Res Develop.1995; 5:115-121.
3. Kurreck J. Antisense technologies: Improvement through novel chemical modifications. Eur J Biochem. 2003; 270:1628-1644.
4. Nishikawa M, Ogawa K, Umeki Y, Mohri K, Kawasaki Y, Watanabe H, Takahashi N, Kusuki E, Takahashi R, Takahashi Y, Takakura Y. Injectable, self-gelling, biodegradable, and immunomodulatory DNA hydrogel for antigen delivery. J Control Release. 2014; 180:25-32.
5. Nishikawa M, Mizuno Y, Mohri K, Matsuoka N, Rattanakiat S, Takahashi Y, Funabashi H, Luo D, Takakura Y. Biodegradable CpG DNA hydrogels for sustained delivery of doxorubicin and immunostimulatory signals in tumor-bearing mice. Biomaterials. 2011; 32:488-494.
6. Umeki Y, Mohri K, Kawasaki Y, Watanabe H, Takahashi R, Takahashi Y, Takakura Y, Nishikawa M. Induction of potent antitumor immunity by sustained release of cationic antigen from a DNA-based hydrogel with adjuvant activity. Adv Funct Mater. 2015; 25:5758-5767.

(Received August 30, 2016; Revised September 21, 2016; Accepted September 23, 2016)

Commentary

DOI: 10.5582/ddt.2016.01070

Can colorectal delivery technology provide a platform for enteral oligonucleotide-based therapeutics?

Masahiro Murakami*, Chie Watanabe

Laboratory of Pharmaceutics, Faculty of Pharmacy, Osaka Ohtani University, Osaka, Japan.

Summary **Nucleic acid-based therapeutics including antisense and siRNA oligonucleotides has been expected as an innovative treatment for intractable diseases. Oral drug delivery is the most patient-friendly route of administration but developing an effective delivery system for oligonucleotides remains a major challenge. In this commentary, we discuss the potential benefits of the colorectal route as another platform for the development of oral oligonucleotide therapeutics. The importance of the targeting or the availability of oligonucleotides in targeted tissue is highlighted in contrast to systemic availability, while the liver-targeted enteral siRNA delivery technology that we recently developed is introduced.**

Keywords: Oligonucleotide, drug delivery, siRNA, large intestine, liver, lymph

Oligonucleotides are promising candidates for effective therapeutic entities, not only for genetic or intractable diseases, but also for various other illnesses (*1,2*). Most major chronic diseases that account for the majority of deaths are refractory in nature. It is becoming clear that nucleic acid medicines are effective treatments for these diseases. Suppressing disease-specific gene expression using small interfering RNA (siRNA) or antisense oligonuclotide is quite effective and a promising treatment modality (*3*), but the success of this technique depends on nucleic acid molecules selectively reaching the target gene in the body. It also goes without saying that the *in vivo* stability and target specificity of the nucleic acid molecules themselves are important factors. Advances in nucleic acid synthesis techniques with chemical modifications including the introduction of phosphorothioate linkages and 2'-*O*-methylation of the ribose moieties have led to the development of nucleic acids that are resistant to nucleolytic enzymes and are extremely stable *in vivo*, improvements in the selectivity and affinity towards target genes, and significant reductions in the risk of off-target adverse effects (*4-9*). The cost of synthesizing nucleic acid molecules has also continued to decline, while the cost-benefit ratio, which has been a bottleneck for oral drug development, has also been rapidly improving (*10*). However, many significant hurdles must be overcome to develop oral drugs based on nucleic acids. First, there is an issue with stability with respect to enzyme degradation in the alimentary canal and permeability through the intestinal epithelium by nucleic acids, which are polyanionic macromolecules. Another unresolved issue is the mechanism by which they are transported selectively to the target tissue. On the other hand, there have been a number of recent reports on the oral and enteral delivery of nucleic acid molecules, including in humans, suggesting its feasibility (*11-13*). However, these studies have focused on absorption through the small intestine and accordingly it is necessary to include large quantities of nucleic acids as well as absorption promoters. Therefore, these results may not provide sufficient grounds for initiating drug development based on high-cost nucleic acid molecules. We designed a delivery system aimed at the systemic liver-specific delivery of nucleic acid molecules from the large intestine, including the colon and rectum (*14*). This system succeeded in suppressing serum lipid levels by specifically delivering siRNA in mice from the colon to the target organ, which was the liver, where the targeted *ApoB* gene was suppressed. In this system, vitamin E was bonded to the siRNA to achieve liver-specific delivery. In order to improve

**Address correspondence to:*
Dr. Masahiro Murakami, Laboratory of Pharmaceutics, Faculty of Pharmacy, Osaka Ohtani University, 3-11-1 Nisikiori-Kita, Tondabayashi-shi, Osaka 584-8540, Japan.
E-mail: murakam@osaka-ohtani.ac.jp

intestinal epithelial permeability, this was prepared in the form of nanoparticles combined with long-chain unsaturated fatty acids. By post-prandial administration when chylomicron synthesis is elevated, effective and specific delivery from the alimentary canal to the liver was achieved. This system is characterized by utilizing an endogenous transport carrier without the use of an artificial carrier, such as a virus or polymer. In addition, the importance of targeting or the availability of oligonucleotides in targeted tissue should be highlighted in contrast to systemic availability, which does not directly reflect the effects of oligonucleotide. This is because a lower systemic availability can be compensated by a higher accumulation of the oligonucleotide in the target tissue.

There are differences between drug preparations targeting the small intestine and those targeting the colon and rectum. The small intestine has the advantage of high rates of synthesis and internal chylomicron secretion. However, there is a high likelihood of significant nucleic acid losses as well as reductions or fluctuations in the effectiveness of absorption promoters. This occurs by many mechanisms, including high decomposition activity owing to the secretion of digestive enzymes, significant dilution of active ingredients and adjuvants eluted from drugs by food and digestive fluids in the gut lumen, and a relatively low residence time. In addition, the small intestine has much larger surface area for digestion and lower susceptibility to the effects of most absorption enhancers compared to the large intestine (*15*). Therefore, it is necessary to load large amounts of nucleic acids and absorption promoters, resulting in high costs. In addition, the risk of adverse effects may also be high.

On the other hand, water absorption takes place in the colon and accordingly there is a relatively low degree of dilution and a significant reduction in enzyme activity compared to the upper gastrointestinal tract. In addition, the local physicochemical environment in the colon and rectum can be temporarily controlled to an extent using additives. In our system, the formation of complexes with chylomicrons is the key to targeted delivery to the liver, but the chylomicrons secreted in the small intestine accumulate at high concentrations in intestinal lymphatics and eventually thoracic lymph duct. Macromolecules, such as siRNA, exhibit excellent selective transfer to the lymphatic system, and molecules with hydrophobic modifications have particularly high self-associating properties as well as a high rate of bonding with proteins, potentially enabling increased targeting to the lymphatic system (*16*). As a result, vitamin E-modified siRNA that passes through the colonic epithelium progresses within lymph vessels and has many opportunities to form complexes with chylomicrons before entering the systemic circulation *via* the thoracic duct. Macromolecular movement towards the lymphatic system increases as the molecular weight increases, but absorption through the gastrointestinal tract decreases with molecular weight (*17*). As a result, it is highly likely that an optimal molecular weight exists for the liver-specific delivery of nucleic acid molecules *via* lymph vessels from the gastrointestinal tract. However, further insight in this area will require additional research.

Our systemic delivery technique for nucleic acids *via* the large intestine not only has the potential to be developed into a drug for use as an enema or suppository, but could also be developed into an oral drug, taking advantage of a colonic drug delivery system (*18-20*). Thus, this colorectal delivery technique may provide a new foundation for the development of oligonucleotide-based oral therapeutics.

References

1. Juliano R, Alam MR, Dixit V, Kang H. Mechanisms and strategies for effective delivery of antisense and siRNA oligonucleotides. Nucleic Acids Res. 2008; 36:4158-4171.
2. Yu B, Zhao X, Lee LJ, Lee RJ. Targeted delivery systems for oligonucleotide therapeutics. AAPS J. 2009; 11:195-203.
3. Kole R, Krainer AR, Altman S. RNA therapeutics: Beyond RNA interference and antisense oligonucleotides. Nat Rev Drug Discov. 2012; 11:125-140.
4. Kurreck J. Antisense technologies. Improvement through novel chemical modifications. Eur J Biochem. 2003; 270:1628-1644.
5. Freier SM, Altmann KH. The ups and downs of nucleic acid duplex stability: Structure-stability studies on chemically-modified DNA:RNA duplexes. Nucleic Acids Res. 1997; 25:4429-4443.
6. Obika S, Nanbu D, Hari Y, Andoh J, Morio K, Doi T, Imanishi T. Stability and structural features of the duplexes containing nucleoside analogues with a fixed N-type conformation, 2′-O,4′-C-methyleneribonucleosides. Tetrahedron Lett. 1998; 39:5401-5404.
7. Singh SK, Koshkin AA, Wengel J, Nielsen P. LNA (locked nucleic acids): Synthesis and high-affinity nucleic acid recognition. Chem Commun. 1998; 4:455-456.
8. Straarup EM, Fisker N, Hedtjärn M, Lindholm MW, Rosenbohm C, Aarup V, Hansen HF, Ørum H, Hansen JB, Koch T. Short locked nucleic acid antisense oligonucleotides potently reduce apolipoprotein B mRNA and serum cholesterol in mice and non-human primates. Nucleic Acids Res. 2010; 38:7100-7111.
9. Nishina K, Piao W, Yoshida-Tanaka K, et al. DNA/RNA heteroduplex oligonucleotide for highly efficient gene silencing. Nat Commun. 2015; 6:7969.
10. Hardee GE. Oral delivery of nucleic acid-based therapeutics. Ther Deliv. 2012; 3:143-145.
11. Date AA, Hanes J, Ensign LM. Nanoparticles for oral delivery: Design, evaluation and state-of-the-art. J Control Rel. 2016; 240:504-526.
12. Akhtar S. Oral delivery of siRNA and antisense oligonucleotides. J Drug Targeting. 2009; 17:491-495.
13. Tillman LG, Geary RS, Hardee GE. Oral delivery of antisense oligonucleotides in man. J Pharm Sci. 2008; 97:225-236.

14. Murakami M, Nishina K, Watanabe C, Yoshida-Tanaka K, Piao W, Kuwahara H, Horikiri Y, Miyata K, Nishiyama N, Kataoka K, Yoshida M, Mizusawa H, Yokota T. Enteral siRNA delivery technique for therapeutic gene silencing in the liver *via* the lymphatic route. Sci Rep. 2015; 5:17035.
15. Muranishi S. Absorption enhancers. Crit Rev Ther Drug Carrier Syst. 1990; 7:1-33.
16. Reddy LH, Murthy RS. Lymphatic transport of orally administered drugs. Indian J Exp Biol. 2002; 40:1097-1109.
17. Muranishi S, Takada K, Yoshikawa H, Murakami M. Enhanced absorption and lymphatic transport of macromolecules *via* the rectal route. In: Delivery Systems for Peptide Drugs (Davis SS, Illum L, Tomlinson E, eds.). NATO ASI Series, Springer, US, 1986; pp. 177-189.
18. Amidon S, Brown JE, Dave VS. Colon-targeted oral drug delivery systems: Design trends and approaches. AAPS PharmSciTech. 2015; 16:731-741.
19. Prasanth VV, Jayaprakash R, Mathew ST. Colon specific drug delivery systems: A review on various pharmaceutical approaches. JAPS. 2012:163-169.
20. Shibata N, Ohno T, Shimokawa T, Hu Z, Yoshikawa Y, Koga K, Murakami M, Takada K. Application of pressure-controlled colon delivery capsule to oral administration of glycyrrhizin in dogs. J Pharm Pharmacol. 2001; 53:441-447.

(Received October 11, 2016; Revised October 17, 2016; Accepted October 25, 2016)

DD&T
Drug Discoveries & Therapeutics

Guide for Authors

1. Scope of Articles

Drug Discoveries & Therapeutics welcomes contributions in all fields of pharmaceutical and therapeutic research such as medicinal chemistry, pharmacology, pharmaceutical analysis, pharmaceutics, pharmaceutical administration, and experimental and clinical studies of effects, mechanisms, or uses of various treatments. Studies in drug-related fields such as biology, biochemistry, physiology, microbiology, and immunology are also within the scope of this journal.

2. Submission Types

Original Articles should be well-documented, novel, and significant to the field as a whole. An Original Article should be arranged into the following sections: Title page, Abstract, Introduction, Materials and Methods, Results, Discussion, Acknowledgments, and References. Original articles should not exceed 5,000 words in length (excluding references) and should be limited to a maximum of 50 references. Articles may contain a maximum of 10 figures and/or tables.

Brief Reports definitively documenting either experimental results or informative clinical observations will be considered for publication in this category. Brief Reports are not intended for publication of incomplete or preliminary findings. Brief Reports should not exceed 3,000 words in length (excluding references) and should be limited to a maximum of 4 figures and/or tables and 30 references. A Brief Report contains the same sections as an Original Article, but the Results and Discussion sections should be combined.

Reviews should present a full and up-to-date account of recent developments within an area of research. Normally, reviews should not exceed 8,000 words in length (excluding references) and should be limited to a maximum of 100 references. Mini reviews are also accepted.

Policy Forum articles discuss research and policy issues in areas related to life science such as public health, the medical care system, and social science and may address governmental issues at district, national, and international levels of discourse. Policy Forum articles should not exceed 2,000 words in length (excluding references).

Case Reports should be detailed reports of the symptoms, signs, diagnosis, treatment, and follow-up of an individual patient. Case reports may contain a demographic profile of the patient but usually describe an unusual or novel occurrence. Unreported or unusual side effects or adverse interactions involving medications will also be considered. Case Reports should not exceed 3,000 words in length (excluding references).

News articles should report the latest events in health sciences and medical research from around the world. News should not exceed 500 words in length.

Letters should present considered opinions in response to articles published in Drug Discoveries & Therapeutics in the last 6 months or issues of general interest. Letters should not exceed 800 words in length and may contain a maximum of 10 references.

3. Editorial Policies

Ethics: Drug Discoveries & Therapeutics requires that authors of reports of investigations in humans or animals indicate that those studies were formally approved by a relevant ethics committee or review board.

Conflict of Interest: All authors are required to disclose any actual or potential conflict of interest including financial interests or relationships with other people or organizations that might raise questions of bias in the work reported. If no conflict of interest exists for each author, please state "There is no conflict of interest to disclose".

Submission Declaration: When a manuscript is considered for submission to Drug Discoveries & Therapeutics, the authors should confirm that 1) no part of this manuscript is currently under consideration for publication elsewhere; 2) this manuscript does not contain the same information in whole or in part as manuscripts that have been published, accepted, or are under review elsewhere, except in the form of an abstract, a letter to the editor, or part of a published lecture or academic thesis; 3) authorization for publication has been obtained from the authors' employer or institution; and 4) all contributing authors have agreed to submit this manuscript.

Cover Letter: The manuscript must be accompanied by a cover letter signed by the corresponding author on behalf of all authors. The letter should indicate the basic findings of the work and their significance. The letter should also include a statement affirming that all authors concur with the submission and that the material submitted for publication has not been published previously or is not under consideration for publication elsewhere. The cover letter should be submitted in PDF format. For example of Cover Letter, please visit http://www.ddtjournal.com/downcentre.php (Download Centre).

Copyright: A signed JOURNAL PUBLISHING AGREEMENT (JPA) must be provided by post, fax, or as a scanned file before acceptance of the article. Only forms with a hand-written signature are accepted. This copyright will ensure the widest possible dissemination of information. A form facilitating transfer of copyright can be downloaded by clicking the appropriate link and can be returned to the e-mail address or fax number noted on the form (Please visit Download Centre). Please note that your manuscript will not proceed to the next step in publication until the JPA form is received. In addition, if excerpts from other copyrighted works are included, the author(s) must obtain written permission from the copyright owners and credit the source(s) in the article.

Suggested Reviewers: A list of up to 3 reviewers who are qualified to assess the scientific merit of the study is welcomed. Reviewer information including names, affiliations, addresses, and e-mail should be provided at the same time the manuscript is submitted online. Please do not suggest reviewers with known conflicts of interest, including participants or anyone with a stake in the proposed research; anyone from the same institution; former students, advisors, or research collaborators (within the last three years); or close personal contacts. Please note that the Editor-in-Chief may accept one or more of the proposed reviewers or may request a review by other qualified persons.

Language Editing: Manuscripts prepared by authors whose native language is not English should have their work proofread by a native English speaker before submission. If not, this might delay the publication of your manuscript in Drug Discoveries & Therapeutics.

The Editing Support Organization can provide English proofreading, Japanese-English translation, and Chinese-English translation services to authors who want to publish in Drug Discoveries & Therapeutics and need assistance before submitting a manuscript. Authors can visit this organization directly at http://www.iacmhr.com/iac-eso/support.php?lang=en. IAC-ESO was established to facilitate manuscript preparation by researchers whose native language is not English and to help edit works intended for international academic journals.

4. Manuscript Preparation

Manuscripts should be written in clear, grammatically correct English and submitted as a Microsoft Word file in a single-column format. Manuscripts must be paginated and typed in 12-point Times New Roman font with 24-point line spacing. Please do not embed figures in the text. Abbreviations should be used as little as possible and should be explained at first mention unless the term is a well-known abbreviation (*e.g.* DNA). Single words should not be abbreviated.

Title page: The title page must include 1) the title of the paper (Please note the title should be short, informative, and contain the major key words); 2) full name(s) and affiliation(s) of the author(s), 3) abbreviated names of the author(s), 4) full name, mailing address, telephone/fax numbers, and e-mail address of the corresponding author; and 5) conflicts of interest (if you have an actual or potential conflict of interest to disclose, it must be included as a footnote on the title page of the manuscript; if no conflict of interest exists for each author, please state "There is no conflict of interest to disclose"). Please visit Download Centre and refer to the title page of the manuscript sample.

Abstract: The abstract should briefly state the purpose of the study, methods, main findings, and conclusions. For article types including Original Article, Brief Report, Review, Policy Forum, and Case Report, a one-paragraph abstract consisting of no more than 250 words must be included in the manuscript. For News and Letters, a brief summary of main content in 150 words or fewer should be included in the manuscript. Abbreviations must be kept to a minimum and non-standard abbreviations explained in brackets at first mention. References should be avoided in the abstract. Key words or phrases that do not occur in the title should be included in the Abstract page.

Introduction: The introduction should be a concise statement of the basis for the study and its scientific context.

Materials and Methods: The description should be brief but with sufficient detail to enable others to reproduce the experiments. Procedures that have been published previously should not be described in detail but appropriate references should simply be cited. Only new and significant modifications of previously published procedures require complete description. Names of products and manufacturers with their locations (city and state/country) should be given and sources of animals and cell lines should always be indicated. All clinical investigations must have been conducted in accordance with Declaration of Helsinki principles. All human and animal studies must have been approved by the appropriate institutional review board(s) and a specific declaration of approval must be made within this section.

Results: The description of the experimental results should be succinct but in sufficient detail to allow the experiments to be analyzed and interpreted by an independent reader. If necessary, subheadings may be used for an orderly presentation. All figures and tables must be referred to in the text.

Discussion: The data should be interpreted concisely without repeating material already presented in the Results section. Speculation is permissible, but it must be well-founded, and discussion of the wider implications of the findings is encouraged. Conclusions derived from the study should be included in this section.

Acknowledgments: All funding sources should be credited in the Acknowledgments section. In addition, people who contributed to the work but who do not meet the criteria for authors should be listed along with their contributions.

References: References should be numbered in the order in which they appear in the text. Citing of unpublished results, personal communications, conference abstracts, and theses in the reference list is not recommended but these sources may be mentioned in the text. In the reference list, cite the names of all authors when there are fifteen or fewer authors; if there are sixteen or more authors, list the first three followed by *et al*. Names of journals should be abbreviated in the style used in PubMed. Authors are responsible for the accuracy of the references. Examples are given below:

Example 1 (Sample journal reference):
Nakata M, Tang W. Japan-China Joint Medical Workshop on Drug Discoveries and Therapeutics 2008: The need of Asian pharmaceutical researchers' cooperation. Drug Discov Ther. 2008; 2:262-263.

Example 2 (Sample journal reference with more than 15 authors):
Darby S, Hill D, Auvinen A, *et al*. Radon in homes and risk of lung cancer: Collaborative analysis of individual data from 13 European case-control studies. BMJ. 2005; 330:223.

Example 3 (Sample book reference):
Shalev AY. Post-traumatic stress disorder: Diagnosis, history and life course. In: Post-traumatic Stress Disorder, Diagnosis, Management and Treatment (Nutt DJ, Davidson JR, Zohar J, eds.). Martin Dunitz, London, UK, 2000; pp. 1-15.

Example 4 (Sample web page reference):
World Health Organization. The World Health Report 2008 – primary health care: Now more than ever. *http://www.who.int/whr/2008/whr08_en.pdf* (accessed September 23, 2010).

Tables: All tables should be prepared in Microsoft Word or Excel and should be arranged at the end of the manuscript after the References section. Please note that tables should not in image format. All tables should have a concise title and should be numbered consecutively with Arabic numerals. If necessary, additional information should be given below the table.

Figure Legend: The figure legend should be typed on a separate page of the main manuscript and should include a short title and explanation. The legend should be concise but comprehensive and should be understood without referring to the text. Symbols used in figures must be explained.

Figure Preparation: All figures should be clear and cited in numerical order in the text. Figures must fit a one- or two-column format on the journal page: 8.3 cm (3.3 in.) wide for a single column, 17.3 cm (6.8 in.) wide for a double column; maximum height: 24.0 cm (9.5 in.). Please make sure that artwork files are in an acceptable format (TIFF or JPEG) at minimum resolution (600 dpi for illustrations, graphs, and annotated artwork, and 300 dpi for micrographs and photographs). Please provide all figures as separate files. Please note that low-resolution images are one of the leading causes of article resubmission and schedule delays. All color figures will be reproduced in full color in the online edition of the journal at no cost to authors.

Units and Symbols: Units and symbols conforming to the International System of Units (SI) should be used for physicochemical quantities. Solidus notation (*e.g.* mg/kg, mg/mL, mol/mm^2/min) should be used. Please refer to the SI Guide www.bipm.org/en/si/ for standard units.

Supplemental data: Supplemental data might be useful for supporting and enhancing your scientific research and Drug Discoveries & Therapeutics accepts the submission of these materials which will be only published online alongside the electronic version of your article. Supplemental files (figures, tables, and other text materials) should be prepared according to the above guidelines, numbered in Arabic numerals (*e.g.*, Figure S1, Figure S2, and Table S1, Table S2) and referred to in the text. All figures and tables should have titles and legends. All figure legends, tables and supplemental text materials should be placed at the end of the paper. Please note all of these supplemental data should be provided at the time of initial submission and note that the editors reserve the right to limit the size and length of Supplemental Data.

5. Submission Checklist

The Submission Checklist will be useful during the final checking of a manuscript prior to sending it to Drug Discoveries & Therapeutics for review. Please visit Download Centre and download the Submission Checklist file.

6. Online submission

Manuscripts should be submitted to Drug Discoveries & Therapeutics online at http://www.ddtjournal.com. The manuscript file should be smaller than 5 MB in size. If for any reason you are unable to submit a file online, please contact the Editorial Office by e-mail at office@ddtjournal.com

7. Accepted manuscripts

Proofs: Galley proofs in PDF format will be sent to the corresponding author *via* e-mail. Corrections must be returned to the editor (proof-editing@ddtjournal.com) within 3 working days.

Offprints: Authors will be provided with electronic offprints of their article. Paper offprints can be ordered at prices quoted on the order form that accompanies the proofs.

Page Charge: A page charge of $140 will be assessed for each printed page of an accepted manuscript. The charge for printing color figures is $340 for each page. Under exceptional circumstances, the author(s) may apply to the editorial office for a waiver of the publication charges at the time of submission.

(Revised February 2013)

Editorial and Head Office:

Pearl City Koishikawa 603
2-4-5 Kasuga, Bunkyo-ku
Tokyo 112-0003
Japan
Tel: +81-3-5840-9697
Fax: +81-3-5840-9698
E-mail: office@ddtjournal.com

DD&T
Drug Discoveries & Therapeutics

JOURNAL PUBLISHING AGREEMENT (JPA)

Manuscript No.:

Title:

Corresponding author:

The International Advancement Center for Medicine & Health Research Co., Ltd. (IACMHR Co., Ltd.) is pleased to accept the above article for publication in Drug Discoveries & Therapeutics. The International Research and Cooperation Association for Bio & Socio-Sciences Advancement (IRCA-BSSA) reserves all rights to the published article. Your written acceptance of this JOURNAL PUBLISHING AGREEMENT is required before the article can be published. Please read this form carefully and sign it if you agree to its terms. The signed JOURNAL PUBLISHING AGREEMENT should be sent to the Drug Discoveries & Therapeutics office (Pearl City Koishikawa 603, 2-4-5 Kasuga, Bunkyo-ku, Tokyo 112-0003, Japan; E-mail: office@ddtjournal.com; Tel: +81-3-5840-9697; Fax: +81-3-5840-9698).

1. Authorship Criteria

As the corresponding author, I certify on behalf of all of the authors that:

1) The article is an original work and does not involve fraud, fabrication, or plagiarism.
2) The article has not been published previously and is not currently under consideration for publication elsewhere. If accepted by Drug Discoveries & Therapeutics, the article will not be submitted for publication to any other journal.
3) The article contains no libelous or other unlawful statements and does not contain any materials that infringes upon individual privacy or proprietary rights or any statutory copyright.
4) I have obtained written permission from copyright owners for any excerpts from copyrighted works that are included and have credited the sources in my article.
5) All authors have made significant contributions to the study including the conception and design of this work, the analysis of the data, and the writing of the manuscript.
6) All authors have reviewed this manuscript and take responsibility for its content and approve its publication.
7) I have informed all of the authors of the terms of this publishing agreement and I am signing on their behalf as their agent.

2. Copyright Transfer Agreement

I hereby assign and transfer to IACMHR Co., Ltd. all exclusive rights of copyright ownership to the above work in the journal Drug Discoveries & Therapeutics, including but not limited to the right 1) to publish, republish, derivate, distribute, transmit, sell, and otherwise use the work and other related material worldwide, in whole or in part, in all languages, in electronic, printed, or any other forms of media now known or hereafter developed and the right 2) to authorize or license third parties to do any of the above.

I understand that these exclusive rights will become the property of IACMHR Co., Ltd., from the date the article is accepted for publication in the journal Drug Discoveries & Therapeutics. I also understand that IACMHR Co., Ltd. as a copyright owner has sole authority to license and permit reproductions of the article.

I understand that except for copyright, other proprietary rights related to the Work (*e.g.* patent or other rights to any process or procedure) shall be retained by the authors. To reproduce any text, figures, tables, or illustrations from this Work in future works of their own, the authors must obtain written permission from IACMHR Co., Ltd.; such permission cannot be unreasonably withheld by IACMHR Co., Ltd.

3. Conflict of Interest Disclosure

I confirm that all funding sources supporting the work and all institutions or people who contributed to the work but who do not meet the criteria for authors are acknowledged. I also confirm that all commercial affiliations, stock ownership, equity interests, or patent-licensing arrangements that could be considered to pose a financial conflict of interest in connection with the article have been disclosed.

Corresponding Author's Name (Signature):

Date: